UNIVERSIDADE FEDERAL DO CEARÁ
CENTRO DE CIÊNCIAS
DEPARTAMENTO DE BIOQUÍMICA E BIOLOGIA MOLECULAR
PROGRAMA DE PÓS-GRADUAÇÃO EM BIOQUÍMICA

GYEDRE DOS SANTOS ARAÚJO

ANÁLISE COMPARATIVA DO METABOLOMA E PROTEOMA DE FOLHAS DE MILHO NA ACLIMATAÇÃO À SALINIDADE INDUZIDA PELO PRÉ-TRATAMENTO COM H_2O_2

FORTALEZA
2021

GYEDRE DOS SANTOS ARAÚJO

ANÁLISE COMPARATIVA DO METABOLOMA E PROTEOMA DE FOLHAS DE MILHO NA ACLIMATAÇÃO À SALINIDADE INDUZIDA PELO PRÉ-TRATAMENTO COM H_2O_2

Tese apresentada ao Programa de Pós-Graduação em Bioquímica da Universidade Federal do Ceará, como requisito parcial para obtenção do título de Doutor em Bioquímica. Área de concentração: Bioquímica Vegetal

Orientador: Prof. Dr. Enéas Gomes Filho
Coorientador: Dr. Elton Camelo Marques

FORTALEZA
2021

Dados Internacionais de Catalogação na Publicação
Universidade Federal do Ceará
Biblioteca Universitária
Gerada automaticamente pelo módulo Catalog, mediante os dados fornecidos pelo(a) autor(a)

A689a Araújo, Gyedre dos Santos.
Análise comparativa do metaboloma e proteoma de folhas de milho na aclimatação à salinidade induzida pelo pré-tratamento com H2O2 / Gyedre dos Santos Araújo. – 2021.
99 f. : il. color.

Tese (doutorado) – Universidade Federal do Ceará, Centro de Ciências, Programa de Pós-Graduação em Bioquímica , Fortaleza, 2021.
Orientação: Prof. Dr. Enéas Gomes Filho.
Coorientação: Prof. Dr. Elton Camelo Marques.

1. Estresse salino. 2. Fotossíntese. 3. Metabolismo. 4. Ultraestrutura de cloroplastos. 5. Fluorescência da clorofila. I. Título.

CDD 572

GYEDRE DOS SANTOS ARAÚJO

ANÁLISE COMPARATIVA DO METABOLOMA E PROTEOMA DE FOLHAS DE MILHO NA ACLIMATAÇÃO À SALINIDADE INDUZIDA PELO PRÉ-TRATAMENTO COM H_2O_2

Tese apresentada ao Programa de Pós-Graduação em Bioquímica do Departamento de Bioquímica e Biologia Molecular da Universidade Federal do Ceará, como requisito parcial para obtenção do título de Doutor em Bioquímica. Área de concentração: Bioquímica Vegetal.

Aprovada em: __/__/___.

BANCA EXAMINADORA

_____
Prof. Dr. Enéas Gomes Filho (Orientador)
Universidade Federal do Ceará (UFC)

_____
Profa. Dra. Maria Raquel Alcântara Miranda
Universidade Federal do Ceará (UFC)

_____
Profa. Dr. Humberto Henrique de Carvalho
Universidade Federal do Ceará (UFC)

_____
Prof. Dr. José Hélio Costa
Universidade Federal do Ceará (UFC)

_____
Profa. Dra. Valdineia Soares Freitas
Instituto Federal do Ceará (IFCE)

_____
Dr. Fabrício Eulálio Leite Carvalho
Universidade Federal do Ceará (UFC)

Ao meu filho, ***Theo***

... com amor.

AGRADECIMENTOS

A *Deus*, por guiar meus passos, cuidar de mim e me sustentar em todos os momentos.

Aos meus pais, *Joaquim Bizerra de Araújo* e *Antônia dos Santos Araújo*, pelo amor incondicional, por tudo que me ensinaram, pelo imenso esforço e incentivo durante toda essa jornada.

À minha irmã, *Gessica dos Santos Araújo*, por me acompanhar nessa caminhada, pelo companherismo e apoio que sempre deu em minhas decisões, por torcer por mim e vibrar com minhas conquistas.

Ao meu esposo, *João Paulo de Sousa Almeida*, pelo seu amor e carinho, pelo cuidado, compreensão, pelo incentivo diário e pela ajuda essencial para esta conquista.

Ao professor Dr. *Enéas Gomes Filho*, responsável pela minha iniciação científca, um agradecimento especial pela orientação, confiança e incentivo à minha formação.

Ao professor Dr. *Humberto Henrique de Carvalho*, pelo incentivo, pelos ensinamentos transmitidos e pela ajuda na produção dos artigos científicos resultantes deste trabalho.

Ao Dr. *Lineker Lopes*, pela convivência, dedicação e grande contribuição na produção dos artigos científicos resultantes deste trabalho.

Ao professor Dr. *Emílio de Castro Miguel*, da Central Analítica da UFC, pela valiosa colaboração e disponibilização do espaço e dos recursos de seu laboratório, e aos técnicos *Sergimar Kennedy de Paiva* e *Marlos de Medeiros* pelo auxílio durante as análises de microscopia eletrônica de transmissão.

Ao professor Dr. *Celso Shiniti Nagano*, pela grandiosa colaboração e disponibilização dos recursos de seu laboratório, e ao Dr. *Fábio Roger Vasconcelos*, pela ajuda nas análises proteômicas.

Aos professores Dra. *Maria Raquel Alcântara de Miranda* e Dr. *José Hélio Costa*, por aceitarem participar de minha banca examinadora, pelos ensinamentos e por sempre permitirem o uso de seus laboratórios para a realização de análises, e ao Dr. *Fabricio Eulálio Leite Carvalho*, pelas valiosas críticas e sugestões a este trabalho.

À amiga *Stelamaris de Oliveira Paula Marinho*, pela amizade e parceria, pelo carinho, pelo convívio nos dias alegres e também nos dias difíceis, pela ajuda nos experimentos, pela contribuição durante as análises, pelo apoio e incentivo em todos os momentos.

Aos amigos queridos *Valdinéia Soares Freitas*, *Rosilene Oliveira Mesquita*, *Nara Lídia Alencar*, *Alexcyane Feijão*, *Marilena Braga*, *Daniel Farias, Elton Marques* e *Rafael Miranda*, pelos diversos ensimamentos transmitidos, incentivo, pela convivência e pelos encontros rodeados de alegria.

Aos amigos *Lindefânia Melo, Domingos Neto* e *Francisco Dalton Barreto*, pela amizade, convívio e por tornarem os dias de trabalho mais agradáveis.

Aos amigos do Laboratório de Fisiologia Vegetal, *Cibelle Gadelha*, *Karollyny Roger*, *Lucas Pacheco*, *Isabelle Mary Pereira*, *Igor Rafael*, como também aos que já passaram pelo laboratório, *Carlos Eduardo*, *Daniel Coelho*, *Analya Roberta*, *Valéria Batista*, *Paulo André*, *Igor Moura* e *Luckas Huriel*, pela convivência, amizade, pelos momentos de descontração e pela ajuda direta ou indireta no andamento deste trabalho.

À Universidade Federal do Ceará, em especial ao Departamento de Bioquímica e Biologia Molecular, pela oportunidade de realização deste trabalho.

À Coordenação de Aperfeiçoamento de Pessoal de Nível Superior (CAPES), pela concessão de bolsa de doutorado durante os anos de 2015 a 2018.

Ao Instituto Nacional de Ciência e Tecnologia em Salinidade (INCTSal), que por meio do Conselho Nacional de Desenvolvimento Científico e Tecnológico (CNPq) e Apoio ao Desenvolvimento Científico e Tecnológico (FUNCAP), concederam auxílio financeiro para execução deste trabalho.

E por fim, a todas as pessoas que contribuíram de alguma forma para o desenvolvimento deste trabalho e que não foram mencionadas.

"*A ciência não é somente um discípulo da razão, mas também do romance e da paixão*."
Stephen Hawking

RESUMO

A salinidade é um dos principais fatores limitantes à produtividade das culturas agrícolas, pois restringe o crescimento e desenvolvimento vegetal, afetando quase todas as características fisiológicas, morfológicas, bioquímicas e moleculares das plantas. Assim, a aclimatação ao estresse salino é essencial para sobrevivência e reprodução nessa condição adversa. O uso de pré-tratamento foliar com peróxido de hidrogênio (H_2O_2) em baixa concentrações pode atenuar os efeitos deletérios do estresse salino e com isso contribuir para aclimatação de plantas à tais condições. Entretanto, os mecanismos envolvidos na eficiência fotossintética, bem como a regulação de metabólitos e proteínas em plantas de milho pré-tratadas com H_2O_2 submetidas à salinidade não estão totalmente esclarecidos. Este estudo foi desenvolvido para testar a hipótese de que o uso do pré-tratamento com H_2O_2 mitiga os efeitos prejudiciais da salinidade na maquinaria fotossintética por afetar positivamente a modulação de metabólitos e proteínas envolvidas com a tolerância ao sal. Para isso, foram realizados dois experimentos com plantas de milho do genótipo BR 5011, considerado sensível à salinidade, pré-tratadas com solução de 10 mM de H_2O_2 e, então, estressadas com 80 mM de NaCl, sob condições de casa de vegetação. No primeiro experimento; que objetivou analisar a eficiência fotossintética, integridade estrutural dos cloroplastos e regulação dos metabólitos das plantas de milho; foi observado que a salinidade afetou drasticamente os parâmetros de trocas gasosas, da eficiência quântica máxima (Fv/Fm) do fotossistema II e os teores de clorofila *b* e *total*. Além disso, o estresse com NaCl aumentou os teores de espécies reativas de oxigênio (H_2O_2 e $^{\cdot}O_2^-$), ocasionou danos estruturais nos cloroplastos e promoveu perturbações no conjunto de metabólitos das plantas de milho, quando comparadas às condições de controle. No entanto, nossos resultados sugerem que plantas pré-tratadas com H_2O_2 melhoraram o desempenho fotossintético por evitar o excesso de energia induzida pela salinidade, induzindo assim acréscimos nos valores de Fv/Fm, *quenching* não-fotoquímico (NPQ) e taxa de transporte de elétrons (ETR), bem como apresentaram manutenção do empilhamento dos tilacóides, redução nos teores de H_2O_2 e $^{\cdot}O_2^-$ e modulação positiva de metabólitos, principalmente açúcares e aminoácidos, que contribuíram para a manutenção do equilíbrio osmótico e redução do estresse oxidativo. O segundo experimento teve como objetivo principal relacionar as análises de crescimento e o acúmulo de íons (Na^+ e K^+) com as alterações no perfil proteômico de plantas de milho. Nessa ocasião, o estresse salino imposto afetou significativamente os parâmetros de crescimento, bem como

aumentou a relação Na^+/K^+ nas folhas e promoveu alterações negativas no proteoma foliar. Em contraste, o uso do pré-tratamento com H_2O_2 influenciou positivamente na aparência fenotípica nas plantas sob salinidade, confirmada pela melhora das análises de crescimento e redução dos teores de íons Na^+ nas folhas. Adicionalmente, houve regulação de importantes proteínas que participam de vias metabólicas relacionadas à tolerância ao estresse salino. No geral, essas observações revelam que o pré-tratamento com H_2O_2 ativa mecanismos envolvidos na modulação positiva de importantes metabólitos e proteínas, que alivia os efeitos prejudiciais da salinidade na maquinara fotossintética de plantas de milho e aumenta a tolerância ao estresse salino.

Palavras-chave: Estresse salino. Fotossíntese. Metabolismo. Ultraestrutura de cloroplastos. Fluorescência da clorofila. *Zea Mays*.

ABSTRACT

Salinity is one of the major limiting factors crop productivity, it restricts plant growth and development, affecting almost all physiological, morphological, biochemical and molecular characteristics of plants. Thus, acclimation to salt stress is essential for survival and reproduction under this adverse condition. The use of hydrogen peroxide (H_2O_2) foliar pretreatment at low concentrations can attenuate the deleterious effects of salt stress and thus contribute to plant acclimation to such conditions. However, the mechanisms involved in the photosynthetic efficiency and the metabolites and proteins regulation of H_2O_2 pretreated maize plants under salinity are not fully understood. This study was designed in order to test the hypothesis that the use of H_2O_2 pretreatment mitigates the harmful effects of salinity on photosynthetic machinery by positively affecting the modulation of metabolites and proteins involved with salt tolerance. Therefore, two experiments were conducted with maize plants of genotype BR 5011, considered sensitive to salinity, pretreated with 10 mM H_2O_2 and then stressed with 80 mM NaCl under greenhouse conditions. In the first experiment; which aimed to analyze the photosynthetic efficiency, the structural integrity of chloroplasts and metabolites regulation of maize plants; was observed that salinity drastically affected the gas exchange parameters, maximum quantum efficiency (Fv/Fm) of photosystem II and chlorophyll *b* and *total* contents. In addition, NaCl-stress increased the reactive oxygen species (H_2O_2 and $^{\cdot}O_2^-$) contents, caused structural damage to chloroplasts and promoted disturbances in the metabolite set of maize plants when compared to control conditions. However, our results suggest that H_2O_2-pretreated plants improve photosynthetic performance by avoiding salinity-induced excess energy, thus inducing increases in Fv/Fm, non-photochemical quenching (NPQ) and electron transport rate (ETR) values. In parallel, there was maintenance of thylakoids stacking, reduction in H_2O_2 and $^{\cdot}O_2^-$ contents and positive modulation of metabolites, mainly sugars and amino acids, which contributed to the maintenance of osmotic balance and reduction of oxidative stress. The second experiment aimed to relate growth analysis and ion accumulation (Na^+ and K^+) with changes in the proteomic profiling of maize plants. The imposed salt stress significantly affected the growth parameters, as well as increased the Na^+/K^+ ratio in leaves and promoted negative alterations in leaf proteome. In contrast, the use of H_2O_2 pretreatment positively influenced the phenotypic appearance in plants under salinity, confirmed by improved growth analyzes and reduced Na^+ ion foliar contents. Additionally, there was

regulation of important proteins that participate in metabolic pathways related to salt stress tolerance. In conclusion, these observations reveal that H_2O_2 pretreatment activates mechanisms involved in the positive modulation of crucial metabolites and proteins, which alleviates the harmful effects of salinity on photosynthetic machinery of the maize plants and increases the tolerance to salt stress.

Keywords: Salt stress. Photosynthesis. Metabolism. Chloroplast ultrastructure. Chlorophyll fluorescence. *Zea Mays*.

LISTA DE FIGURAS

LISTA DE TABELAS

SUMÁRIO

1 INTRODUÇÃO

A salinidade é um dos principais estresses abióticos que restringem a produtividade das culturas em todo o mundo, afetando quase todas as características fisiológicas, morfológicas, bioquímicas e moleculares das plantas (SEKHON *et al.*, 2016; ISAYENKOV *et al*., 2019). Esse problema tem sido agravado pela utilização de certas práticas agrícolas, particularmente em regiões áridas e semiáridas, onde os solos marginais são incorporados na agricultura em paralelo ao uso de água de irrigação de baixa qualidade e a um manejo inadequado do solo (MEDEIROS *et al*., 2016).

A salinidade afeta o crescimento e o desenvolvimento vegetal por alterar a homeostase osmótica e/ou iônica das plantas. A redução do potencial hídrico do solo promove diminuição da disponibilidade de água para a planta e, consequentemente, a pressão de turgor das células é reduzida, afetando diretamente os processos de divisão e expansão celulares. Por outro lado, o acúmulo de íons tóxicos prejudica as relações minerais das plantas, e isso eventualmente gera desequilíbrios e distúrbios nutricionais (LIANG *et al*., 2018). Juntos, esses efeitos adversos observados em muitas plantas são frequentemente associados a reduções na taxa fotossintética, que impacta negativamente a difusão do dióxido de carbono (CO_2) através do complexo estomático, além de causar danos à estrutura dos cloroplastos e às enzimas envolvidas na assimilação de CO_2 (HUANG *et al*., 2014; SINGH *et al*., 2017). O estresse salino também provoca um desequilíbrio no estado redox das células, gerando estresse oxidativo através da produção excessiva de espécies reativas de oxigênio (EROs), tais como o peróxido de hidrogênio (H_2O_2) e os radicais superóxido ($^{\bullet}O_2^-$) e hidroxil ($HO^{\bullet}$) (DAS; ROYCHOUDHURY, 2014; ANJUM *et al*., 2015).

A aclimatação ao estresse salino ou a quaisquer condições adversas é essencial para a sobrevivência, o crescimento e a reprodução das plantas. Nos últimos anos, a pré-exposição ou pré-tratamento (*priming*) de plantas a estresses moderados ou moléculas sinalizadoras vem sendo associado às respostas de defesa, podendo aumentar a aclimatação de plantas a estresses abióticos (FORMAN *et al*., 2010; WANG *et al*., 2014). Essa técnica é conhecida como tolerância cruzada e permite o acúmulo de proteínas de sinalização ou fatores de transcrição de forma inativa, que são modulados após exposição a um estresse severo, resultando em um mecanismo de defesa mais eficiente (BRUCE *et al*., 2007; KOLLIST *et al*., 2019). O pré-tratamento com H_2O_2 a fim de induzir respostas de defesa a estresses abióticos tem sido

proposto devido à importância dessa molécula em muitos processos fisiológicos, tais como fotossíntese e modulação de vias de resposta ao estresse (NIU; LIAO, 2016). Vários estudos têm demostrado que a aplicação de H_2O_2 contribui para manter os teores de EROs baixos, além de aumentar a atividade de enzimas antioxidantes, através da mudança na transcrição de genes, induzindo assim a aclimatação de plantas ao estresse salino (GONDIM *et al*., 2013; ASHFAQUE *et al*.; 2014; SATHIYARAJ *et al*., 2014).

Nos últimos anos, análises proteômicas e metabolômicas, além de estudos da eficiência fotossintética, têm contribuído com o fornecimento de novas percepções acerca da tolerância à salinidade, revelando proteínas e metabólitos cruciais na aclimatação das plantas ao estresse salino (SINGH *et al*., 2017; WANG *et al*., 2019; ZHANG *et al*., 2019).

Tendo em vista que estudar os mecanismos que contribuem para a tolerância à salinidade é de grande importância, especialmente através da caracterização conjunta de aspectos fisiológicos, bioquímicos, estruturais e moleculares envolvidos no processo de aclimatação à salinidade, e dado o efeito benéfico da aplicação de H_2O_2 nas plantas, o presente trabalho visou avaliar o papel do pré-tratamento com H_2O_2 na maquinaria fotossintética, bem como na modulação de proteínas e metabólitos associados com as vias de proteção contra o estresse salino, esclarecendo respostas envolvidas na aclimatação de plantas de milho a esse estresse.

2 FUNDAMENTAÇÃO TEÓRICA

2.1 Salinidade na maquinaria fotossintética

Dentre os processos fisiológicos mais afetados pelo estresse salino, destaca-se a fotossíntese, responsável por fixar o CO_2 e sintetizar compostos orgânicos, utilizando água e energia solar. É o processo fisiológico mais importante relacionado com a produtividade das culturas e é extremamente sensível ao estresse salino (NAJAFPOUR; PASHAEI, 2012). Os efeitos da salinidade sobre a fotossíntese, em paralelo à redução do crescimento foliar (MUNNS *et al*. 2006; NEBAUER, 2013), podem ser associados diretamente a alterações no aparato fotossintético, como a redução do conteúdo de pigmentos fotossintéticos e do transporte de elétrons nos cloroplastos, causando, consequentemente, decréscimos na eficiência do fotossistema II (PSII) (CHAVES *et al*., 2011; YAN *et al*., 2012; HUANG *et al*., 2014).

Durante o estresse salino, as mudanças nas relações hídricas associadas com o acúmulo de íons no interior dos tecidos fotossintéticos têm implicações consideráveis na atividade fotossintética de muitas culturas. Na maioria das plantas, o excesso de sais no ambiente radicular provoca um rápido fechamento dos estômatos, prejudicando a assimilação de CO_2. Esse efeito provoca um desequilíbrio entre a absorção de luz e a utilização de energia, gerando fortes perturbações em praticamente todos as etapas da fotossíntese (CHAVES; FLEXAS, 2009). As respostas estomáticas induzidas pelo efeito osmótico no ambiente radicular são decorrentes do desequilíbrio hídrico que ocorre durante o estresse salino. Essas respostas são provavelmente reguladas por sinais da raiz, através principalmente do hormônio ácido abscísico (ABA), que é acumulado nessas condições adversas (JANICKA-RUSSAK; KLOBUS, 2007; ZÖRB *et al*., 2013). Além de afetar a condutância estomática, o efeito osmótico da salinidade leva à redução da área foliar, prejudicando a produção de fotoassimilados e afetando o rendimento das plantas (AHMAD *et al*., 2013).

Além dos efeitos de natureza estomática, a salinidade também implica limitações bioquímicas à maquinaria fotossintética, provocadas pelo efeito iônico do estresse salino, dentre as quais estão a redução do conteúdo total de clorofilas, devido a uma biossíntese prejudicada ou à degradação acelerada dos pigmentos. Adicionalmente os carotenoides, que desempenham um papel importante na fotoproteção do aparato fotossintético e funcionam como precursores na sinalização durante o desenvolvimento das plantas sob estresse, também podem ser afetados (GOMATHI; RAKKIYAPAN, 2011; ASHRAF; HARRIS, 2013).

O potencial metabólico da fotossíntese é também influenciado pela atividade das enzimas envolvidas na fixação do CO_2 e na regeneração da ribulose-1,5-bifosfato (RuBP) (REDONDO-GÓMEZ *et al*., 2007; HE *et al*., 2014), especialmente a ribulose-1,5-bisfosfato carboxilase/oxigenase (Rubisco) e a fosfoenolpiruvato carboxilase (PEPCase). Sob salinidade, a redução na síntese e na atividade de tais enzimas têm sido considerada uma das limitações bioquímicas da fotossíntese mais importantes, o que interfere consideravelmente na síntese de carboidratos (ABDEL-LATIF, 2008; LU *et al*. 2009; YAMANE *et al*., 2012; ASHRAF; HARRIS, 2013; HE *et al*., 2014). Além disso, mudanças na ultraestrutura dos cloroplastos, principalmente pela desorganização das membranas dos tilacoides, também estão correlacionadas com a menor eficiência e a degradação de enzimas envolvidas na fixação de carbono, como a Rubisco (KRUPINSKA, 2006).

Outra consequência do excesso de sais nas plantas é a limitação no transporte de elétrons nos cloroplastos, causando decréscimos na eficiência fotoquímica do PSII (SALEEM *et al*., 2011; MIRANDA *et al*., 2013). Dessa forma, a produção e o acúmulo excessivo de EROs torna-se um dos principais efetores dessa ineficiência. A produção de EROs é um evento bioquímico normal do metabolismo celular, que ocorre em vários locais na célula vegetal, principalmente nos cloroplastos, nas mitocôndrias e nos peroxissomos, a partir da redução monovalente do oxigênio molecular (O_2). As EROs mais comumente encontradas são o H_2O_2 e os radicais $^{\bullet}O_2^-$ e $HO^{\bullet}$ (AZEVEDO-NETO *et al*., 2005; YAMANE *et al*., 2012). No entanto, quando as plantas são submetidas a estresses ambientais, a produção de EROs geralmente aumenta, levando a um desequilíbrio redox e a estresse oxidativo, que afetam as funções normais da célula. Nessa condição, pode haver danos a proteínas, DNA e lipídios, culminando eventualmente em uma disfunção metabólica permanente e até na morte da planta (GILL; TUTEJA, 2010; DAS; ROYCHOUDHURY, 2014; ANJUM *et al*., 2015).

As reduções na eficiência fotoquímica podem ser decorrentes de danos à integridade dos tilacoides nos cloroplastos, gerando excesso de energia nos tecidos fotossintéticos, o qual, se não for seguramente dissipado, causa danos extremos ao metabolismo celular vegetal (YAMANE *et al*., 2003; ARAGÃO *et al*., 2012; SANTOS *et al*., 2013). Excessos de energia podem ser dissipados como fluorescência ou na forma de calor, ou ainda ser transferidos para o O_2 em vez de para o $NADP^+$, gerando acúmulo de EROs, que podem levar à fotoinibição (KRIEGER-LISZKAY *et al*., 2008; YU *et al*., 2014). Dessa forma, os mecanismos de dissipação de energia constituem um importante indicativo da eficiência do aparato fotossintético em diversas culturas. Dentre eles, pode-se citar o ciclo das xantofilas, ou dissipação térmica, que desempenha um papel significante na captação de luz e na minimização do excesso de energia das plantas (MISRA *et al*. 2006; SILVA *et al*., 2010; WILHELM; SELMAR, 2011; KUCZYŃSKA *et al*. 2012). Nesse processo, o excesso de energia durante o transporte de elétrons aumenta a acidificação do lúmen dos tilacoides e proporciona uma rápida conversão da violaxantina em zeaxantina, através do intermediário anteraxantina, pela ação da violaxantina de-epoxidase. Adicionalmente, ocorre a protonação de proteínas associadas com os complexos coletores de luz do PSII (LHCII). Essas mudanças produzem alterações conformacionais em LCHII e, assim, aumentam a dissipação térmica, para minimizar a pressão de excitação no PSII (BAKER, 2008; ROACH *et al*.; 2012; YU *et al*., 2014).

Diversos pesquisadores têm empregado a mensuração da fluorescência da clorofila *a* como forma de investigar a eficiência da fotossíntese de plantas sob condições de estresse. Essa técnica tem sido difundida principalmente por ser um método não destrutivo e que permite analisar qualitativa e quantitativamente a absorção e o aproveitamento da energia luminosa através do PSII, bem como suas possíveis relações com a capacidade fotossintética. Dessa maneira, mensurações simultâneas de fluorescência da clorofila *a* e de trocas gasosas permitem um melhor entendimento dos efeitos da salinidade sobre o aparato fotossintético e têm sido bastante úteis na seleção de plantas mais tolerantes a condições ambientais adversas (BAKER *et al*., 2008; RAZAVI *et al*., 2008; LIMA NETO *et al*., 2014).

2.2 Aclimatação de plantas a estresses

De modo geral, a salinidade promove alterações nas condições ótimas de crescimento, perturbando o funcionamento fisiológico e bioquímico e o componente estrutural das plantas, o que limita seu crescimento e seu desenvolvimento e pode até levar à morte delas. Para sobreviver em condições de estresse, as plantas dependem da sua capacidade de se aclimatar a tais condições adversas. A aclimatação é um processo que envolve mudanças temporárias no metabolismo da planta (fisiológicas, bioquímicas e morfológicas), permitindo que um indivíduo adquira maior tolerância ao estresse, em comparação àqueles que não se encontram aclimatados. Esse processo não está associado a alterações no genoma vegetal, mas sim a uma plasticidade fenotípica, não sendo, portanto, transmitida para as gerações futuras (PRISCO; GOMES-FILHO, 2010; SOUZA; LÜTTGE, 2015).

Quando as plantas são submetidas a condições ambientais adversas, a percepção do estresse e a subsequente aclimatação dessas plantas a tais condições, como a salinidade, seguem vias complexas de transdução de sinal e envolvem um grande número de componentes moleculares (GOLLDACK *et al*., 2014). O estresse é percebido extracelularmente pelos receptores da membrana plasmática e, em seguida, é ativada uma cascata de sinalização, que inclui a geração de moléculas secundárias sinalizadoras no meio intracelular. Essa cascata resulta na expressão de múltiplos genes de resposta ao estresse, que levam a mudanças profundas na composição do conjunto de proteínas, proporcionando, assim, a aclimatação das plantas, pela sobrevivência e pela superação em condições desfavoráveis (KOSOVÁ *et al*., 2011; HUANG *et al*., 2012).

Nos últimos anos, parte dos estudos sobre estresse salino está voltada para a intensificação da aclimatação das plantas a estresses abióticos. Embora seja possível construir plantas transgênicas tolerantes à salinidade, isso não vem sendo utilizado em larga escala (MUNNS, 2005; COMINELLI *et al*., 2013). A complexidade dos mecanismos de tolerância, que por vezes é uma característica multigênica, e a diversidade das respostas das plantas aos estresses têm contribuído para esse insucesso (ASHRAF *et al*., 2008). Nas condições de campo, as plantas estão submetidas frequentemente a estresses múltiplos, os quais variam em intensidade e duração, afetando diferencialmente o crescimento, que dependerá ainda do estágio de desenvolvimento em que elas se encontram (COMINELLI *et al*., 2013).

Quando a aclimatação a um determinado estresse é intensificada pela exposição a um estresse anterior (de mesmo tipo ou diferente), têm-se a tolerância cruzada. O emprego de moléculas sinalizadoras para induzir a aclimatação a estresses abióticos pela tolerância cruzada tem se tornado uma importante estratégia para aumentar a capacidade de as plantas crescerem em condições ambientais adversas (NAHAR *et al*., 2014; TENG *et al*., 2014; WANG *et al*., 2014). É nesse contexto que a tolerância cruzada torna-se importante, principalmente para a agricultura, pois, através desse processo, as plantas podem ser selecionadas por apresentarem maior tolerância a um tipo de estresse (AZEVEDO-NETO *et al*., 2008). A pré-exposição das plantas a um fator estressante ou sinalizador antecedente, parece ser integrada com diferentes redes de sinalização em plantas, tais como, rede de proteínas quinases e sinalização do Ca^{+2}, que são componentes fundamentais para o início da transdução do sinal, pois permitem que o estímulo extracelular seja traduzido a uma mudança intracelular (WEI *et al*., 2014; ZHOU *et al*., 2014). Além disso, a modulação da expressão gênica e o metabolismo das proteínas e metabólitos estão associados com importantes vias nas respostas ao estresse abiótico. Juntos, esses fatores podem desencadear a "memória de estresse" das culturas, permitindo que as plantas estejam melhor preparadas para responder a estresses posteriores (BRUCE *et al*., 2007; BALMER *et al*., 2015; MARTINEZ-MEDINA *et al*., 2016).

2.3 Papel do H_2O_2 na aclimatação ao estresse salino

Uma das técnicas utilizadas para intensificar a aclimatação a estresses abióticos é a aplicação de compostos orgânicos, inorgânicos ou reguladores do crescimento no meio de cultivo das plantas, sendo as raízes, nesse caso, o órgão que entra em contato direto com a substância, ou por aspersão desses compostos nas folhas (ASHRAF *et al*., 2008). Essas

substâncias, dependendo da sua concentração, ora atuam como indutores de estresse, ora como moléculas sinalizadoras; o H_2O_2 e o óxido nítrico (NO) são exemplos dessas moléculas (KHAN *et al*., 2012; FILIPPOU *et al*., 2013). Têm-se utilizado ainda o pré-tratamento com poliaminas (DUAN *et al*., 2008), ácido abscísico (ABA) (LI *et al*., 2010), glicose (HU *et al*., 2012) e oligoquitosana (MA *et al*., 2012), dentre outras substâncias, como meio para atenuar os efeitos deletérios do estresse salino. Em todos esses casos, as plantas podem ser mantidas na presença dessas substâncias exógenas durante todo o desenvolvimento delas, ou apenas em um período que antecede a exposição ao estresse (pré-tratamento), e se os efeitos nocivos do estresse puderem ser atenuados nos estádios iniciais do desenvolvimento, as chances de a planta estabelecer-se com sucesso são consideravelmente aumentadas (ASHRAF; FOOLAD, 2005).

As evidências de que essa abordagem condiciona as plantas a responderem mais rápida e eficientemente a estresses são cada vez mais notórias. Dentre os vários estudos que já foram realizados, destaca-se o uso do pré-tratamento com H_2O_2, a fim de aumentar a tolerância à salinidade (AZEVEDO NETO *et al*., 2005; GONDIM *et al*., 2013). O H_2O_2 é um componente vital para o desenvolvimento, o metabolismo e a homeostase de diferentes organismos, e nas últimas décadas, tem recebido um interesse considerável entre as EROs (BIENERT *et al*., 2006; HOSSAIN *et al*., 2015). O H_2O_2 é uma das EROs mais estáveis, e nas plantas está envolvido em processos tais como alongamento celular, diferenciação e morfogênese, bem como na defesa e nas respostas de aclimatação a vários estresses ambientais (TSUKAGOSHI *et al*., 2010; BHATTACHARJEE, 2012). Resultando da redução de dois elétrons a partir do O_2, o H_2O_2 não é um radical livre, não apresenta carga (HALLIWEL, 2006) e possui a meia-vida celular mais longa dentre as EROs (1 ms). Além disso, por possuir um pequeno tamanho, o H_2O_2 pode atuar como molécula sinalizadora, pois atravessa membranas celulares e percorre diferentes compartimentos celulares (BIENERT *et al*., 2006; MARUTA *et al*., 2012; NOCTOR *et al*., 2014).

Embora o H_2O_2 seja considerado subproduto do metabolismo celular e, quando se encontra em concentrações mais elevadas, esteja associado com toxicidade e danos oxidativos, ele é empregado pelas plantas, em baixas concentrações, como iniciador da sinalização em diferentes processos celulares, tornando-o uma molécula versátil. Portanto, é necessário que as células possuam processos de regulação das concentrações de H_2O_2, mantendo assim em equilíbrio a produção e a eliminação dessa espécie reativa de oxigênio (GECHEV; HILLE, 2005; BHATTACHARJEE, 2012).

Alguns estudos com plantas têm demonstrado que o pré-tratamento com concentrações apropriadas de H_2O_2 pode conferir tolerância a estresses ambientais, através da modulação de vários processos fisiológicos, tais como a fotossíntese, e de múltiplas vias de resposta ao estresse, como as vias de remoção das EROs (WANG *et al*., 2010; GONDIM *et al*., 2013; LIU *et al*., 2014). Fedina *et al*. (2009) observaram que plântulas de *Hordeum vulgare* pré-tratadas com H_2O_2 apresentaram altas taxas de fixação de CO_2 e baixos teores de malondialdeído (MDA) e de H_2O_2, quando submetidas por 4 e 7 dias a NaCl a 150 mM, em comparação com as plantas submetidas somente ao estresse salino. De modo similar, Li *et al*. (2011) relataram que a aplicação de H_2O_2 reduziu a peroxidação de lipídios e aumentou os teores de glutationa (GSH) e a atividade das enzimas peroxidase do ascorbato (APX), catalase (CAT), dismutase do superóxido (SOD) e peroxidase (POD) em plantas de trigo sob estresse salino.

As evidências de que o metabolismo do H_2O_2 pode ser importante para induzir aclimatação à salinidade são cada vez mais concretas. Gondim *et al*. (2013), em estudos com aplicação de H_2O_2 em plantas de milho (*Zea mays* L.) sob salinidade, observaram que as taxas de fotossíntese líquida, transpiração, condutância estomática e concentração interna de CO_2 foram reduzidas em plantas sob salinidade, porém, quando essas plantas foram pré-tratadas com H_2O_2, o impacto negativo da salinidade foi atenuado. Além disso, nesse mesmo estudo, as plantas pulverizadas com H_2O_2 tiveram os teores relativos de água e de clorofila mais elevados, e baixo acúmulo de H_2O_2 foliar, o que se correlacionou positivamente com a melhora nas trocas gasosas, em comparação com plantas não pré-tratadas submetidas a condições salinas, permitindo maior eficiência fotossintética e melhoria no crescimento das plantas de milho sob salinidade.

Recentemente, Ashfaque *et al*. (2014) conduziram um experimento para estudar o papel do H_2O_2 na mitigação dos efeitos do estresse salino em plantas de trigo (*Triticum aestivum* L.). Nesse estudo, os autores observaram que o pré-tratamento das plantas com H_2O_2 influenciou positivamente o crescimento sob condições salinas, reduzindo o acúmulo de Na^+ e Cl^- e aumentando os teores de prolina e a assimilação de nitrogênio. Já em plântulas de *Panax ginseng*, Sathiyaraj *et al*. (2014) demostraram que o pré-tratamento com H_2O_2 aumentou as atividades das enzimas APX, CAT e peroxidase da glutationa (GPX) e decresceu o acúmulo de MDA, H_2O_2 e $\cdot O_2^-$, elevando consideravelmente a tolerância das plantas ao estresse salino.

Todas essas evidências demostram que o pré-tratamento com H_2O_2 é uma estratégia promissora para atenuar os efeitos deletérios do estresse salino, pois além de ativar efetivamente

mecanismos antioxidantes, proporciona também respostas fotossintéticas relevantes e um melhor crescimento e desenvolvimento sob salinidade. Contudo, embora o H_2O_2 seja reconhecidamente um agente indutor de tolerância cruzada, pouco se sabe sobre como o pré-tratamento com H_2O_2 afeta a eficiência da maquinaria fotossintética e aumenta a assimilação de CO_2 nas plantas.

2.4 Proteômica e metabolômica de plantas sob estresse salino

Durante os últimos anos, a proteômica e a metabolômica vegetais tornaram-se importantes ferramentas no estudo das complexas interações moleculares envolvidas nas respostas a estresses abióticos, incluindo o estresse salino (LLANES *et al*., 2018; FRUKH *et al*., 2019). Durante a aclimatação das plantas a estresses, a expressão de genes é alterada e o transcriptoma, o proteoma e o metaboloma das plantas são modificados. Na maioria dos casos, alterações na transcrição gênica nem sempre são acompanhadas por mudanças no proteoma (KOSOVÁ *et al*., 2011), portanto estudar as alterações no proteoma durante a aclimatação é de grande relevância, uma vez que as proteínas são os efetores diretos das respostas das plantas a estresses.

A análise sistemática global de proteínas expressas, denominada coletivamente de proteoma, tornou-se um dos enfoques mais promissores para se compreender a função e a regulação dos genes responsáveis pelos mecanismos de tolerância das plantas a estresses ambientais. Assim, a proteômica permite avaliar simultaneamente o perfil de muitas proteínas e, em paralelo, a identificação de alterações pós-traducionais induzidas por estresses, inclusive a salinidade (SOBHANIAN *et al*., 2011; KOSOVÁ et al., 2018). Com isso, as proteínas diretamente envolvidas nas respostas ao estresse podem contribuir significativamente para desvendar as possíveis relações entre a abundância de proteínas e a aclimatação das plantas a estresses.

Em estudos com estresse salino, a maioria das pesquisas comparam o proteoma isolado de plantas não estressadas (controle) com as de plantas submetidas a condições de estresse. Outra abordagem inclui a comparação do proteoma de dois diferentes genótipos ou espécies de plantas com tolerância diferencial a um dado estresse (HAKEEM *et al*., 2012; MA *et al*., 2014). Pesquisas destinadas à comparação de diversos proteomas são na maior parte dominadas pela separação das proteínas por eletroforese bidimensional, seguida pela identificação delas por espectrometria de massas (CARUSO *et al*., 2008; AGRAWAL *et al*., 2013).

Vários pesquisadores têm empregado uma abordagem proteômica no estudo de diferentes cultivares e espécies de plantas sob condições de salinidade. Como resultado, tem sido observado que as proteínas alteradas e identificadas pertenciam a importantes processos fisiológicos, tais como o metabolismo do carbono, incluindo proteínas que participam na fixação do carbono pelo ciclo de Calvin-Benson e as associadas com reações fotossintéticas primárias, especialmente as que compõem a cadeia transportadora de elétrons e o metabolismo dos carboidratos. Além disso, a síntese de proteínas com funções de proteção e as relacionadas com os mecanismos antioxidantes, conhecidas como eliminadoras de EROs, também sofreram alterações com a salinidade (ABREU *et al*., 2014; MOSTEK *et al*., 2015; ZHANG *et al*., 2019).

Apesar da ampla utilização da proteômica como uma ferramenta capaz de fornecer novas percepções e esclarecer os efeitos da salinidade na gama de proteínas relacionadas a processos fisiológicos essenciais, tais como a fotossíntese, os estudos atuais revelam que a contribuição dela para elucidar o papel fisiológico dessas proteínas na tolerância das plantas ao estresse salino tem sido limitada, visto que os estudos proteômicos revelam apenas a quantidade e a função dos peptídeos/proteínas, mas não discriminam a atividade da proteína, e esse é um fator importante para a interpretação em termos de fisiologia vegetal. No entanto, as limitações da proteômica podem ser atenuadas com auxílio de ferramentas de bioinformática e de técnicas particulares de proteômica, tais como proteômica redox e fosfoproteômica, além da integração com outras ferramentas, como transcriptômica e atividades enzimáticas (STRÖHE *et al*., 2006; LV *et al*., 2014; SILVEIRA *et al*., 2016).

A metabolômica pode ser definida como o estudo do "metaboloma", o conjunto de metabólitos presentes em uma célula ou tecido vegetal sob determinadas condições. Associada a técnicas cromatográficas, como cromatografia líquida-espectrometria de massas (LC-MS) ou cromatografia gasosa-espectrometria de massas (GC-MS), essa ferramenta faz uma abordagem poderosa para alcançar conhecimento integrado sobre as redes metabólicas que regulam as respostas a estresses (LLANES *et al*., 2018). Nas plantas, os estudos metabolômicos visam a identificar e quantificar metabólitos primários e secundários envolvidos em vários processos biológicos. Os metabólitos primários são altamente conservados em sua estrutura e abundância e são fundamentais para o crescimento e desenvolvimento das plantas, enquanto os metabólitos secundários ajudam as plantas a se comunicarem com o meio ambiente e diferem amplamente entre as espécies vegetais (SCOSSA *et al*., 2016; SINGH *et al*., 2017).

Em resposta à salinidade, ocorrem alterações no metabolismo das plantas, que é modulado a fim de manter a homeostase celular e garantir a sobrevivência, mesmo nessas condições adversas (HAMANISHI *et al*., 2015). Estudos têm sido empregados para identificar metabólitos envolvidos no restabelecimento da homeostase, bem como para detectar grupos de compostos envolvidos na tolerância ao estresse salino (RICHTER *et al*. 2015; WANG *et al*. 2019). Compostos tais como aminoácidos, carboidratos e ácidos orgânicos são os que geralmente têm seus teores alterados pela salinidade. Analisando o perfil metabólico de *Lolium perenne* em resposta ao estresse salino, determinado por GC-MS, foi observado que muitos metabólitos envolvidos no metabolismo dos carboidratos aumentaram acentuadamente em plantas sob estresse (HU *et al*., 2016). Nesse estudo, a sacarose representou 42,2% do total de carboidratos, o que se correlacionou com funções cruciais que essa molécula possui, tais como sinalizadora na regulação fonte-dreno, além de atuar na estrutura e metabolismo das plantas.

Estudos metabolômicos também ressaltam a modulação de fitohormônios e compostos antioxidantes em plantas submetidas ao estresse salino. Esses metabólitos ajudam na redução da concentração de Na^+ e melhoram o ajuste osmótico, além de estabilizar membranas de cloroplastos e reduzir a formação de EROs (WANG *et al*., 2015; BENDALY *et al*., 2016). Portanto, os estudos do metaboloma e proteoma de plantas submetidas à salinidade, seguido de identificação, quantificação e função das proteínas e metabólitos mais relevantes, contribuem significantemente para o entendimento dos mecanismos que governam as respostas à salinidade.

2.5 A cultura do milho

O milho é uma monocotiledônea, anual, herbácea, pertencente à família Poaceae, subfamília Panicoidae, gênero *Zea* e espécie *Zea mays*. (DUARTE, 2000). Sua importância econômica está centrada na diversidade de utilização, sendo responsável pelo fornecimento de diversos produtos para a alimentação humana e animal e como matéria-prima para a agroindústria (PAES, 2006; DEMARCHI, 2011). Além disso, o milho é utilizado para produção de bioetanol. O Brasil desempenha um papel importante na produção de milho, pois responde por cerca de 6,5% da produção mundial de grãos, com ocupação total de 16 milhões de hectares (FAO, 2019). Apesar da capacidade de adaptação ecológica, o milho tem sua produtividade limitada em muitas áreas do mundo, devido a certas condições adversas, como a salinização do solo e da água de irrigação (LERAYER, 2006; HICHEM *et al*., 2009). Essa espécie é

considerada moderadamente sensível à salinidade, com limiar de crescimento afetado a partir de 1,6 dS m^{-1}, embora esse efeito varie entre os diferentes cultivares existentes (MASS; HOFFMAN, 1977).

Dada a importância econômica do milho e sua relativa sensibilidade aos sais, estudar os efeitos do pré-tratamento com H_2O_2 na indução dessa espécie à aclimatação ao estresse salino torna-se relevante. Além disso, a eficiência fotossintética de plantas de milho nessas condições adversas é pouco explorada, assim como não se sabe com exatidão quais proteínas e metabólitos estão envolvidos nesse processo. Portanto, o presente estudo poderá esclarecer as respostas relacionadas ao desempenho fotossintético, assim como também auxiliar na seleção de marcadores moleculares envolvidos na aclimatação das plantas de milho à salinidade, os quais serão úteis para os programas de melhoramento genético dessa espécie.

3 HIPÓTESE

O pré-tratamento com H_2O_2 ativa mecanismos para evitar o acúmulo excessivo de EROs na maquinaria fotossintética, permitindo a integridade do aparato e a maior eficiência fotossintética, bem como promove alterações no metaboloma e no proteoma associadas com as vias metabólicas de proteção contra o estresse, induzindo a aclimatação de plantas de milho à salinidade.

4 OBJETIVOS

4.1 Objetivos gerais

Pretende-se averiguar a modulação do aparato fotossintético de plantas de milho pré-tratadas com H_2O_2 frente à salinidade, bem como investigar os efeitos do pré-tratamento com H_2O_2 e do estresse salino sobre o padrão proteico de folhas e de cloroplastos, analisando os aspectos fisiológicos, bioquímicos, estruturais e moleculares envolvidos na aclimatação dessa espécie a tais condições.

4.2 Objetivos específicos

- Avaliar os efeitos da salinidade e do pré-tratamento com H_2O_2 nos parâmetros de crescimento (área foliar e massa seca) de plantas de milho;

- Mensurar as trocas gasosas (taxa de fotossíntese líquida, transpiração, condutância estomática e eficiência da carboxilação da Rubisco), a eficiência do PSII (fluorescência da clorofila *a*) e os teores de pigmentos foliares (clorofilas e carotenoides) de plantas de milho pré-tratadas com H_2O_2 e submetidas à salinidade;

- Determinar o teor relativo de água e o potencial osmótico de folhas de plantas de milho pré-tratadas com H_2O_2 e submetidas à salinidade;

- Quantificar os teores de EROs ($^{\bullet}O_2^-$ e H_2O_2) nas folhas de plantas de milho pré-tratadas com H_2O_2 e submetidas à salinidade;

- Investigar a ultraestrutura de cloroplastos de folhas de plantas de milho pré-tratadas com H_2O_2 e submetidas à salinidade;

- Determinar a atividade da enzima fosfoenolpiruvato carboxilase (PEPCase) nos tecidos foliares de plantas de milho pré-tratadas com H_2O_2 e submetidas à salinidade;

- Elaborar mapas proteômicos reprodutíveis e de qualidade de folhas de plantas de milho, avaliando a influência dos tratamentos sobre os padrões eletroforéticos bidimensionais;

- Analisar os mapas proteômicos e identificar as proteínas diferencialmente sintetizadas de folhas de plantas de milho pré-tratadas com H_2O_2 e sob condições de salinidade;

- Identificar as proteínas responsivas ao estresse salino em folhas de plantas de milho pré-tratadas com H_2O_2;

- Identificar e mensurar, por meio de GC-MS, metabólitos considerados responsivos ao pré-tratamento com H_2O_2 e à salinidade em folhas de plantas de milho.

5 ESTRATÉGIA EXPERIMENTAL

Para testar a hipótese levantada e alcançar os objetivos propostos, o presente estudo foi desenvolvido em duas etapas, que consistiram de experimentos dependentes. A princípio, plantas de milho cultivadas em solução nutritiva foram pré-tratadas com H_2O_2 e, após 48 horas, submetidas ao estresse salino com NaCl a 80 mM. Para averiguar as alterações no metabolismo fotossintético de milho decorrentes do pré-tratamento com H_2O_2 e relacioná-las à aclimatação ao estresse salino, foram avaliadas as trocas gasosas e a fluorescência da clorofila *a*, o potencial osmótico foliar e os teores de pigmentos fotossintéticos. Em paralelo, foram determinados os teores foliares de $^{\cdot}O_2^-$ e H_2O_2, bem como investigada a ultraestrutura de cloroplastos, para averiguar se o pré-tratamento com H_2O_2 reduz a produção excessiva de EROs nos tecidos

foliares e mantêm a integridade estrutural do aparato fotossintético de plantas sob estresse salino. Foram determinadas também as modificações no conjunto de metabólitos de folhas, por meio de cromatografia gasosa acoplada à espectrometria de massas, bem como a atividade da enzima PEPCase, com o objetivo de investigar se as maiores taxas de assimilação de CO_2 em plantas de milho pré-tratadas com H_2O_2 são decorrentes da maior eficiência dessa enzima do metabolismo do carbono. Essa etapa possibilitou correlacionar as variáveis fisiológicas, fotoquímicas, bioquímicas e estruturais com a aclimatação das plantas de milho ao estresse salino. Durante a segunda etapa, foram avaliados os parâmetros de crescimento (produção de biomassa e área foliar), teor relativo de água e teores de íons Na^+ e K^+, bem como realizada uma análise proteômica diferencial em folhas de milho, utilizando as técnicas de eletroforese 2D-SDS PAGE e de espectrometria de massas, em função do pré-tratamento com H_2O_2 e da salinidade. Nessa ocasião, a abordagem das análises fisiológicas e as proteínas que apresentaram modulação positiva no perfil proteico, em função do pré-tratamento com H_2O_2, foram considerados responsivos e determinantes para a aclimatação de plantas de milho ao estresse salino.

6 H_2O_2 PRIMING PROMOTES SALT TOLERANCE IN MAIZE BY PROTECTING CHLOROPLASTS ULTRASTRUCTURE AND PRIMARY METABOLITES MODULATION

(Artigo publicado no periódico *Plant Science*)

Gyedre dos Santos Araújo[1] · Stelamaris de Oliveira Paula-Marinho[1] · Sergimar Kennedy de Paiva Pinheiro[2] · Emílio de Castro Miguel[2] · Lineker de Sousa Lopes[1] · Elton Camelo Marques[1] · Humberto Henrique de Carvalho[1] · Enéas Gomes-Filho[3]

[1] Department of Biochemistry and Molecular Biology, Federal University of Ceará, Brazil
[2] Department of Metallurgical and Materials Engineering, and Analytical Center, Federal University of Ceará, Fortaleza, Brazil
[3] Department of Biochemistry and Molecular Biology, and National Institute of Science and Technology in Salinity (INCTSal / CNPq), Federal University of Ceará, Fortaleza, Brazil

Abstract

Hydrogen peroxide priming has emerged as a powerful strategy to trigger multiple responses involved in plant acclimation that reinforce tolerance to abiotic stresses, including salt stress. Thus, this study aimed to investigate the impact of foliar H_2O_2 priming on the physiological, biochemical, and ultrastructural traits related to photosynthesis of salt-stressed plants. Besides, we provided comparative leaf metabolomic profiles of *Zea mays* plants under such conditions. For this, H_2O or H_2O_2 pretreated plants were grown under saline conditions for 12-days. Salinity drastically affected photosynthetic parameters and structural chloroplasts integrity, also increased reactive oxygen species contents promoting disturbance in the plant metabolism when compared to non-saline conditions. Our results suggest that H_2O_2-pretreated plants improved photosynthetic performance avoiding salinity-induced energy excess and ultrastructural damage by preserving stacking thylakoids. It displayed modulation of some metabolites, as arabitol, glucose, asparagine, and tyrosine, which may contribute to the maintenance of osmotic balance and reduced oxidative stress. Hence, our study brings new insights into an understanding of plant acclimation to salinity by H_2O_2 priming based on photosynthesis maintenance and metabolite modulation.

Keywords: Acclimation · Metabolomic · Photosynthesis · Salt stress · *Zea mays*

6.1 Introduction

Maize (*Zea mays* L.) plants have been one of the most energy sources for human and animal nutrition in the world (SEKHON *et al*., 2016; FAO, 2019). Nevertheless, maize growth and quality of grains can be severely affected by salinity, drought, high temperatures, among other adverse environmental conditions (SABAGH *et al*., 2020) that are responsible for a yield reduction of over 50% in major global crops (CAO *et al*., 2017). Salinity has a notable negative impact on crops worldwide, in which physiological, biochemical, morphological, and molecular processes are impaired by osmotic stress and ionic toxicity generated by salinity, leading to a series of secondary stresses, including oxidative burst (CHOUDHURY, 2017; ISAYENKOV; MAATHUIS, 2019). Salinity directly affects the integrity of chloroplast ultrastructure and causes lamellar disorders, affecting photosynthesis processes (BORGES, 2004). It can additionally reduce the content of photosynthetic pigments and electron transport

in the thylakoid membrane (HUANG *et al*., 2014; ABDELRAHEEM *et al*., 2019). Salt stress also can alter the activity of carbon-fixing enzymes and the regulation of plant metabolism (SINGH *et al*., 2017). That way, efficient acclimation to salt stress includes several structural or molecular changes. Also, the priming technique can be a helpful tool to reach acclimation inducing molecular mechanisms associated with salt tolerance in plant crops (FILIPPOU *et al*., 2013; SAVVIDES *et al*., 2016, GONZÁLEZ-BOSCH, 2018).

Overall, the priming can be achieved by pretreatment with synthetic or natural compounds as H_2O_2 applied on seed, root, or leaves (ASHRAF *et al*., 2018; THAKUR *et al*., 2019). The H_2O_2 is one of the reactive oxygen species (ROS) produced during cell metabolism; at low levels, it functions as a signaling agent, but in excess generates oxidative stress in plant cells, which usually occurs under severe environmental stresses (SINGH *et al*., 2019). The linkage of H_2O_2 and abiotic stress in the intracellular signaling for physiological responses remain not entirely clear, bearing in mind that the acclimation responses depend on specific ROS signatures to tailor plant to the exact stress encounters it (CHOUDHURY *et al*., 2017). Meanwhile, a promising improvement in photosynthesis by H_2O_2 priming can be related to carbon fixation enzymes activity, PSII efficiency, and protection of cellular organelles, such as chloroplasts (GAO, 2010; KHAN *et al*., 2016). Also, previous studies have demonstrated that application exogenous of a 10 mM H_2O_2 solution as a priming agent in maize leaves confers tolerance to salt stress (GONDIM *et al*., 2012; 2013). This H_2O_2 priming modulated various cellular processes associated with high antioxidant enzyme activities and increased soluble protein and soluble carbohydrates contents too.

Over the last years, the untargeted plant metabolomics has risen as a powerful research tool to study mechanisms of stress tolerance mainly because of the different modulate compounds (DEBNATH *et al*., 2018; WANG *et. al*., 2019). Although an overall metabolic reprogramming occurs in plants exposed to abiotic stresses, it is quite different among species. Some species synthesize and accumulate low quantities of specific metabolites, whereas some others do not do so at all (SINGH *et al*., 2017; LLANES *et al*., 2018). Thus, it becomes relevant to understand the metabolic reprogramming of primed plants under stress, accessing the primary metabolism and its relationship with other physiological responses. Given the economic importance of maize and its relative sensitivity to salinity, a better understanding regarding salt-tolerance by H_2O_2 priming becomes especially pertinent. Our purpose was to investigate if salt tolerance induced by H_2O_2 exogenous reported in maize by other studies be

the result of regulation and upkeep of photosynthetic machinery coupled with positive modulation of key metabolites as carbohydrates.

6.2 Material and methods

6.2.1 *Plant material and experimental conditions*

The maize (*Zea mays* L.) cultivar was BR 5011, considered sensitive to salinity (AZEVEDO-NETO *et al*., 2004). The seeds surfaces were sanitized in a 1% NaClO solution for 10 min before sown. After seven days of sowing, uniform seedlings were transferred to 10-L trays containing half-strength Hoagland's nutrient solution (HOAGLAND; ARNON, 1950) for five days, as an acclimation time. Then, 15 mL plant^{-1} of 10 mM H_2O_2 solution or an equal volume of distilled water was sprayed directly on the leaves, both containing 0.025% Tween 20 detergent, to break water surface tension facilitate H_2O_2 diffusion into mesophyll cells. The application with a 10 mM H_2O_2 solution was defined based on previous studies with promising results [GONDIM *et al*., 2012]. This pretreatment was performed around 6:00 am and repeated the next day. Two days after the priming end, the plants were transferred to a 6-L plastic pot containing half-strength Hoagland's nutrient solution without and with saline treatment. The saline treatment (80 mM NaCl) was first applied in two installments to avoid osmotic shock, so the NaCl concentration was increased daily by 40 mM until the desired level. After that, the 80 mM NaCl treatment was applied in its entirety to each solution change. All nutrient solutions were renewed every four days, and the pH was maintained between 5.5 and 6.0. The experiments were conducted in a greenhouse located in the tropical semiarid region of Northeastern Brazil under average values of temperature, relative humidity, and photosynthetic photon flux density (PPFD) of 32.3 °C, 44.8%, and 1,050 μmol photon m^{-2} s^{-1}, respectively. The plants were kept under twelve days of salt stress. At the end of the experiment, they were harvested and grouped into four treatments according to growth conditions: water-pretreated (1) and H_2O_2-pretreated (2) plants both under non-salt conditions, and water-pretreated (3) and H_2O_2-pretreated (4) plants both under salt stress.

6.2.2 *Gas exchange and chlorophyll a fluorescence*

The gas exchange and chlorophyll *a* fluorescence were performed in the middle third of the fully expanded leaves under constant CO_2 concentration and PPFD of 400 μmol mol^{-1} CO_2

and 1,200 μmol photons m^{-2} s^{-1}, respectively. Two measurements were performed by repetition, and the chamber size used was 2 cm^2. Rates of CO_2 assimilation (*A*), transpiration (*E*), stomatal conductance (g_s), and carboxylation efficiency (*A/Ci*) were measured employing a portable photosynthetic system (IRGA, mod. LI-6400XT, LI-COR, Lincoln, USA) coupled with artificial light. The chlorophyll *a* fluorescence parameters [maximum (Fm) and variable (Fv) fluorescence in dark-adapted leaves, maximum (Fm') and dynamic (Fs) equilibrium state in the presence of light, and basal fluorescence (Fo') after excitation state of photosystem I] were measured using a fluorometer (6400-40, LI-COR, USA) coupled to IRGA. From the chlorophyll *a* fluorescence, the following photochemical parameters were estimated: maximum quantum yield of PSII [Fv/Fm = (Fm - Fo)/Fm], effective quantum yield of PSII [ΦPSII = (Fm' - Fs)/Fm'], photochemical [qP = (Fm' - Fs)/(Fm' - Fo')] and non-photochemical [NPQ = (Fm - Fm')/Fm'] quenching, and electron transport rate (ETR = ΦPSII x PPFD x 0.5 x 0.84) (BILGER *et al*., 1995).

6.2.3 *Measurement of osmotic potential*

For determination of osmotic potential (Ψs), the sap was extracted from 350 mg of maize leaves expanded newly harvested by pressing the plant material with the aid of a disposable syringe. Then the obtained liquid (extract) was centrifuged at 6,000*g* for 5 min, and the supernatant used to determine the Ψs using the osmometer (VAPRO 5520, Wescor, Utah, USA) (CALLISTER *et al*., 2006).

6.2.4 *Photosynthetic pigments contents*

Contents of chlorophyll *a* (Chl *a*), *b* (Chl *b*), and total (Chl *total*), and carotenoids (Car) were determined from leaf discs of 1 cm^2, a total fresh mass of approximately 0.25 g, obtained from the middle third of fully expanded leaves. For pigments extraction, tubes containing the leaf discs were incubating in dimethyl sulfoxide saturated with $CaCO_3$, during 48 h at room temperature. After, the tubes were kept in the dark for 24 h and then incubated in a 65 °C water bath for 30 min. Photosynthetic pigments were spectrophotometrically measured by reading the absorbance at A_{480}, A_{649}, and A_{665}. The concentrations were calculated through the following equations: Chl *a* = $12.47_{A665} - 3.62_{A649}$, Chl *b* = $25.06_{A649} - 6.50_{A665}$, Chl *total* = $7.15_{A665} + 18.71_{A649,}$ and Car = $(1000_{A480} - 1.29$ Chl *a* – 53.78 Chl *b*)/220 (WELLBURN, 1994).

6.2.5 *ROS contents*

The leaf extracts used for the determination of H_2O_2 contents were prepared according to methods of Cheeseman (2006), with some modifications. Approximately 0.5 g of fresh tissue from fully expanded leaves was macerated with liquid nitrogen, followed by homogenization at 4 ° C with 100 mM potassium phosphate buffer solution, pH 6.3. The homogenate was centrifuged at 12,000*g* at 4 °C for 15 min, and the supernatant immediately evaluated. The reaction for H_2O_2 determination consisted of 350 µL plant extract; 350µL 12 mM phenol; 100 µL 0.5 mM 4-aminoantipyrine; 350 µL 84 mM phosphate buffer (pH 7.0) and 40 µL 1 U mL^{-1} HRP (horseradish peroxidase) diluted in 100 mM phosphate buffer pH 6.0. The reaction mixture was shaken and heated at 37 °C for 30 min. The H_2O_2 concentration of the reaction medium was determined by reading at 505 nm and comparing with a standard curve obtained from increasing H_2O_2 concentrations as standard according to methods of Fernando and Soysa (2015).

The determination of superoxide radical ($^{\bullet}O_2^-$) content was performed according to Klein *et al*. (2018) with some modifications. The fresh leaf tissue (0.25 g) macerated in liquid nitrogen was homogenized at 4 °C in 65 mM potassium phosphate buffer pH 7.8. The homogenate was centrifuged at 10,000*g* for 10 min at 4 °C, and the supernatant used immediately. The reaction occurred by the addition of 250 µL extract to a mixture composed of 65 mM phosphate buffer (pH 7.8) and 50 µL 10 mM hydroxylamine. The tubes were shaken and incubated at 25 °C for one hour. Next, 1000 µL of the mixture from 58 mM sulfanilamide and 7 mM N-naphthyl ethylenediamine (1:1) were added. Finally, 1000 µL ethyl ether was added to the tubes. The $^{\bullet}O_2^-$ concentration was determined by absorbance of pink aqueous phase at 530 nm and based on a standard curve obtained from increasing $NaNO_2$ concentrations.

6.2.6 *Phosphoenolpyruvate carboxylase activity*

Extracts for determination of phosphoenolpyruvate carboxylase activity (PEPcase, EC 4.1.1.31) were prepared according to Echevarria *et al*. (1994), with some modifications. Initially, approximately 0.25 g of fresh material from fully expanded leaves were macerated with liquid nitrogen and homogenized with 1.0 mL 100 mM Tris-HCl buffer (pH 7.5) containing 5% glycerol, 10 mM $MgCl_2$, 1.0 mM EDTA, 1.0 mM Na_3VO_4, 5.0 mM dithiothreitol (DTT), 2% polyvinylpyrrolidone (PVP), and 1mM phenylmethanesulfonyl fluoride (PMSF).

The homogenate was centrifuged at 15,000*g* for 2 min, and the supernatant used immediately in the enzymatic assay. All extraction steps were performed at 4 °C.

PEPcase activity was estimated by NADH oxidation kinetics in the presence of malate dehydrogenase (MDH). The 100 µl extract was added to reaction medium composed by 100 mM HEPES-KOH buffer (pH 8.0) containing 5 mM $MgCl_2$, 2.5 mM phosphoenolpyruvate (PEP), 1 mM $NaHCO_3$, 0.2 mM NADH, and 5 U mL^{-1} malate dehydrogenase enzyme (MDH) at 30 °C. The reaction was monitored by absorbance decay at 340 nm. For each mol of malate produced is oxidized 1 mol of NADH, so the results were expressed as nmol NADH h^{-1} mg^{-1} protein, using the NADH molar extinction coefficient (6.22 mM^{-1} cm^{-1}). Protein concentrations were determined by the Bradford method (Bradford, 1976) by absorbance readings at 595 nm and using bovine serum albumin (Sigma-Aldrich, USA) as standard.

6.2.7 *Chloroplast ultrastructure*

For chloroplast ultrastructure, approximately 2 mm^2 leaf fragments from fully expanded leaves were fixed for 24 h in 50 mM phosphate buffer (pH 7.2) containing 2.5% glutaraldehyde and 4% paraformaldehyde. Subsequently, the material was rinsed three times in buffer and 45 min apart for each wash. Posteriorly, the samples were post-fixed with 1% osmium tetroxide (OsO4) in 50 mM phosphate buffer for 60 min and then rinsed again in the same buffer. The samples were then dehydrated with increasing series of 50%, 70%, 90% and 100% acetone for 45 min each step, and after infiltrated in epoxy resin (EMbed 812) according to the methodology described by Yamane *et al*. (2012), with some modifications. The resin polymerization was performed at 60 °C. Ultrathin sections (70 nm) were placed on copper grids (300 mesh) and stained with 2% uranyl acetate for 40 min, followed by 0.5% lead citrate for 5 min. Finally, to generate chloroplast ultrastructure images, the sections were analyzed using a transmission electron microscope (JEOL JEM 1011) at 100 kV.

6.2.8 *Metabolomic analysis*

Extraction and derivatization of metabolites were performed as described by Lisec *et al*. (2006) with adjustments. Approximately 50 mg of fully expanded leaf tissue (frozen) was macerated using liquid N_2 and homogenized with 100% methanol (HPLC grade) containing ribitol (0.2 mg mL^{-1}) as a quantitative internal standard. The homogenate was incubated at 70 °C for 15 min under constant shaking. Then, the samples extracts were centrifuged at 12,000*g*

for 10 min, and the supernatants were transferred to microtubes containing 100% chloroform and ultrapure H_2O at 1:2 (v/v) ratio to separate polar and nonpolar phases inside the tubes. After vigorous vortexing, new centrifugation was conducted at 2,200 *g* for 10 min. A 150 µL of the upper polar phase was carefully collected and transferred to another microtube. Samples were dehydrated and concentrated in vacuo system (SpeedVac Concentrator, Eppendorf, Hamburg, Germany), then stored at -80 °C. The metabolites were derivatized using 20 µL methoxyamine hydrochloride (20 mg mL^{-1} pyridin) for two hours at 37 °C. Subsequently with 35 µL *N*-methyl-*N*- (trimethylsilyl)trifluoroacetamide for 30 min at 37 °C.

Separation and identification of metabolites were performed according to Roessner et al. (2001). Samples were analyzed by a gas chromatography system coupled to mass spectrometry (GC-MS, QP-PLUS-2010, Shimadzu, Tokyo, Japan), using an RTX-5MS capillary column (30.0 m x 0.25 mm x 0.25 µm). A volume of 1 µL of each derivatized sample was injected with a split ratio of 1:5. The injection temperature was 250 °C, and helium carrier gas was at 1.2 mL min^{-1} constant flow rate. The temperature programming was as follows: 2 min at 80 °C, 10 °C min^{-1} ramp to 315 °C, and then held at 315 ºC for 8 min. The transfer line and ion source were heated at 230 ºC and 250 ºC, respectively. Ionization was performed in an electron impact at 70 eV. The spectra in full scan mode were acquired from m/z 40 to 700. The solvent delay time was 3 min. Blank samples containing only derivatizing were done to identify possible contaminants.

Both chromatogram and mass spectral analysis were analyzed using the Xcalibur™ 2.1 software (Thermo Fisher Scientific, Waltham, MA, USA). All compounds were identified based on their retention times and mass spectrum fragmentation in comparison with an internal library composed by a mix of standards and its mass spectra previously identified based on the Golm Metabolome Database (GMD). The relative value of each metabolite was determined by the division of their respective peak areas by internal standard peak area (ribitol) and, after divided by the fresh weight of the sample.

6.2.9 *Experimental design and statistical analysis*

The experimental design was completely randomized, with a 2 × 2 factorial scheme. It was composed of two saline conditions [non-salt conditions (0 mM NaCl) and salt stress (80 mM NaCl)], and two leaf pretreatments [water-pretreated (0 mM H_2O_2) and H_2O_2-pretreated (10 mM H_2O_2)]. Each treatment was composed of four replicates consisting of two plants each.

The physiological and biochemical data were submitted to a two-way analysis of variance (ANOVA), and the main values were compared by *F*-test ($p < 0.05$). Statistical analyses were performed using the Sisvar® 5.3 software. Also, these data were divided by the standard deviation of each variable (Autoscaling) for chemometrics analysis [PCA (Principal Component Analysis)] by MetabolAnalyst 4.0 (https://www.metaboanalyst.ca).

The relative values of metabolites were normalized by the control treatment and converted to $\log_2$ values to generate a Heatmap by MultiExperiment Viewer (MeV) 4.9 software. Besides, multivariate analysis was conducted log-transformed data by MetaboAnalyst 4.0. The transformed metabolic data were submitted to chemometrics analysis [PLS-DA (Partial Least Squares Discriminant Analysis)] and Variable Importance in Projection (VIP) scores, based on the first component of the PLS-DA model, was performed to identify potential biomarkers. Those metabolites with VIP > 1.3 were considered essential for treatment separation (SINELNIKOV *et al*., 2015). They were also submitted to a one-way ANOVA, and mean treatment values were separated by Tukey's test ($p < 0.05$). Besides, the log-transformed physiological, biochemical, and metabolic data were submitted to correlation analysis [Pearson correlation ($p < 0.05$)] by MetabolAnalyst 4.0.

6.3 Results

6.3.1 *Gas exchange and Chlorophyll parameters*

H_2O_2 priming did not affect any gas exchange parameters of maize leaves in the absence of NaCl (Figure 1). Conversely, salinity significantly reduced all gas exchange parameters of water-pretreated plants except for *A/Ci*, which increased by 20%. Thus, *A*, *E,* and g_s rates decreased by 24%, 21%, and 48%, respectively. However, foliar H_2O_2 priming was able to prevent damage caused by salt stress on *A* and *E*, although it did not attenuate the g_s reduction

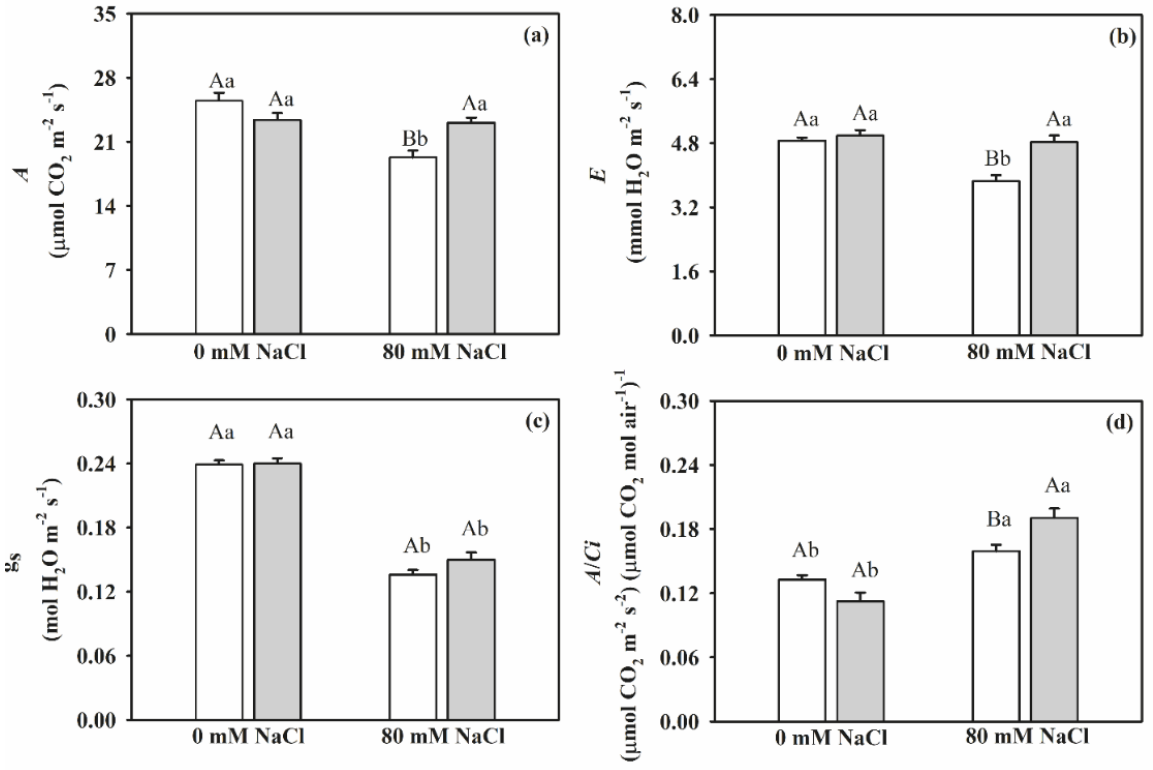

Figure 1. Gas exchange measurements in the leaves of maize cv. BR 5011 water-pretreated (*white bars*) or H_2O_2-pretreated (*gray bars*) under non-salt conditions or salt stress conditions for twelve days. Rates of CO_2 assimilation (*A*, a), transpiration (*E*, b), stomatal conductance (g_s, c), and Rubisco carboxylation efficiency (*A*/*Ci*, d). For each variable, the capital letters and lowercase letters compare the H_2O_2 pretreatments and salinity treatments, respectively, according to *F*-test ($p < 0.05$). Error bars represent ± standard error and means represent $n = 5$.

(Figure 1a-c). Also, H_2O_2 priming increased the *A/Ci* ratio by 20% under salt conditions (Figure 1d). Salinity did not reduce the ΦPSII and ETR values; H_2O_2 priming nevertheless slightly increased these parameters under non-saline conditions (Table 1). Additionally, the salt stress reduced the Fv/Fm values by 18%, but H_2O_2 priming decreased this reduction to 12%. In contrast, salt stress increased NPQ by 115%, and H_2O_2 primed plants under salt stress increased it more by 61%, in comparison to only salt-stress treatment. While H_2O_2 priming and salinity single treatments equally increased qP values; however, no change occurred by the combined action of both treatments. Also, no significant difference in the photosynthetic pigments analyzed was perceived by H_2O_2 priming either in non-saline or saline conditions (Table 1). On the other hand, Chl *a*, Chl *b*, and Chl *total* contents decreased by 21, 58, and 42%, respectively, under salt stress. Differently, carotenoid content was increased by 30% under salt stress. Also, H_2O_2 priming did not significantly alter photosynthetic pigments under non-saline and saline conditions, except for an increase under non-saline conditions in the carotenoid content similar to that produced by saline stress.

Table 1. Chlorophyll *a* fluorescence parameters and photosynthetic pigments in leaves of maize cv. BR 5011 water-pretreated (C) or H_2O_2-pretreated (H) under non-salt conditions and water-pretreated (S) or H_2O_2-pretreated (HS) under salt stress conditions for twelve days. Values represent the means (n = 5) ± standard error

Treatments	Chlorophyll *a* fluorescence variables [a]				
	ΦPSII [b]	**Fv/Fm [b]**	**NPQ [b]**	**qP [b]**	**ETR**
C	0.34±0.01 Ba	0.61±0.01 Aa	0.55±0.08 Bb	0.56±0.03 Bb	192.74±9.07Ba
H	0.39±0.01 Aa	0.58±0.01 Aa	0.70±0.02 Ab	0.67±0.01 Aa	204.44±3.31Aa
S	0.36±0.00 Aa	0.50±0.01 Bb	1.18±0.03 Ba	0.71±0.02 Aa	182.63±2.52Aa
HS	0.36±0.02 Ab	0.54±0.01 Ab	1.90±0.08 Aa	0.67±0.03 Aa	190.70±3.08Ab

Treatments	Photosynthetic pigments contents (μg g^{-1} DM) [a]			
	Chl *a*	**Chl *b***	**Chl *total***	**Car [b]**
C	373.7 ± 17.1 Aa	503.4 ± 29.8 Aa	877.1 ± 31.8 Aa	46.8 ± 4.9 Ab
H	385.6 ± 16.5 Aa	498.6 ± 14.7 Aa	884.2 ± 38.1 Aa	55.8 ± 5.5 Aa
S	294.4 ± 17.8 Ab	210.7 ± 11.1 Ab	505.9 ± 17.5 Ab	60.8 ± 1.7 Aa
HS	255.1 ± 11.2 Ab	313.8 ± 3.7 Ab	538.9 ± 23.2 Ab	49.3 ± 3.3 Aa

[a] For each variable, the capital letters and lowercase letters compare the H_2O_2 pretreatments and salinity treatments, respectively, according to F-test ($p < 0.05$). [b] Significant interaction between treatments ($p < 0.05$).

6.3.2 *Osmotic potential and reactive oxygen species*

The H_2O_2 priming did not modify the Ψs of leaves under non-saline conditions, and the salinity reduced the Ψs by 32% (Figure 2a). However, H_2O_2 priming under salinity induced a further 24% reduction of this value, in comparison to salt treatment alone. The H_2O_2 priming promoted an increase of 33% in the $\cdot O_2^-$ content but did not change H_2O_2 contents under non-saline conditions (Figure 2b, c), and salinity promoted the growth of 26 and 36% of $\cdot O_2^-$ and H_2O_2 contents in water-pretreated plants, respectively. In contrast, H_2O_2 priming significantly reduced $\cdot O_2^-$ and H_2O_2 contents in plants under salinity, making the values similar to those of water-pretreated plants without salt stress. The $\cdot O_2^-$ and H_2O_2 reductions stimulated by H_2O_2 priming under salinity were 17 and 26%, respectively, when compared to single salt treatment.

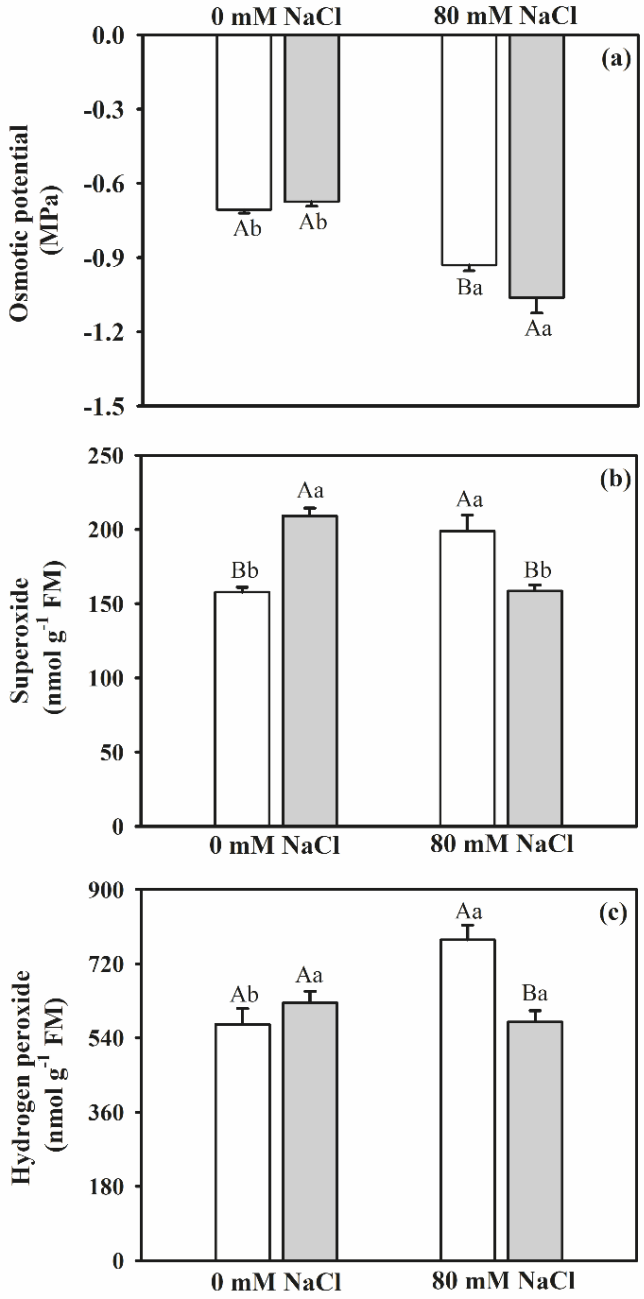

Figure 2. Osmotic potential and reactive oxygen species in the leaves of maize cv. BR 5011 water-pretreated (*white bars*) or H_2O_2-pretreated (*gray bars*) under non-salt conditions or salt stress conditions for twelve days. Osmotic potential (a), and contents of superoxide radical (b) and hydrogen peroxide (c). For each variable, the capital letters and lowercase letters compare the H_2O_2 pretreatments and salinity treatments, respectively, according to *F*-test ($p < 0.05$). Error bars represent ± standard error and means represent $n = 5$.

6.7.3 *PEPcase activity and chloroplast ultrastructure*

H_2O_2 priming reduced PEPcase activity in both the absence and presence of NaCl (Figure 3). In contrast, salt treatment remarkably enhanced the enzyme activity, with an increase of 123% in water-pretreated plants. However, H_2O_2 priming promoted a 52% reduction of

PEPcase activity under salinity. This decrease reached the value of PEPcase activity observed for water-pretreated plants without salinity. Also, the salinity caused damage in the mesophyll cells of maize leaves. In the absence of salinity, chloroplast ultrastructure exhibited a typical regular arrangement, characterized by well-stacked thylakoids and well-developed grana (Figure 4a, e). The application of H_2O_2 priming subtly reduced the thylakoid stacking under non-salt conditions (Figure 4b, f). Besides, salinity treatment promoted the unstacking and ripple in the thylakoid membranes (Figure 4c, g). In contrast, the chloroplast of H_2O_2-pretreated plants under salt stress seemed to be like those of the water-pretreated plants under non-salt conditions, since it showed no abnormalities in their ultrastructure, as well as well-stacked thylakoid membranes (Figure 4d, h).

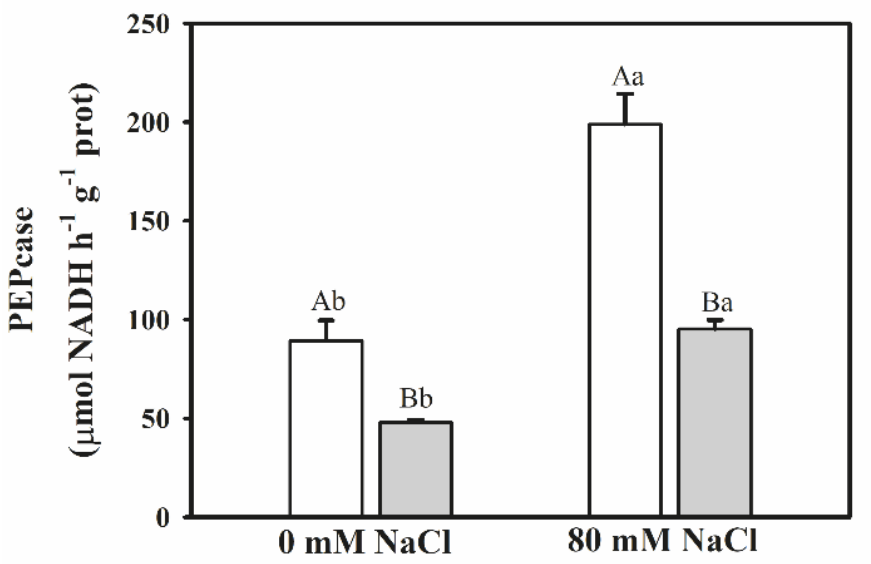

Figure 3. Phosphoenolpyruvate carboxylase (PEPcase) activity in the leaves of maize cv. BR 5011 water-pretreated (*white bars*) or H_2O_2-pretreated (*gray bars*) under non-salt conditions or salt stress conditions for twelve days. The capital letters and lowercase letters compare the H_2O_2 pretreatments and salinity treatments, respectively, according to *F*-test ($p < 0.05$). Error bars represent ± standard error and means represent $n = 5$.

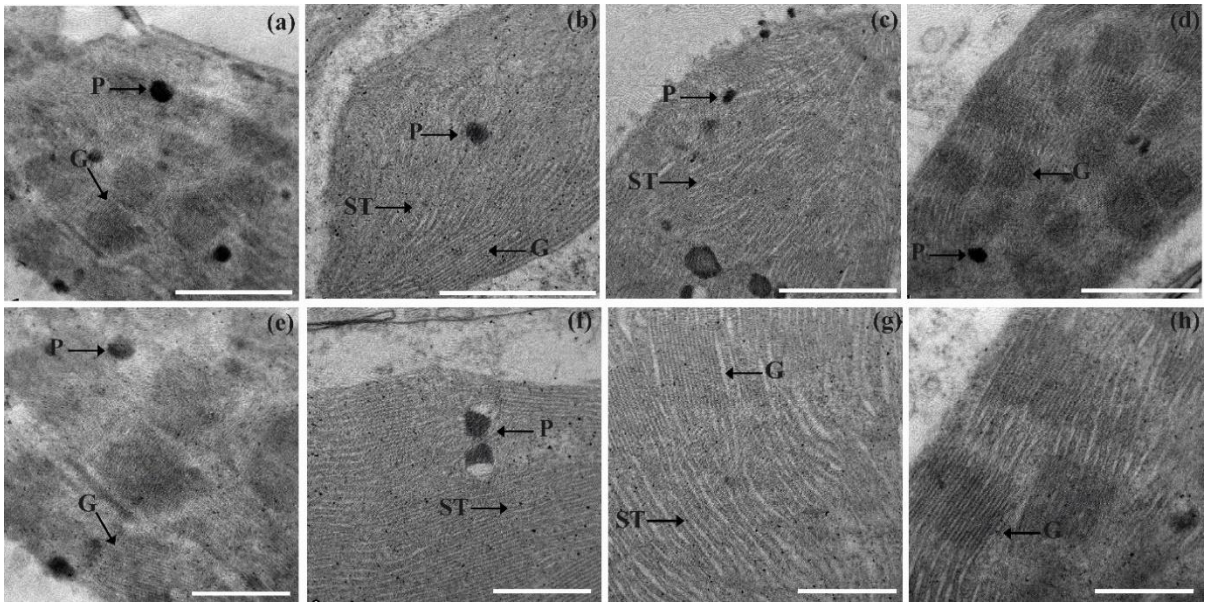

Figure 4. Chloroplast ultrastructure by transmission electron microscopy in the mesophyll cells of maize cv. BR 5011 water-pretreated (a, e) or H_2O_2-pretreated (b, f) under non-salt conditions and water-pretreated (c, g) or H_2O_2-pretreated (d, h) under salt stress conditions for twelve days. Bars: 1 µm (a-d) and bars: 0.5 µm (e-h). G – grana; P – plastoglobule; ST – stromal thylakoids.

6.3.4 *PCA of physiological and biochemical data*

According to PCA analysis gathering physiological and biochemical data, there was a clear separation between H_2O_2-pretreated and water-pretreated plants under both saline and non-saline conditions (Figure 5a). However, the most evident separation was between the groups water-pretreated (S), and H_2O_2-pretreated (HS) plants both under salt stress. Also, between these two groups and the other two rest groups, water-pretreated (C) and H_2O_2-pretreated (H) plants both under non-salt conditions. The PCA showed that the first two components accounted for 72.8% of the total variability. Loading plots showed the variation of each physiological and biochemical parameters (Figure 5b). The first component (PC1) was positively influenced by 8 of 17 parameters, and it was negatively affected by 9 of 17 parameters (Figure 5b). Meanwhile, the second component (PC2) was positively impacted by 10 of 17 parameters, and it was negatively affected by 7 of 17 parameters.

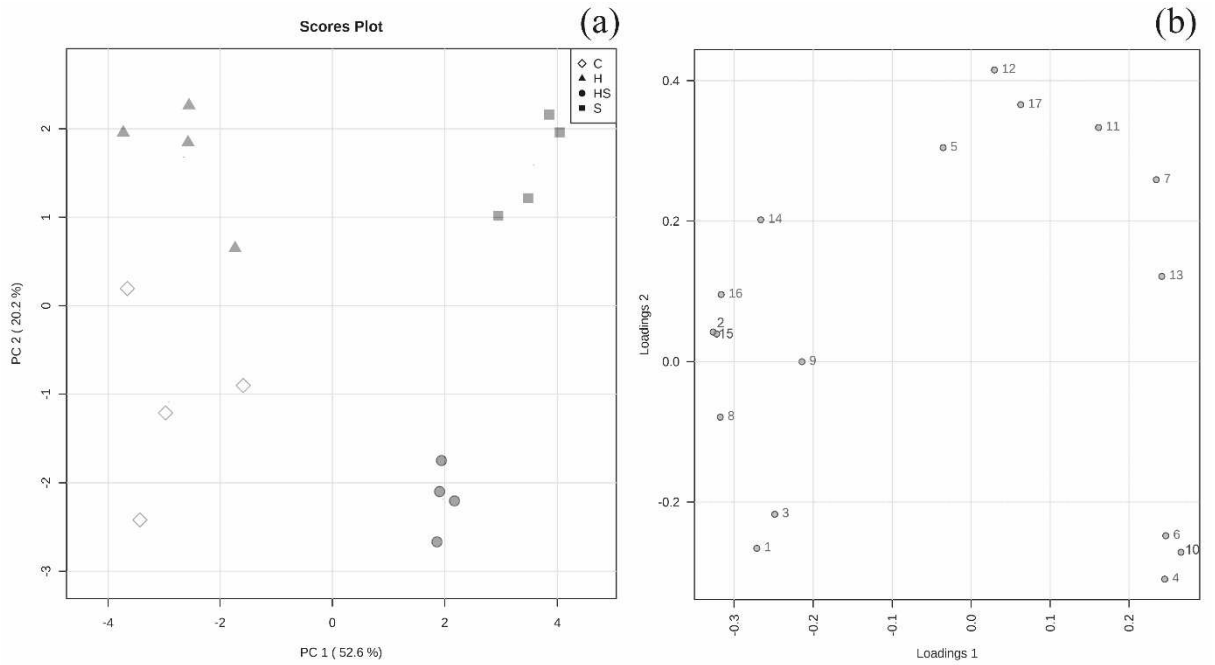

Figure 5. Principal component analysis (PCA) of physiological and biochemical parameters in maize cv. BR 5011 water-pretreated (C) or H_2O_2-pretreated (H) under non-salt conditions and water-pretreated (S) or H_2O_2-pretreated (HS) under salt stress conditions for twelve days. Scores plot (a) and loading plot (b) of the first and second components (PC 1 and PC 2) indicating the clustering of samples into four groups. Paraments list: 1 *A*, 2 g_s, 3 *E*, 4 *A*/*Ci*, 5 ΦPSII, 6 NPQ, 7 qP, 8 Fv'/Fm', 9 ETR, 10 Ψs, 11 H_2O_2, 12 $\cdot O_2^-$, 13 PEPcase, 14 Chl *a*, 15 Chl *b*, 16 Chl *total*, 17 Car.

6.3.5 *Metabolomic profiling*

Fifty-one compounds were identified in maize leaves (Tables 2 and 3). A heatmap also was built, showing the profile of each treatment normalized by the relative intensity values of the metabolites of water-pretreated plants under non-salt conditions, group C (Figure 6). Carbohydrates, organic acids, and amino acids were the major compound groups classified. Twenty sugars and derivatives were detected, including erythritol, arabitol, ribulose-5-phosphate, galactinol, and raffinose, among others. Fourteen organic acids, including pyruvic acid, succinic acid, citric acid, and glyceric acid, among others, comprised the second major group. Ten amino acids and derivates were identified, including valine, serine, proline, asparagine, and tyrosine, among others. Finally, five phenolic compounds (shikimic acid, quinic acid, cinnamic acid, caffeic acid, and caffeoylquinic acid), and two nitrogenous compounds (uracil and spermine) were detected. In relative intensity terms, sucrose was the most predominant metabolite identified, followed by maleic acid, malonic acid, valine, and xylose. While aconitic acid, spermine, maltitol, uracil, and fumaric acid were among the five less predominant identified metabolites (Table 2).

Table 2. Metabolites identified and retention time reached in leaves of maize plants cv. BR 5011 by GC-MS. For details of treatments and metabolites, see Table 3.

Metabolites	Retention time (min)	Metabolites	Retention time (min)
Pyruvic acid	5.15	Arabitol	16.86
Valine	5.92	Tyrosine	16.94
Uracil	7.17	Xylitol	17.36
Serine	8.34	Threitol	18.63
Proline	8.91	Butyric acid	19.43
Glycine	9.07	Ribose-5-phosphate	19.51
Succinic acid	9.13	Glucopyranoside	20.42
Glyceric acid	9.45	Glucose	20.64
Alanine	9.87	Ribulose-5-phosphate	20.80
Hexanoic acid	10.72	Glucoheptonic acid	21.14
Malonic acid	11.64	Spermine	21.74
Glutaric acid	11.73	Melezitose	22.22
Aspartic acid	12.05	Lactic acid	22.58
Pyroglutamic acid	12.10	Sucrose	23.49
Fumaric acid	12.63	Palatinose	24.97
Aconitic acid	13.53	Maltotriose	25.15
Itaconic acid	13.78	Maltitol	25.81
Asparagine	13.94	Galactinol	26.11
Erythritol	14.68	Trehalose	26.56
Maleic acid	14.81	Cinnamic acid	26.82
Shikimic acid	15.51	Caffeic acid, trans	26.94
Citric acid	15.69	Isomaltose	27.07
Dehydroascorbic acid	16.07	Caffeoylquinic acid	27.55
Quinic acid	16.22	Oxalic acid	29.77
Xylose	16.37	Raffinose	30.06
Lyxose	16.48		

Table 3. Relative intensity values of metabolites in leaves of maize plants cv. 5011 under no-salinity and no-pretreated (Control**),** H_2O_2-pretreated (H_2O_2), 80 mM NaCl and no-pretreated (80 mM NaCl**),** and H_2O_2-pretreated under salinity (H_2O_2 + NaCl) conditions for twelve days. Values represent the means of four repetitions ± standard error.

Metabolites	Relative intensity [a, b]			
	Control	H_2O_2	80 mM NaCl	H_2O_2 + NaCl
Sugars and derivates				
Erythritol	16.01 ± 0.72 Aa	14.94 ± 1.30 Aa	14.79 ± 1.18 Aa	9.50 ± 0.61 Bb
Xylose	30.12 ± 0.27 Aa	27.59 ± 0.71 Aa	28.50 ± 0.99 Aa	29.70 ± 1.14 Aa
Lyxose	20.60 ± 0.54 Aa	18.35 ± 0.88 Ab	19.80 ± 0.84 Aa	22.42 ± 1.39 Aa
Arabitol	3.75 ± 0.08 Aa	3.52 ± 0.13 Ab	3.75 ± 0.19 Ba	4.87 ± 0.37 Aa
Xylitol	1.45 ± 0.13 Aa	0.88 ± 0.10 Ba	1.46 ± 0.03 Aa	0.62 ± 0.04 Ba
Threitol	20.27 ± 1.47 Aa	17.23 ± 1.83 Aa	17.84 ±1.14 Aa	14.48 ± 1.34 Aa
Ribose-5-phosphate	1.02 ± 0.06 Aa	1.41 ± 0.23 Aa	1.36 ± 0.06 Aa	1.03 ± 0.14 Aa
Glucopyranoside	0.94 ± 0.10 Aa	1.13 ± 0.01 Aa	0.62 ± 0.05 Ab	0.69 ± 0.04 Ab
Glucose	6.12 ± 0.36 Ab	4.59 ± 0.24 Ab	15.48 ± 2.14 Ba	25.77 ± 4.75 Aa
Ribulose-5-phosphate	0.34 ± 0.05 Ab	0.33 ± 0.03 Ab	0.61 ± 0.02 Aa	0.55 ± 0.06 Aa
Glucoheptonic acid	2.99 ± 0.33 Aa	2.82 ± 0.22 Aa	1.69 ± 0.23 Ab	1.28 ± 0.08 Ab
Melezitose	4.47 ± 0.79 Ba	10.23 ± 1.53 Aa	6.51 ± 1.14 Aa	5.48 ± 0.39 Ab
Sucrose	178.2 ± 10.6 Aa	200.7 ± 4.9 Aa	200.5 ± 16.7 Aa	152.2 ± 10.7 Bb
Palatinose	15.75 ± 2.43 Aa	16.63 ± 0.73 Aa	21.95 ± 1.64 Aa	16.39 ± 1.99 Aa

Maltotriose	1.06 ± 0.17 Aa	0.75 ± 0.07 Aa	1.41 ± 0.19 Aa	0.85 ± 0.14 Ba
Maltitol	0.18 ± 0.03 Ab	0.46 ± 0.09 Aa	0.73 ± 0.17 Aa	0.68 ± 0.04 Aa
Galactinol	1.23 ± 0.13 Ab	2.06 ± 0.16 Aa	3.93 ± 0.70 Aa	2.82 ± 0.36 Aa
Trehalose	1.32 ± 0.18 Ab	1.17 ± 0.10 Aa	2.43 ± 0.24 Aa	1.25 ± 0.09 Ba
Isomaltose	9.14 ± 0.50 Bb	21.61 ± 1.37 Aa	21.39 ± 2.43 Aa	15.38 ± 0.64 Bb
Raffinose	1.53 ± 0.19 Ab	3.47 ± 0.43 Ab	19.26 ± 1.61 Aa	8.13 ± 1.39 Ba
Organic acids				
Pyruvic acid	5.67 ± 0.33 Aa	5.38 ± 0.42 Aa	6.10 ± 0.49 Aa	2.64 ± 0.30 Bb
Succinic acid	2.85 ± 0.38 Ba	4.61 ± 0.68 Aa	3.94 ± 0.41 Aa	4.11 ± 0.47 Aa
Glyceric acid	3.93 ± 0.37 Aa	3.22 ± 0.30 Aa	1.60 ± 0.13 Ab	0.92 ± 0.03 Ab
Hexanoic acid	4.88 ± 0.44 Aa	3.37 ± 0.77 Aa	5.76 ± 0.89 Aa	2.48 ± 0.10 Ba
Malonic acid	47.36 ± 3.75 Aa	54.47±9.44 Aa	28.59 ± 1.21 Ab	23.74 ± 0.92 Ab
Fumaric acid	0.17 ± 0.02 Aa	0.14 ± 0.02 Aa	0.13 ± 0.02 Aa	0.15 ± 0.01 Aa
Aconitic acid	0.42 ± 0.01 Aa	0.50 ± 0.07 Aa	0.17 ± 0.00 Ab	0.14 ± 0.01 Ab
Itaconic acid	1.47 ± 0.11 Aa	1.86 ± 0.26 Ab	1.42 ± 0.30 Ba	2.48 ± 0.05 Aa
Maleic acid	122.5 ± 3.0 Aa	108.7 ± 11.9Aa	51.9 ± 6.0 Ab	37.4 ± 2.1 Ab
Citric acid	3.88 ± 0.23 Aa	4.8 ± 0.86 Aa	2.57 ± 0.37 Aa	2.65 ± 0.33 Ab
Dehydroascorbic acid	2.58 ± 0.37 Ba	3.80 ± 0.15 Aa	2.61 ± 0.30 Aa	1.84 ± 0.22 Ab
Butyric acid	4.45 ± 0.56 Aa	5.36 ± 0.86 Aa	5.60 ± 0.75 Aa	5.18 ±0 .44 Aa
Lactic acid	3.38 ± 0.52 Ba	7.74 ± 0.91 Aa	4.93 ± 0.66 Aa	3.30 ± 0.25 Ab
Oxalic acid	2.71 ± 0.29 Aa	2.51 ± 0.40 Aa	2.88 ± 0.47 Aa	1.44 ± 0.05 Ba
Amino acids and derivates				
Valine	39.95 ± 2.11 Aa	38.42 ± 5.80 Aa	43.42 ± 3.22 Aa	30.08 ± 0.90 Ba
Serine	3.50 ± 0.20 Ab	2.47 ± 0.27 Aa	4.77 ± 0.44 Aa	2.95 ± 0.43 Ba
Proline	1.76 ± 0.15 Aa	1.38 ± 0.22 Aa	1.98 ± 0.29 Aa	1.21 ± 0.12 Ba
Glycine	13.98 ± 2.26 Aa	19.13 ± 3.12 Aa	6.26 ± 0.72 Ab	8.54 ± 0.95 Ab
Alanine	4.79 ± 0.49 Aa	4.78 ± 0.74 Aa	4.54 ± 0.55 Aa	2.62 ± 0.26 Ba
Aspartic acid	4.17 ± 0.72 Aa	5.06 ± 0.90 Aa	2.90 ± 0.42 Ba	5.23 ± 0.62 Aa
Pyroglutamic acid	26.29 ± 1.21 Aa	26.79 ± 1.62 Aa	18.69 ± 1.80 Ab	12.66 ± 0.81 Bb
Glutaric acid	14.36 ± 1.99 Aa	7.35 ± 1.48 Ba	7.58 ± 0.59 Ab	7.06 ± 0.79 Aa
Asparagine	0.99 ± 0.10 Bb	5.27 ± 0.68 Ab	6.53 ± 0.82 Ba	9.39 ± 0.92 Aa
Tyrosine	2.92 ± 0.22 Aa	2.88 ± 0.26 Aa	1.25 ± 0.05 Bb	2.78 ± 0.40 Aa
Phenolic compounds				
Shikimic acid	3.99 ± 0.19 Aa	5.38 ± 0.88 Aa	1.34 ± 0.08 Ab	1.50 ± 0.14 Ab
Quinic acid	11.80 ± 0.50 Ba	20.26 ± 1.92 Aa	4.77 ± 0.34 Ab	3.00 ± 0.04 Ab
Cinnamic acid	5.46 ± 0.59 Ab	6.35 ± 1.10 Ab	11.94 ± 1.16 Aa	13.61 ± 1.66 Aa
Caffeic acid	12.22 ± 1.61 Aa	9.57 ± 0.89 Ab	16.86 ± 1.13 Aa	17.34 ± 3.10 Aa
Caffeoylquinic acid	4.72 ± 0.46 Aa	9.08 ± 2.42 Aa	5.19 ± 0.86 Aa	1.30 ± 0.29 Ab
Nitrogenous compounds				
Uracil	0.17 ± 0.01 Aa	0.09 ± 0.01 Ba	0.13 ± 0.02 Ab	0.09 ± 0.01 Ba
Spermine	0.27 ± 0.02 Ab	0.32 ± 0.02 Aa	0.41 ± 0.01 Aa	0.31 ± 0.04 Ba

[a] The capital letters and lowercase letters compare the H_2O_2 pre-treatments and salinity treatments, respectively, according to *F*-test ($p < 0.05$).
[b] Ratio of metabolite peak area to ribitol peak area

In the absence of NaCl, H_2O_2 priming promoted a significant increase of six metabolites (maltitol, isomaltose, raffinose, lactic acid, asparagine, and quinic acid) and reduction three metabolites (xylitol, glutaric acid, and uracil) (Figure 6; Table 2). Also, the salinity increased the relative intensity values of eight metabolites (glucose, ribulose-5-phosphate, maltitol, galactinol, trehalose, raffinose, asparagine, and cinnamic acid), but it reduced other eleven

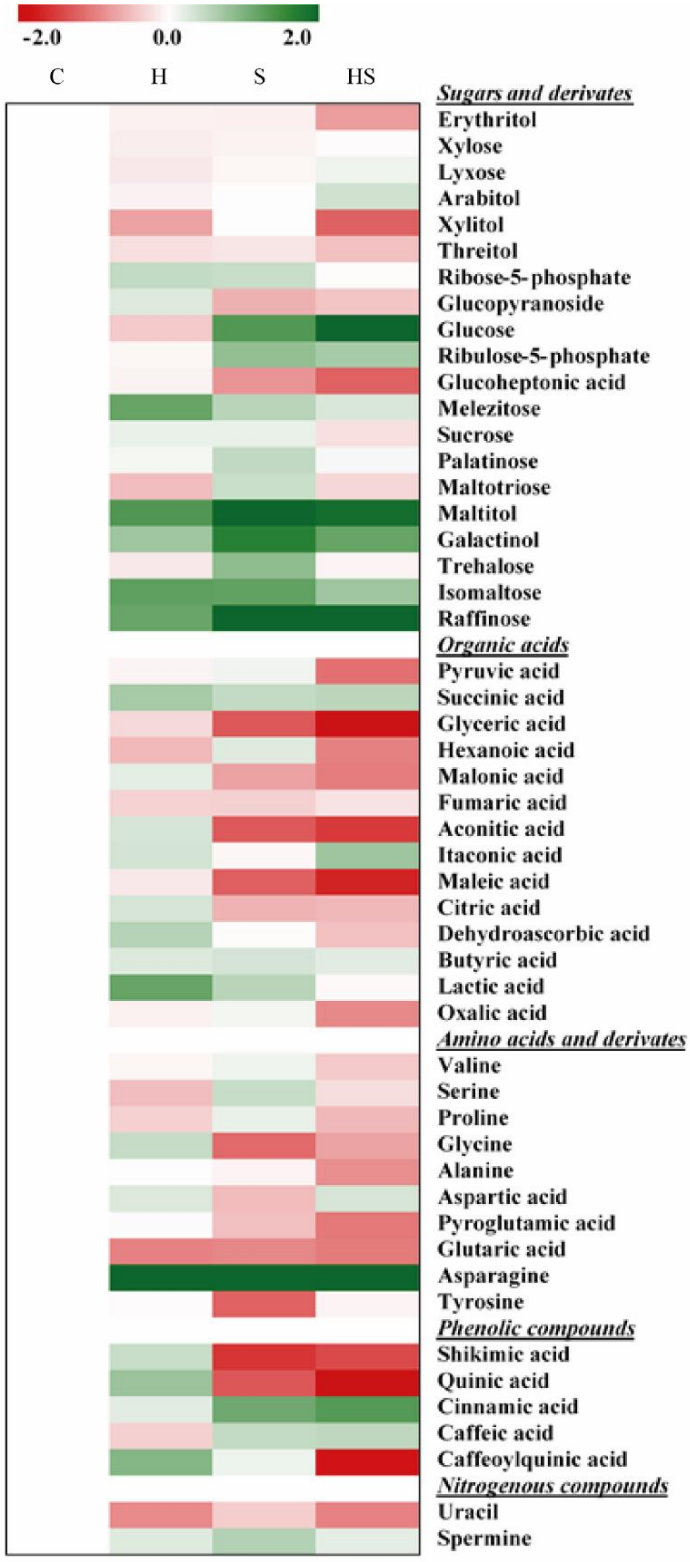

Figure 6. Heat map of normalized values of metabolites in leaves of maize cv. BR 5011 water-pretreated (C) or H_2O_2-pretreated (H) under non-salt conditions and water-pretreated (S) or H_2O_2-pretreated (HS) under salt stress conditions for twelve days. The Heat map shows a high (green scale) or low (red scale) relative amount of each metabolite in comparison to control plants (uncolored scale). Each square represents the mean of four biological replicates, and the statistical difference was obtained according to *F*-test ($p < 0.05$). For more details, see Table 2.

metabolites (glucopyranoside, glucoheptonic acid, glyceric acid, malonic acid, aconitic acid, maleic acid, glycine, pyroglutamic acid, tyrosine, shikimic acid, and quinic acid) (Figure 6; Table 2). Moreover, H_2O_2 priming altered the metabolic profile of maize leaves under salinity, increasing the relative intensity values of four metabolites (arabitol, glucose, asparagine, and tyrosine) when compared to water-pretreated plants under salinity (Figure 6; Table 2). Conversely, H_2O_2 priming reduced other eleven metabolites, including sugars and derivates (erythritol, xylitol, trehalose, and raffinose), organic acids (pyruvic acid, glyceric acid, hexanoic acid, and oxalic acid), amino acid derivative (pyroglutamic acid), and phenolic compounds (quinic acid and caffeoylquinic acid).

The PLS-DA showed that the first two components accounted for 65.8% of the total variability in maize leaves (Figure 7a). Loading plots generated show the variation of individual metabolites in the experiment validates the PLS-DA (Figure 7b). Besides, a cross-validation and permutation test ($p < 0.05$) allowed us to use PLS-DA instead of PCA analysis (Figure 7c), which is more efficient to discriminate against the groups. It indicated a distinct separation of the four groups based only on the metabolic profiling of the treatments (Figure 7a). Although the metabolite profile of water-pretreated and H_2O_2-pretreated plants without salinity showed proximity, they presented very distant of metabolite profile under salt stress, as shown by two-dimensional PLS-DA scores plot graph (Figure 7a). Also, the loading plot graph showed metabolites responsible for the separation between groups observed in PLS-DA (Figure 7b). The most positive contributing metabolites for the first component were raffinose, asparagine, glucose, maltitol cinnamic acid, and galactinol. In contrast, the most positive contributing metabolites for the second component were caffeoylquinic acid, lactic acid, pyruvic acid, and quinic acid (Figure 7b). Besides, the variable importance in projection (VIP) *scores* graph displayed the most important metabolites for differentiating the treatments by the abundance of metabolites in each treatment (Fig. 8). VIP plot showed eleven metabolites of more than 1.3 VIP scores, in ascending order of VIP score they are: cinnamic acid, galactinol, maleic acid, aconitic acid, glyceric acid, glucose, shikimic acid, maltitol, quinic acid, asparagine, and raffinose. (Figure 8). Besides, among the 68 analyzed parameters, there are 71 positive correlations and 45 negative correlations with the Pearson coefficient greater than 0.8 (Data not shown).

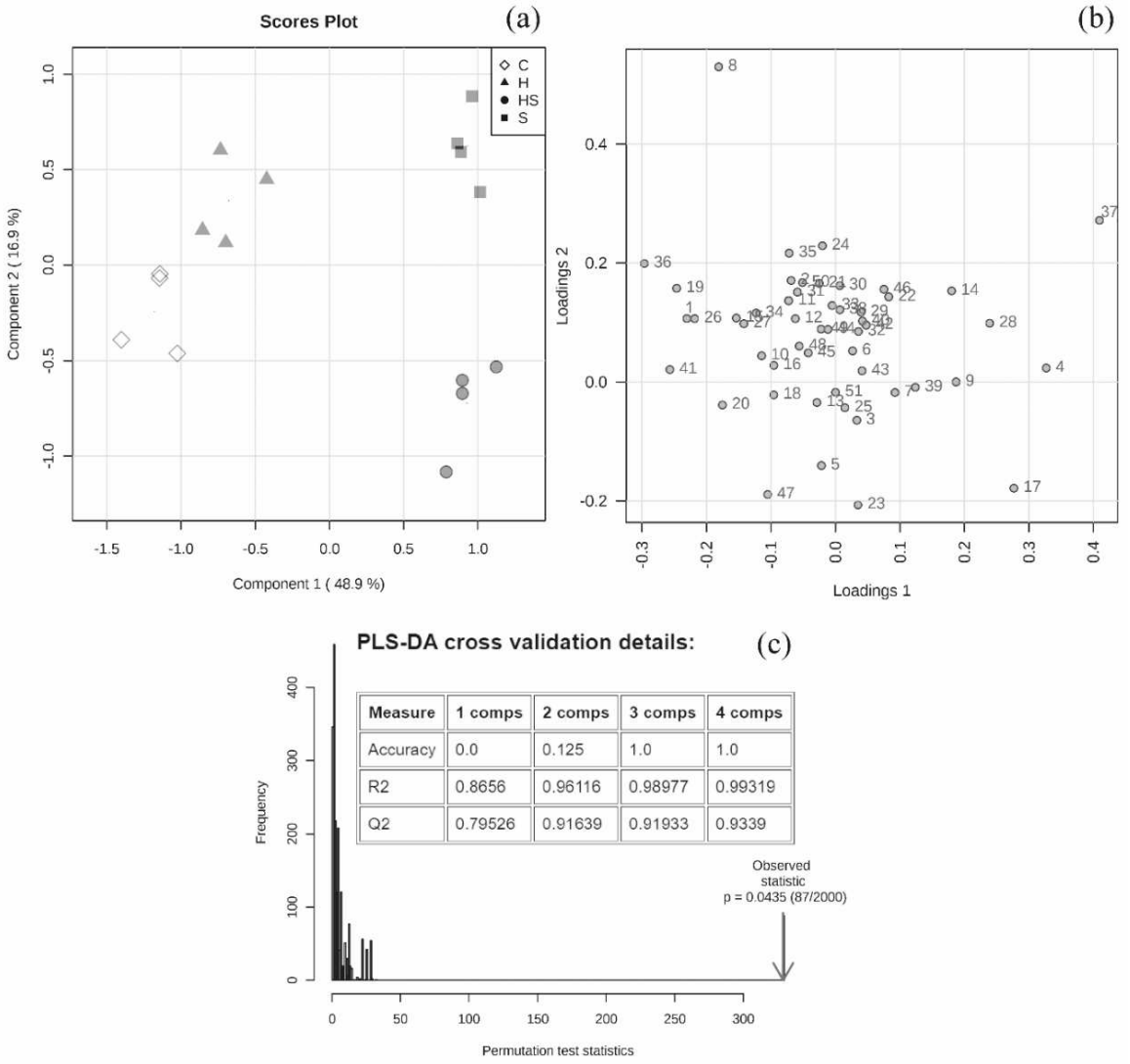

Figure. 7. Partial least squares - discriminant analysis (PLS-DA) of metabolic profiles in leaves of maize cv. BR 5011 water-pretreated (C) or H_2O_2-pretreated (H) under non-salt conditions and water-pretreated (S) or H_2O_2-pretreated (HS) under salt stress conditions for twelve days. Scores plot (a), loading plot (b), and PLS-DA cross-validation and permutation test (c) of the first and second components indicating the clustering of samples into four groups. Metabolites list: 1 Aconitic acid, 2 Alanine, 3 Arabitol, 4 Asparagine, 5 Aspartic acid, 6 Butyric acid, 7 Caffeic acid, 8 Caffeoylquinic acid, 9 Cinnamic acid, 10 Citric acid, 11 Dehydroascorbic acid, 12 Erythritol, 13 Fumaric acid, 14 Galactinol, 15 Glucoheptonic acid, 16 Glucopyranoside, 17 Glucose, 18 Glutaric acid, 19 Glyceric acid, 20 Glycine, 21 Hexanoic acid, 22 Isomaltose, 23 Itaconic acid, 24 Lactic acid, 25 Lyxose, 26 Maleic acid, 27 Malonic acid, 28 Maltitol, 29 Maltotriose, 30 Melezitose, 31 Oxalic acid, 32 Palatinose, 33 Proline, 34 Pyroglutamic acid, 35 Pyruvic acid, 36 Quinic acid, 37 Raffinose, 38 Ribose-5-phosphate, 39 Ribulose-5-phosphate, 40 Serine, 41 Shikimic acid, 42 Spermine, 43 Succinic acid, 44 Sucrose, 45 Threitol, 46 Trehalose, 47 Tyrosine, 48 Uracil, 49 Valine, 50 Xylitol, 51 Xylose.

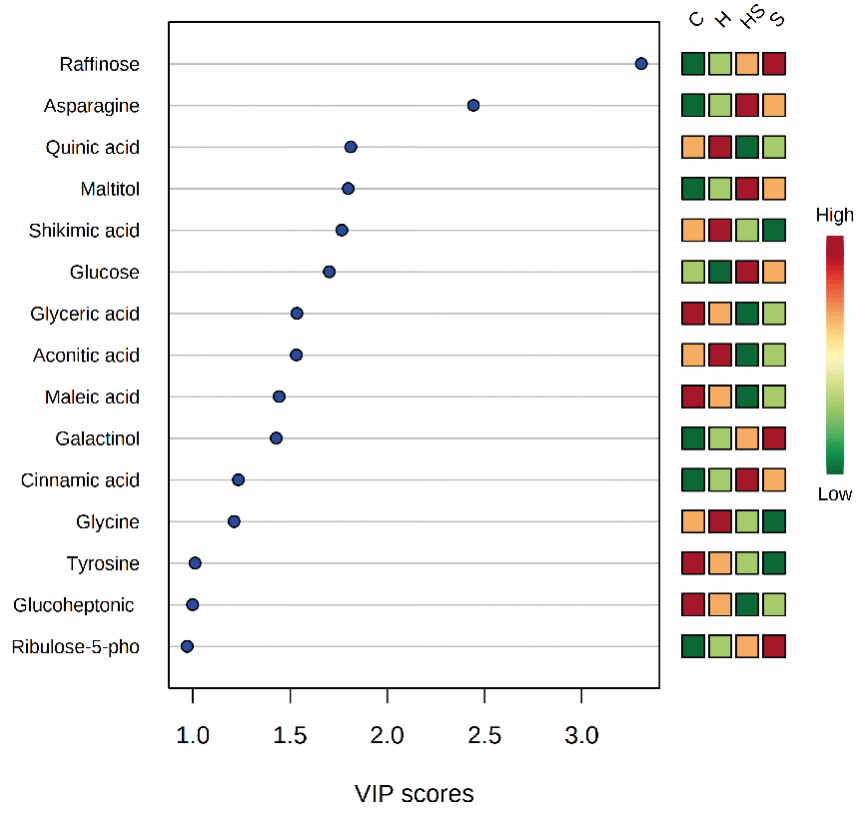

Figure 8. VIP scores plot of metabolites in leaves of maize cv. BR 5011 water-pretreated (C) or H_2O_2-pretreated (H) under non-salt conditions and water-pretreated (S) or H_2O_2-pretreated (HS) under salt stress conditions for twelve days. The selected metabolites were those with a VIP score of greater than 1.0. Red or green squares on the right indicate the high and low abundance of the corresponding metabolite in each treatment, respectively. VIP score was based on the first component of the PLS-DA model.

6.4 Discussion

6.4.1 *H_2O_2 priming protects chloroplast ultrastructure and enhances photosynthetic machinery efficiency of maize leaves under salt stress*

CO_2 assimilation is crucial for plant growth and development. It requires a photosynthetic apparatus that is particularly prepared to adjust to changes in environmental conditions. Therefore, simultaneous investigations of photosynthesis-related parameters from stomata to chloroplast allow a better understanding of salt effects and the priming action to minimize the damage involving environmental, biochemical, and morphological modulations (KALAJI *et al*., 2016). Salt-stressed plants decrease their carbon assimilation capacity by displaying a reduction in gas exchange parameters and severe loss of photosynthetic pigments (MIRANDA *et al*., 2014; SOZHARAJAN *et al*., 2016). Our experimental results showed that salinity significantly reduced the gas exchange parameters, but there was an increase in *A/Ci*

(Figure 1). Despite the losses of carbon assimilation, the maize plant improves its carboxylation efficiency taking better advantage of the low concentration of CO_2 caused by stomatal closure by increasing the activity of PEPcase (Figure 3). Besides, the salinity reduced Fv/Fm and an increase in NPQ and qP, indicating that the amount of energy absorbed not adequately transferred to reaction centers (Table 1). Indeed, the increase in NPQ was associated with heat dissipation in sunflower varieties sensitive to salinity even though it may not be sufficient to avoid damages (ARAÚJO *et al*., 2018).

The C4 plants use PEPcase in the CO_2 assimilation, improving photosynthetic performance, especially in a warm climate with high irradiance and low water availability, which can be significant benefits under other stress conditions too (SAGE, 2004; DOUBNEROVÁ; RYŠLAVÁ, 2011). Also, the PEPcase has a non-photosynthetic role of replenishes intermediates of the citric acid cycle to nitrogen assimilation and multiple biosynthetic pathways (SHI *et al*., 2015; WASSEM, AHMAD, 2019). In this way, an increased PEPcase activity in response to abiotic stresses by an anaplerotic flow is expected (HÝSKOVÁ *et al*., 2014). It acts on defense and repair processes, such as biocompatible osmolytes biosynthesis and ROS detoxification (WANG *et al*., 2016). Remarkably, maize plants invested in high PEPcase activity (Figure 3), which reflected in the accumulation of sugars such as glucose, maltitol, raffinose, among others, in addition to the notable increase in asparagine (Figure 6; Table 2). In contrast, the decrease of PEPcase activity in H_2O_2 pretreated plants under salinity led to levels close to those of control plants (Figure 3). The H_2O_2 priming reduced the need for high PEPcase activity by re-calibrating PEPcase functions, allowing greater CO_2 assimilation and preserving high concentrations of ribulose-5-phosphate and glucose observed in maize leaves under salinity (Figures. 1, 6; Table 2).

The H_2O_2 priming improved Fv/Fm, as well as contributed to most of the excitation energy was dissipated in the form of NPQ without harming qP (Table 1). These effects of H_2O_2 priming can contribute to the normalization of A and E even under low g_s observed under salt stress, taking as reference water-pretreated plants under non-salt conditions (Figure 1). Besides, the higher dissipation in the form of NPQ can contribute to less generation of ROS, mainly singlet oxygen (MÜLLER; NIYOGI, 2001). Admittedly, the reduction of $^{\bullet}O_2^-$ and H_2O_2 in the leaves of H_2O_2-pretreated under salt conditions were notable (Figure 2a). Thus, H_2O_2 priming improved the light energy conversion efficiency of PSII and carboxylation efficiency as well as minimized excess energy in PSII, which results in the improved photosynthetic performance

of maize plants under salt stress (Figure 1d, Table 1). Similar results were observed in mustard (*Brassica juncea* L.) seedlings, where the application of low concentrations of H_2O_2 increased photosynthesis due to an increase in Rubisco activity and PSII efficiency under abiotic stress (KHAN *et al*., 2015).

Furthermore, the *Panax ginseng* and *Brassica napus* seedlings treated with exogenous H_2O_2 showed enhanced salinity tolerance due to decreasing of endogenous ROS contents, including both H_2O_2 and $^{\bullet}O_2^-$ (SATHIYARAJ *et al*., 2014; HASANUZZAMAN *et al*., 2017). Besides, salinity cause damages in the whole chloroplast ultrastructure, which is a reliable stress marker for plants during abiotic stress states (ZECHMANN, 2019). Here, the structural changes were particularly prominent in thylakoids, that exhibited membrane undulations and granal unstacking (Figure 4c, g). However, the exogenous H_2O_2 attenuated the effects of salt stress in maize chloroplast ultrastructure by reducing the oxidative stress generated by salinity by reducing of H_2O_2 and $^{\bullet}O_2^-$, so that practically no damage was observed in its ultrastructure (Figures. 2b, c and 4d, h). Thus, our results reinforce the biochemical benefit of exogenous H_2O_2 in maize plants under salinity to alleviate salt-induced oxidative stress and protect the chloroplast structure against severe damage [SHEN *et al*., 2019]. In this study, H_2O_2 priming, in addition to regulating the ROS scavenging under salt stress, also induced metabolites of different metabolic and regulatory pathways like glucose, organic acids, amino acids, and polyphenols biosynthesis (Figure 6, Table 2).

6.4.2 *Metabolomic profiling of H_2O_2-primed maize leaves reveals metabolites related to relief harmful effects of salt-stress*

The metabolomic approach used in this study allowed us to identify leaf metabolites modulated by maize plants in response to both H_2O_2 priming and salinity. Here, 42 metabolites among a total of 51 remained unchanged in H_2O_2-pretreated plants under non-salt conditions (Table 2), which was supported by a very similar physiological response profile influenced particularly by A, E, g_s, and photosynthetic pigments (Figure 5). Recently, sprayed leaves with active priming compounds, such as jasmonates, salicylic acid, and methionine, were related to defense responses by the modulation of primary and secondary metabolite profiles to reduced plant water loss (BATISTA *et al*., 2019; HASSINI *et al*., 2019). Although exogenous H_2O_2 slightly modified the metabolic profile of maize in the absence of salt, the accumulation of a few metabolites was noticeable (Table 2). Among them, the accumulation of quinic acid, a

phenolic compound, biosynthesized by the shikimate pathway, in part, may contribute to adjusting H_2O_2 levels (Figuress. 2c, 6). In fact, several priming compounds were all found to trigger the accumulation of quinic acids in tobacco cells (MHLONGO *et al*., 2016), and it plays a role as an antioxidant agent acting in plant defense mechanisms and ROS scavenge (ISAH, 2019). Conversely, the presence of NaCl promoted considerable changes in the leaf metabolic profile of maize as increased in cinnamic acid previously reported in Thymus species in response to salinity (BISTGANI *et al*., 2019). However, the presence of salt negatively affected the accumulation of other endogenous phenolic compounds, as shikimic acid and quinic acid, which contribute reduce the antioxidant potential of plants increasing to the harmful effects observed (SHARMA *et al*., 2019). Although, the beneficial of leaves pretreated with H_2O_2 under salinity could not link to these phenolic compounds identified here (Table 2).

In plants, carbohydrate metabolism is involved in crucial processes in response to abiotic stresses as well, playing a critical role in carbon storage, osmotic homeostasis, osmoprotectant, and free radicals elimination (GANGOLA; RAMADOSS, 2018]. Our results showed that salinity increased six sugars and polyols (Figure 6; Table 2). The hydroxyl groups of polyols can be replaced by water molecules and maintain hydrophilic interactions in plant cells, which are crucial for stabilizing macromolecules and membrane structure (GANGOLA; RAMADOSS, 2018]. Indeed, carbohydrate stores are quickly mobilized, releasing soluble sugars that act as compatible solutes under stress (BORRELI *et al*., 2018). Which, in part, supports the high levels of trehalose and raffinose under saline conditions. Such mechanism seems to be elicited in H_2O_2-pretreated plants under salt stress since the reduction of Ψs was accompanied by an increase in glucose and a significant decrease in these two polyols (Figure 6; Table 2). Concurrently, the reduction of raffinose in the leaves can also be related to carbon export (SENGUPTA *et al*., 2015). Furthermore, H_2O_2 priming also increased arabitol content, as well as in salt-tolerant soy plants (JIAO *et al*., 2018), and the gluconeogenesis process may be intensified by H_2O_2 priming since glucose values increased, and pyruvate values decreased (Figure 6; Table 2) contributing to the mitigation of osmotic stress, which is a common phenomenon to promote tolerance to salt stress (GUO *et al*., 2017; POÓR *et al*., 2019). Another highlight is the increase of ribulose-5-phosphate under salinity conditions independently H_2O_2 priming (Figure 6). It is a precursor on the ribulose-1,5-bisphosphate regeneration pathway, which does not necessarily indicate an inhibition of the carboxylation reaction as pointed out in C3 plants (HOSSAIN *et al*., 2017). Once that H_2O_2-pretreated plants under salt stress showed

recovery of *A* and high *A/Ci* in addition to normalization of PEPcase activity (Figures. 1a, d; 3).

Overall, the results here showed a decrease in some organic acids under salinity and H_2O_2 priming, particularly for some Krebs cycle intermediates and their precursors (aconitic acid and maleic acid), as well as glyceric acid, a metabolite involved in the glycolysis pathway. Such depletion is a remarkable metabolic characteristic observed in other plant species under salinity (SANCHEZ *et al*. 2007; RICHTER *et al*., 2015). Besides, increased levels of the amino acid may be attributed to the induction of secondary metabolisms with increased levels of aromatic amino acids, such as tyrosine (Zhang *et al*., 2011). In this hand, an increase of asparagine is related to their role in transporting and storing nitrogen, as well as acts as a regulatory and signaling molecule of stress tolerance in plants (GAUFICHON *et al*., 2010). Also, the increases in asparagine in sunflower leaves (*Helianthus annuus* L.) were related to mitigating the excess energy promoted by salinity (ARAÚJO *et al*., 2018).

Thus, plants under salt stress treatment only, and H_2O_2 pretreated plants under salinity presented differences in the modulation of sugars, as well as distinct adaptation mechanisms, displaying the complexity of carbohydrates in salinity tolerance. However, H_2O_2 priming provides a crucial role in minimizing the harmful effects of salt, because pretreated plants showed higher photosynthetic rates, maintenance of chloroplast ultrastructure, and reduced ROS even under salinity (Figures 1 to 4).

6.5 Conclusion

Our study revealed some mechanisms alleviate harmful by salt stress by H_2O_2 priming. Also, it shows the four best salt stress biomarkers in maize leaves positively elicited by H_2O_2: raffinose, asparagine, quinic acid, and maltitol. The H_2O_2 priming was beneficial mainly by (i) inducing more efficient mechanisms to avoid salinity-induced energy excess, that could be attributed to maintaining high levels of photosynthetic pigments, elevated parameters of photochemical efficiency (Fv/Fm and NPQ), and regular PEPcase activity recovered; (ii) preserving the chloroplast ultrastructure by decrease both endogenous H_2O_2 and $^{\bullet}O_2^-$ contents; and (iii) regulate metabolites to the reestablishment of osmotic homeostasis and the scavenging of ROS.

Acknowledgments

This work was supported by the Conselho Nacional de Desenvolvimento Científico e Tecnológico (CNPq), the Coodenação de Aperfeiçoamento de Pessoal de Nível Superior (CAPES), the Fundação Cearense de Apoio ao Desenvolvimento Científico e Tecnológico (FUNCAP) and Central Analítica-UFC/CT-INFRA/MCTI-SISANO/Pró-Equipamentos CAPES.

7 H_2O_2 priming induces proteomic responses to defense against salt stress in maize

(Artigo publicado no periódico *Plant Molecular Biology*)

Gyedre dos Santos Araújo[1], Lineker de Sousa Lopes[1], Stelamaris de Oliveira Paula-Marinho[1], Rosilene Oliveira Mesquita[2], Celso Shiniti Nagano[3], Fábio Roger Vasconcelos[4], Humberto Henrique de Carvalho[1], Arlindo de Alencar Araripe Noronha Moura[5], Elton Camelo Marques[1], Enéas Gomes-Filho[1,*]

[1] Department of Biochemistry and Molecular Biology, Federal University of Ceará, Fortaleza, CE, Brazil

[2] Department of Phytotechnis, Federal University of Ceará, Fortaleza, CE, Brazil

[3] Department of Fishing Engineering, Federal University of Ceará, Fortaleza, CE, Brazil

[4] Federal Institute of Education, Science and Technology of Ceará (IFCE), Boa Viagem, CE, Brazil

[5] Department of Zootechnics, Federal University of Ceará, Fortaleza, CE, Brazil

Key message

H_2O_2 priming reprograms essential proteins expression to help plants survive, promoting responsive and unresponsive proteins adjustment to salt stress.

Abstract

Priming is a powerful strategy to enhance abiotic stress tolerance in plants. Despite this, there is scarce information about the mechanisms induced by H_2O_2 priming for salt stress tolerance,

particularly on proteome modulation. Improving maize cultivation in areas subject to salinity is imperative for the local economy and food security. Thereby, this study aimed to investigate physiological changes linked with post-translational protein events induced by foliar H_2O_2 priming of *Zea mays* plants under salt stress. As expected, only salt treatment promoted a considerable accumulation of Na^+ ion. It drastically affected growth parameters and relative water content, as well as promoted adverse alteration in the proteome profile, when compared to the absence of salt conditions. Conversely, H_2O_2 priming was beneficial via specific proteome reprogramming, which prepared the maize plants to respond more effectively to salt stress. The identified proteins were associated with photosynthesis and redox homeostasis, critical metabolic pathways for helping plants survive in saline stress by the protection of chloroplasts organization and carbon fixation, as well as state redox. This research provides new proteomic data to improve understanding and forward identifying biotechnological strategies to promote salt stress tolerance.

Keywords: Acclimation, hydrogen peroxide, Na^+ ion toxic, protein modulation, salt tolerance, *Zea mays*.

7.1 Introduction

Plants are exposed to a diversity of environmental pressures, such as abiotic stresses that unfavorably affect the growth and developmental stages of economically important crops (AHMED *et al*., 2020). Among them, salt excess represents one of the significant abiotic stresses that impact agriculture, and consequently, it is a limiting factor that threatens crop productivity worldwide (ISAYENKOV; MAATHUIS, 2019). Salinity disturbs both osmotic and ionic balance in plants. On this hand, osmotic stress can cause cellular turgor limitation and even cell membrane disorder, while ionic stress disrupts plants' mineral relations. Together, these damages lead to water uptake reduction, cell elongation inhibition, enzyme functionality disruption, inhibition of photosynthesis, and, consequently, premature senescence (SHELKE *et al*. 2017).

Acclimation to salt stress or any adverse conditions became essential for survival, growth, and reproduction. In acclimation occurs changes in plants by internal adjustments within tissues and cells, enabling cell metabolism to proceed even under these undesired

conditions (LOPES *et al*., 2020; OLIVEIRA *et al*., 2020). It has been widely recognized that the prior application of some compounds or elicitors triggers the activation of defense response, a technique called priming (GONZÁLEZ-BOSCH, 2018; LOPES *et al*., 2018). The process of priming is a tool used to reach salt stress acclimation. It involves prior exposure of seeds, leaves, or roots to an eliciting factor, inducing the accumulation of signaling proteins or transcription factors in an inactive form, improving plant tolerance in front of future stress exposure (GONDIM *et al*. 2013; SAVVIDES *et al*. 2016). Thereby, H_2O_2 acts as an acclimation inducer to environmental stresses by modulating various physiological and biochemical processes. It leads to higher antioxidant enzyme activities, protection of cellular organelles, and satisfactory photosynthetic efficiency of plants, among others (HOSSAIN *et al*., 2015; HOU *et al*., 2018; BAGHERI *et al*., 2019).

The proteome is the entire set of proteins produced by a living organism, including information on their abundances, variations, and modifications. In this field, proteomics rises as one of the main tools of "omics" to identify some of those proteins. It has been used in several species to understand the cellular activities changes at the protein function level (BUDAK *et al*., 2013; FRUKH *et al*., 2019). Thus, the proteomic strategy has provided successfully insights about salt stress responses in a wide range of crops (OLIVEIRA *et al*., 2020; SUN *et al*., 2017) as well as potential solutions once different priming compounds applied in plants upon stressful conditions induce remarkable changes of proteome profiles. Therefore, it can be valuable to distinguish essential proteins and establish signaling pathways involved in mitigating the effects of stress (LONG *et al*., 2018; BERTINI *et al*., 2019).

Although the salinity problem be well studied and the agronomic and ecological importance of priming be evident, improving biochemical and physiological plant traits, little is known about the molecular mechanisms of H_2O_2 priming under salinity in maize (*Zea mays* L.) at the protein profile level. This crop not only constitutes the major cereal for both humans and animals but has also become a critical resource for industrial use and bio-energy production in the world (FAO 2008; MOURTZINIS *et al*., 2016). Maize is highly productive under suitable growth conditions. However, in many world regions, this C4 plant is mainly grown in semi-arid environments characterized by adverse conditions besides areas many subjects to salinity.

In this present study, we induced acclimation to salt stress by H_2O_2 priming. Also, we performed a comparative proteomic approach composed of two-dimensional electrophoresis (2-DE) and, subsequently, mass spectrometry (ESI-Q-TOF) analysis to assess differentially

synthesized proteins in integration with physiological parameters of salt-sensitive maize plants. The findings here help advance our understanding of the molecular mechanisms involved in the benefic effect of H_2O_2 priming in plants submitted to salt stress, also to enrich the research content in mediating of salinity acclimation in maize. Thus, we provide several differential proteins that play a fundamental role in plant cell metabolism and biological processes that may support future studies.

7.2 Material and methods

7.2.1 *Plant growth and experimental conditions*

Maize seeds (*Zea mays* L.) genotype BR 5011, considered sensitive to salinity (AZEVEDO-NETO *et al*., 2004), were surface-sterilized in 1% NaClO solution for 10 min and subsequently washed. They were sown in plastic containers holding distilled water-moistened vermiculite. After seven days of sowing, the seedlings were transferred to a hydroponic system containing half-strength Hoagland's nutrient solution to acclimation for five days (HOAGLAND; ARNON, 1950). Then, the plants were subjected to pretreatment by spraying 15 mL/plant of 10 mM H_2O_2 solution or distilled water, both containing 0.025% Tween 20 detergent, to break water surface tension and facilitate H_2O_2 diffusion into the leaves (GONDIM *et al*., 2012). It was performed at 6:00 am, and again after 24 h. After 48 h of the first spraying, the plants were subjected to saline treatment by the addition of NaCl. Only in the first application of the salt treatment, the NaCl concentration was increased daily by 40mM until reaching the final concentration of 80 mM to avoid osmotic shock (OLIVEIRA *et al*., 2020). The nutritional solutions were renewed every three days. Also, the pH was corrected to 5.8 with 1.0 M KOH and daily monitored. The plants were cultivated for twelve days after saline treatment. The experiment, therefore, had four treatments: no-pretreated (C) and pretreated (H) plants with H_2O_2 under no-saline condition, and no-pretreated (S) and pretreated (HS) plants with H_2O_2 under salt stress. It was conducted in a greenhouse under a mean temperature of 32.2 ± 4 °C and relative humidity of 63.4 ± 15.9%.

7.2.2 *Growth parameters*

The samples were collected twelve days after the application of salt stress. The plant material was divided into shoots (leaves + stems) and roots. The leaf area (LA) was measured

using a leaf area meter (LI-3100, Li-COR, Inc., Lincoln, NE, USA), being the results expressed in cm^2 $plant^{-1}$. After measuring the fresh mass, the material was dried in a forced-air oven at 60 °C for 48 h for determining the shoot (SDM), root (RDM), and total (TDM) dry mass. The results were expressed as g $plant^{-1}$.

7.2.3 *Relative water content*

Relative water content (RWC) was performed as described by Čatský (1960). Ten leaf discs (1.0 cm in diameter) were weighed to determine fresh mass (FM). After, the leaf discs remained immersed in distilled water for three hours until reaching the turgid mass (TM). Finally, the turgid discs were dried for 72 h at 60 ºC and weighed to determine dry mass (DM). The data obtained were calculated by the following formula: RWC (%) = [(FM-DM) / (TM-DM)] x 100.

7.2.4 *Determination of Na^+ and K^+*

Na^+ and K^+ ions were extracted from leaves, according to Cataldo *et al*. (1975). For this, 50 mg of the dry mass was finely powered and homogenized with 5.0 mL of deionized water for one hour at 40 ºC. The tubes containing the homogenate were vigorously shaken every 15 min and then centrifuged at 3,000 x g for 10 min. The obtained supernatant was filtered on filter paper and stored at -20 °C. Then, it was used for ions determination using flame photometry (Micronal®, model B462, Brazil), according to the methodology described by Malavolta *et al*., 1989, being carried out one read for each ion. The data were expressed as μmol g^{-1} of DM.

7.2.5 *Proteomic analysis*

Protein extraction was performed as described by Mesquita *et al*. (2012), with some modifications. Approximately 500 mg of leaf samples were homogenized with 200 mg polyvinylpolypyrrolidone (PVPP) in 10 mL 40 mM Tris-HCL extraction buffer (pH 7.5), containing 250 mM sucrose, 10 mM EDTA, 1 mM phenylmethylsulfonyl fluoride (PMSF), 1 mM dithiothreitol (DTT), 1% Triton-X 100 and 2% β-mercaptoethanol (v/v). After homogenization, the samples were shaken for 1h at 4 °C and centrifuged at 6.000 × g for 15 min at 4 °C. The supernatant was collected and precipitated with 15 mL of 10% trichloroacetic acid in cold acetone for 12h at -20 °C. After new centrifugation at 6,000 x g for 10 min at 4 °C, the supernatant was discarded, and the precipitate was washed successively with cold acetone

and subsequently with 80% ethanol (v/v). The resulting pellet was vacuum dried and then solubilized in 400 µL of a solution containing 7 M urea, 2 M thiourea, 2% CHAPS, 2% IPG buffer 4-7, and 1% DTT and shaken for one hour. Subsequently, the samples were centrifuged at 10,000 x g for 10 min at 25 °C. The suspension was collected, and protein extracts were quantified using bovine serum albumin (Sigma-Aldrich, USA) as the standard (Bradford 1976). Isoelectric focusing (IEF) was performed on immobilized pH gradient gel strips (Immobiline® DryStrip, 13 cm, pH 4-7, GE-Healthcare). The IPG strips were overnight rehydrated with approximately 1 mg of leaf protein solubilized in rehydration solution (8 M urea, 2% IPG buffer 4-7, 2% CHAPS, 0.3% DTT, and 0.002% bromophenol blue) at room temperature. After rehydration, the isoelectric separation was conducted by an Ettan ™ IPGPhor ™ 3 system (GE Healthcare) at 20 °C using the following settings: 200 V for one hour (Stp); 500 V by 500 Vxh (Stp); 1000 V by 800 Vxh (Grd); 8000 V by 11300 Vxh (Grd); 8000 V by 6500 Vxh (Grd); 500 V for two hours (Stp). After IEF, the protein in the strips was denatured for 15 min with equilibration buffer [50 mM Tris-HCl, (pH 8.8), 6 M urea, 30% glycerol, 2% SDS and bromophenol blue] with 1% DTT for 20 min and thereafter with 2.5% iodoacetamide for 20 min. The second dimension (SDS-PAGE) was performed using a SE 600 Ruby vertical electrophoresis unit (GE-Healthcare: Life sciences, USA). Strips were placed on the top of SDS-PAGE gels (12.5%) and then sealed with 0.5% agarose solution and bromophenol blue. The protein separation run was composed of two steps: 10 mA/gel for 60 min and 40 mA/gel until the indicator (bromophenol blue) tracking dye ran off the gel. 2-D gels electrophoresis were fixed with a solution containing 10% acetic acid and 40% ethanol and then stained with 0.1% colloidal Coomassie Blue G-250 solution for 48 h (NEUHOFF *et al*. 1988).

The 2-D gels were scanned at 300 dpi using a DS-6000 densitometer (Loccus, Cotia, SP, Brazil) and analyzed by the ImageMaster™ 2D Platinum software (version 7.05, GE Life Sciences, USA). For this analysis, was used at least three gels of each treatment employed. The gels were compared in separate groups (one group for each treatment), and a master gel was generated based on a representative gel chosen for each group. Also, the comparisons of the master gels of each treatment allowed the visualization of differentially synthesized spots. Thus, three comparisons of the treatments were analyzed: C x H, C x S, and S x HS. In the comparisons, the gels had their same spots linked by landmarks and identified by numbers. The gel images were also analyzed by PDQuest® software (version 7.3.0; Bio-Rad®, USA) to

elaborate a synthetic gel or master gel containing the complete proteomic profile of maize leaves.

Selected protein spots as differentials were excised from acrylamide gels, and trypsin digested peptides, as proposed by Shevchenko *et al*. (2007), with modifications. The pieces of gels (about 1.0 mm^3) containing the spots were excised and destained by three consecutive washes in 25 mM ammonium bicarbonate solution in 50% acetonitrile (v/v), pH 8.8. After washes, the gel pieces were dehydrated by two consecutive washes with 100% acetonitrile for 5 min. At the end of this process, acetonitrile was removed, and the gels were vacuum dried (SpeedVac Concentrator®, Eppendorf, Hamburg, Germany). The gel fragments were then reduced and alkylated with the 65 mM DTT solutions in 100 mM ammonium bicarbonate and 200 mM iodoacetamide in 100 mM ammonium bicarbonate, respectively. The gel pieces were washed with 100 mM ammonium bicarbonate solution, dehydrated with 100% acetonitrile, and vacuum dried. Finally, they were rehydrated with a 50 mM ammonium bicarbonate solution containing 25 ng μL^{-1} trypsin (Sequencing Grade Modified Trypsin, Promega). The protein/peptide digestion was performed at 37 °C in a water bath for 20 h and extracted from the gel pieces with 5% formic acid solution in 50% acetonitrile in three repetitive steps. The samples were transferred to new microtubes, concentrated in vacuo, and stored at -80 °C for further mass spectrometry analysis.

Tryptic peptides were separated in BEH300 C18 columns (100 × 100 mm) using the nanoAcquity™ (Waters Corp., Milford, USA) system and eluted at 600 $\mu L\ min^{-1}$ with an acetonitrile gradient (5%–85%) containing 0.1% of formic acid. The liquid chromatography system was connected to a nanoelectrospray mass spectrometer source (SYNAPT HDMS system, Waters Corp.). The mass spectrometer was operated in positive mode using a source temperature of 90°C and a capillary voltage of 3.5 kV. The instrument was calibrated with fragments of the double protonated ion phosphoric acid (m/z 686.8461), and the lock mass used during the acquisition was the intact ion. The liquid chromatography-tandem mass spectrometry (ESI-Q-TOF) procedure was performed according to the data-dependent acquisition (DDA) method, selecting MS/MS doubly or triply charged precursor ions. Ions were fragmented by collision-induced dissociation using argon as the collision gas and ramp collision energy that varied according to the charge state of the selected precursor ion. Data acquisition was performed at an m/z range of 300-2.100 for the MS survey (1 scan/s), and at an m/z range of 50-2.500 for MS/MS. Data were collected with MassLynx 4.1 software and processed using

the Protein Lynx Global Server 2.4 (Waters Corp.) and were converted to peak list text files for database searching.

Data were sent to a Mascot server (Matrix Science, London, UK, v. 2.6, www.matrixscience.com) to search the NCBIprot (National Center for Biotechnology Information) and SwissProt databases. The searches were performed according to the following criteria: maximum one trypsin cleavage loss, +1, +2, and +3 charged monoisotopic peptides with variable modification of oxidized methionine residues and fixed variation of carbamidomethylated cysteine residues using MS/MS ion search mode, both limited to the Viridiplantae group. The biological functions of the identified proteins were researched in the protein knowledgebase (UniProtKB) and Mercator - MapMan pipeline. Besides, Plant-Ploc, TargetP, and CELLO programs were used as tools to inform the subcellular localization of proteins.

7.2.6 *Statistical analysis*

The experimental design was completely randomized, in a 2 x 2 factorial arrangement. It was composed of two foliar pretreatments (non-pretreated or pretreated with H_2O_2) and two growth conditions (absence or presence of 80 mM NaCl). Each treatment consisted of five repetitions, and the experimental unit consisted of two plants. The results were submitted to analysis of variance (ANOVA) and means compared by *F*-test ($p \leq 0.05$). Statistical analyses were performed using the Sisvar® 5.3 software. For gel analyses, the proteins/polypeptides in a 2-D gel differentially synthesized were selected by analyzing the images of three gels for each treatment. Significance of abundance protein spot differences was assessed by Student's t-test using the ImageMaster™ 2-D Platinum software. The spots considered differential presented percentage volume rate (% vol) ≥ 1.5 ($p < 0.05$).

7.3 Results

7.3.1 *Growth analysis*

The H_2O_2 priming under no-salt conditions (H treatment) did not change growth parameters, except RDM, which had a 26% increase (Figure 9). The salinity promoted reductions of 41%, 45%, 20%, and 32% in the values of LA, SDM, RDM, and TDM of maize plants no-pretreatment with H_2O_2, respectively. Conversely, H_2O_2 priming was able to attenuate

the effect of salt on growth, except for RDM. The increases observed in LA, SDM, and TDM scores were 16%, 61%, and 32%, respectively, compared to saline treatment. Phenotypically, the H_2O_2-pretreated plants under salinity (HS treatment) had a healthier appearance than the no-pretreated (S treatment) and have shown to be like plants grown under C treatment (Figure 10).

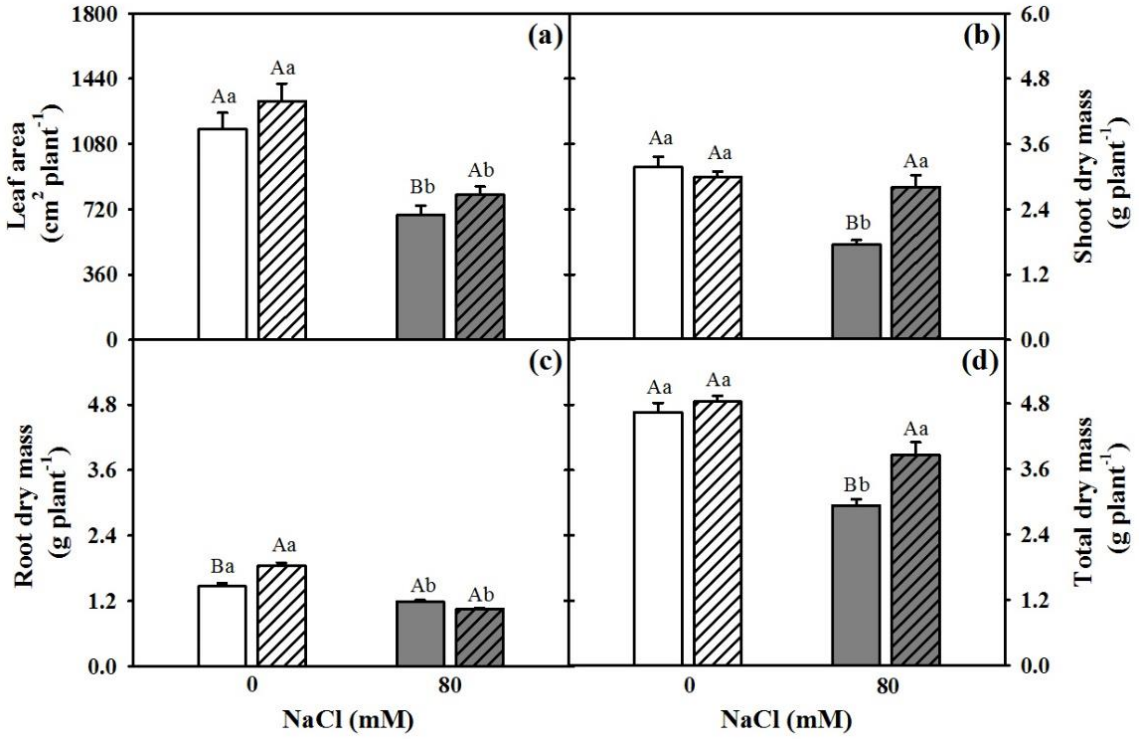

Figure 9. Growth analysis in maize plants no-pretreated (*white bars*) or pretreated (*grey bars*) with H_2O_2 under no-saline or saline (80 mM NaCl) conditions for twelve days. a Leaf area, b shoot, c root, and d total dry mass. The capital letters and lowercase letters compare the H_2O_2 and salinity treatments, respectively, according to *F*-test ($p < 0.05$). Error bars represent ± standard error and means represent n = 5.

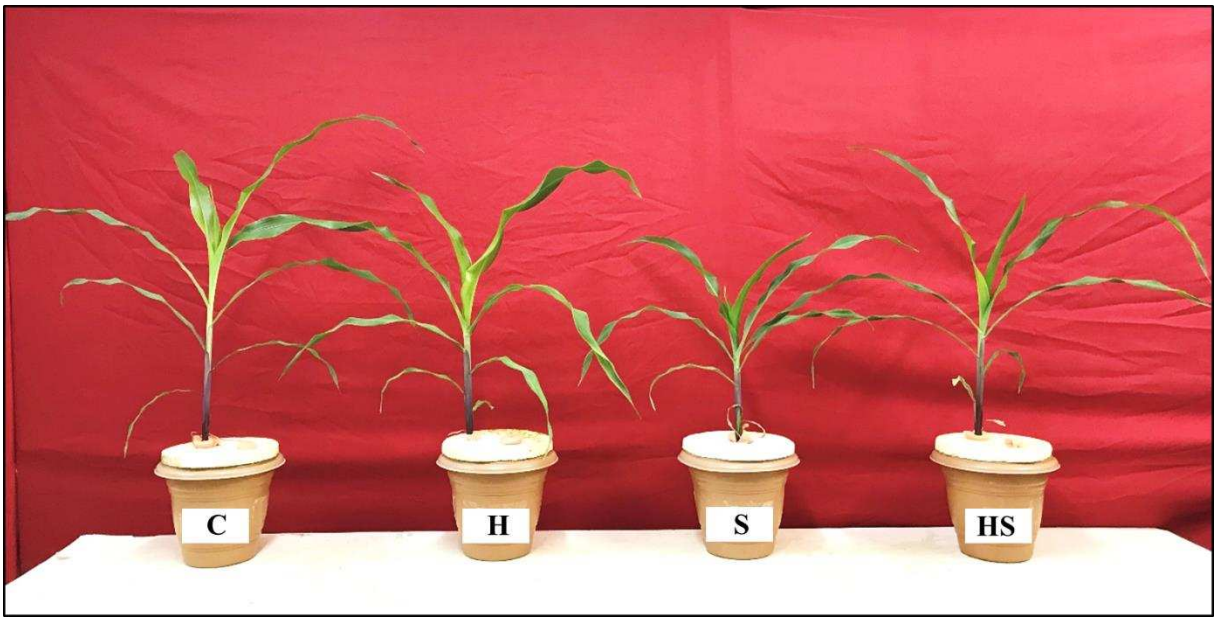

Figure 10. Phenotypic appearance of maize plants no-pretreated (C) and pretreated (H) with H_2O_2 under no-saline conditions, and no-pretreated (S) and pretreated (HS) with H_2O_2 under saline conditions for twelve days.

7.3.2 *Leaf Na^+ and K^+ contents and RWC*

There was no significant difference in Na^+ content between plants of C and H treatments, although there was a 13% reduction in K^+ content (Table 4). As expected, the salt stress remarkably increased the values of Na^+ and decreased K^+ by 31%, promoting a substantial increase of Na^+/K^+ ratio. However, H_2O_2-pretreated plants under salt stress showed a 17% reduction of leaf Na^+ content compared to S treatment, although there was no difference in K^+ content noticed here. Moreover, the RWC was significantly decreased by 9% under saline conditions. However, the H_2O_2 priming provided a significant increase of RWC in plants under saline stress, recovering the RWC as recorded in non-saline conditions (Figure 11).

7.3.3 *Proteomic analysis*

The comparative proteomic analysis investigated responsive leaf proteins to H_2O_2 priming and salinity. The study focused on three 2-D gel comparisons between every two treatments [(C x H), (C x S), and (S x HS)] allowing the visualization of differential spots in the gel imagens (Figure 12). In the C x H comparison, 22 spots with 23 proteins were identified

Table 4. Accumulation of Na^+ and K^+ ions, and Na^+/K^+ ratio in the maize leaves no-pretreated (C) and H_2O_2-pretreated (H) under no-saline conditions, and no-pretreated (S) and H_2O_2-pretreated (HS) under saline conditions for twelve days.

Treatments	Na^+ [a] (µmol g^{-1} de DM)	K^+ (µmol g^{-1} de DM)	Na^+/K^+
C	98.67 ± 0.21 Ab	868.25 ± 39,85 Aa	0.115 ± 0,00 Ab
H	91.24 ± 2.93 Ab	759.28 ± 14,16 Ba	0.120 ± 0,00 Ab
S	1183.85 ± 43.19 Aa	596.51 ± 35,22 Ab	2.013 ± 0,17 Aa
HS	988.269 ± 28.54 Ba	590.94 ± 29,24 Ab	1.680 ± 0,06 Ba

[a]For each variable, the capital letters and lowercase letters compare the H_2O_2 pre-treatments and salinity treatments, respectively, according to *F*-test ($p < 0.05$). Values represent the means of five repetitions ± standard error.

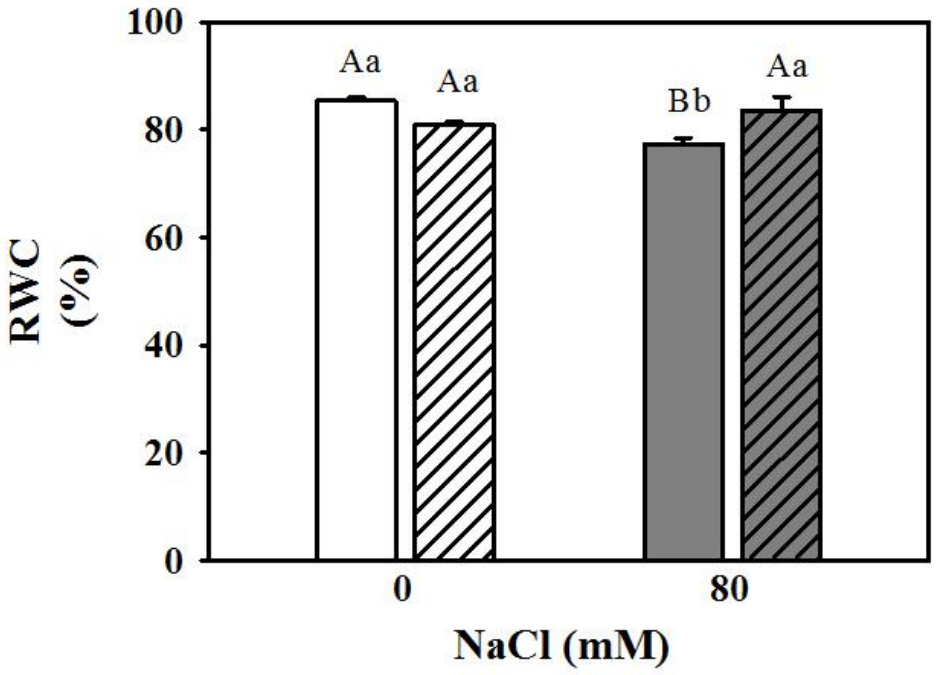

Figure 11. Relative water content in leaves of maize plants no-pretreated (*white bars*) or pretreated (*grey bars*) with H_2O_2 under no-saline or saline (80 mM NaCl) conditions for twelve days. The capital letters and lowercase letters compare the H_2O_2 and salinity treatments, respectively, according to *F*-test ($p < 0.05$). Error bars represent ± standard error and means represent $n = 5$.

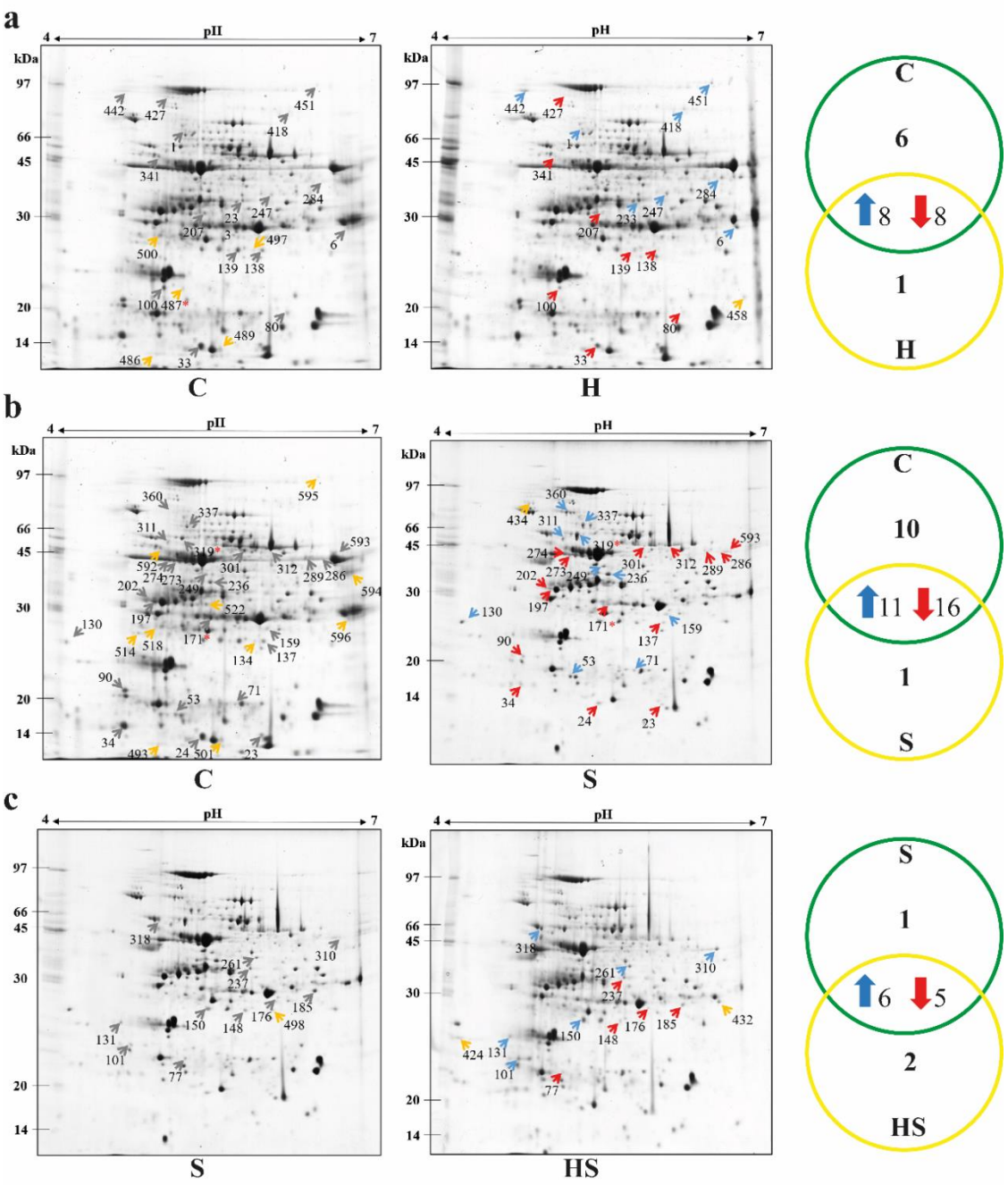

Figure 12. 2-D gels and Venn diagram of leaf proteins of maize plants no-pretreated (C) and pretreated (H) with H_2O_2 under no-saline conditions, and no-pretreated (S) and pretreated (HS) with H_2O_2 under saline conditions for twelve days. The 2-D gels comparisons were a C x H, b C x S, and c S x HS. The proteins (1 mg) were separated in 13 cm IPG strips with pH 4-7 gradient in isoelectric focusing, and 12.5% polyacrylamide gels on the SDS-PAGE. The gels were visualized after staining with Coomassie Blue G-250. Differentially modulated protein spots (intensity ≥ 1.5-fold) were numbered. In 2-D gels, the gray arrows indicate the reference gel's spots that presented differential protein regulation, while blue and red arrows indicate spots of proteins that were significantly upregulated and downregulated, respectively. Also, the orange arrows designate spots with exclusive proteins, thus, represented suppressed or *de novo* synthesized proteins by the imposed treatment. The red asterisks next to the spot number in the gel indicate a spot with two differentially regulated proteins. Spots identified are statistically different by Student's t-test ($p < 0.05$) using biological and analytical replicates ($n = 3$). In the Venn diagram, the values next to the up arrows and blue indicate upregulated proteins while the next down arrows and red indicate

downregulated proteins. Values outside the intersection point indicate the number of unique proteins for each treatment. For more details, see Table 6.

as differentially modulated in response to H_2O_2 priming. Eight proteins were upregulated, eight were downregulated, six were repressed, and one was *de novo* synthesized as represented in the Venn diagram (Figure 12a). Also, in the C x S comparison, 36 spots with 38 proteins were marked as differentially modulated in salinity response. Among them, 11 proteins were upregulated, 16 were downregulated, ten were repressed, and one was *de novo* synthesized (Figure 12b). On the other hand, in the S x HS comparison, only 14 spots with 14 proteins were characterized as differentially modulated in response to H_2O_2 priming under salt conditions, including six upregulated proteins, five downregulated, one repressed, and two *de novo* synthesized (Figure 12c).

The complete proteomic profile of maize leaves represented in a synthetic gel of all spots detected in the three comparisons provided great understanding and visualization (Figure 13a). In general, 55 spots differentially identified were excised from 2-D gels, they were in-gel digested using trypsin, and subjected to mass spectrometry analysis. In three spots were identified two different overlapped proteins: spot 19' (ATP synthase subunit alpha and DNA-directed RNA polymerase subunit beta), spot 30' (fructose-bisphosphate aldolase 2 and ATP synthase subunit alpha). Thus, a total of 58 differentially regulated proteins were identified, which are shown in the Table 5 together with the accession number, biological process involved, molecular weight, and other properties. These proteins were arranged into seven categories based on their functions: energy metabolism, photosynthesis/carbon metabolism, response to stresses, synthesis protein, redox homeostasis, RNA metabolism, and other or uncharacterized proteins according to NCBI and Swissprot databases. (Figure 13b). The C x H comparison revealed that most of the differentially regulated proteins by H_2O_2 priming without salinity were related to photosynthesis/carbon metabolism (26%), energy metabolism (39%), and stress response (18%). The C x S comparison showed that salinity induced the most significant number of changes in the protein profile. The majority was also related to photosynthesis/carbon metabolism (34%), energy metabolism (21%), and stress response (18%). Finally, the S x HS comparison exhibited that most of the differentially regulated proteins by H_2O_2 priming under salinity were linked to energy metabolism (29%), redox homeostasis (29%), stress response (14%), and photosynthesis/carbon metabolism (14%). Each protein's regulation level differently modulated by H_2O_2 priming and salt stress was provided in table 2, including the exclusives proteins of each treatment in each comparison.

In C x H comparison (Table 6), chlorophyll a-b binding protein 8 (spots 18' and 20') and fructose-bisphosphate aldolase (spot 21'), three proteins related to photosynthesis/carbon

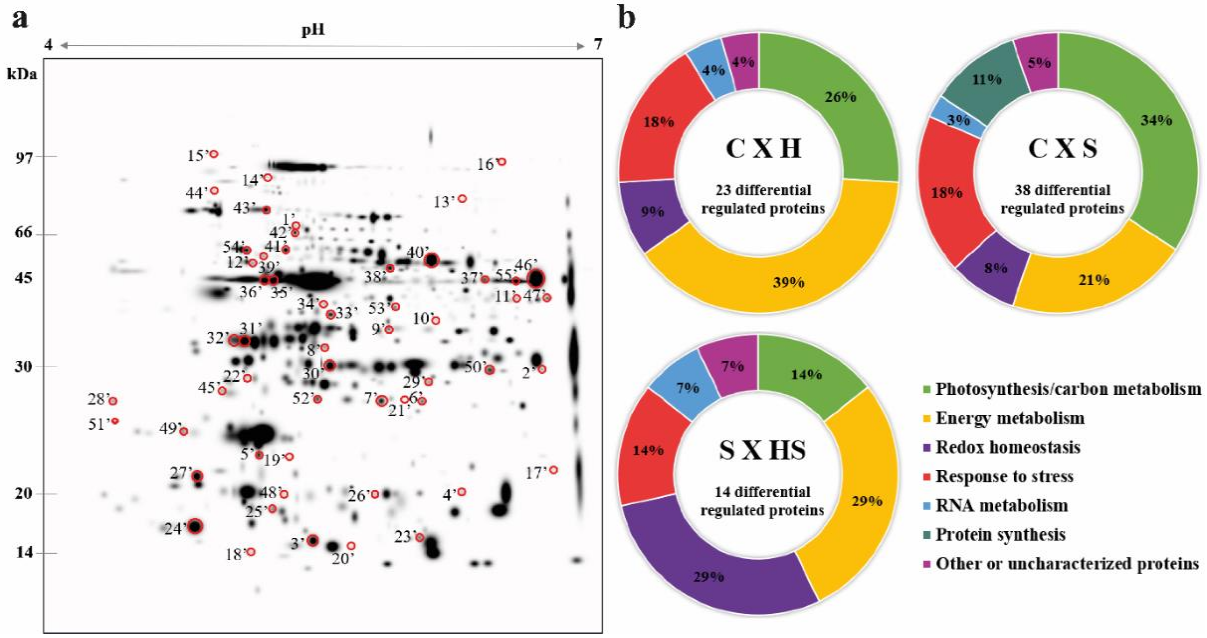

Figure 13. The 55 differentially regulated protein spots plotted in a a synthetic gel image and b functional characterization of the 58 differentially proteins identified in leaves of maize plants no-pretreated (C) and pretreated (H) with H_2O_2 under no-saline conditions, and no-pretreated (S) and pretreated (HS) with H_2O_2 under saline conditions for twelve days for the comparisons C x H, C x S, and S x HS. The proteomic profile of leaves from maize was elaborated by PDQuest® software, and red circles represent the spot position of all three comparisons evaluated. Three differentially regulated protein spots (19', 30', and 41') represent two overlapped proteins. The seven categories were created according to NCBI and Swissprot databases.

metabolism, were repressed by H_2O_2 priming, as well ATP synthase subunit alpha (spot 19'), phosphoglycerate kinase (spot 22'), both proteins related to energy metabolism, and DNA-directed RNA polymerase subunit beta (spot 19'), related to RNA metabolism. Interestingly, NAD(P)-binding Rossmann-fold superfamily protein (spot 17'), related to response stress, was synthesized *de novo* in response to H_2O_2 priming, whereas others were upregulated, e.g., lipoxygenase (spot 15') and FtsH6 - Zea mays FtsH protease (spot 1'), and chaperonin 60 subunit beta 2 (spot 12') was downregulated. Additionally, the exogenous H_2O_2 upregulated the glycine cleavage complex P-protein (spot 16'), a protein related to carbon metabolism, as well as some proteins related to energy metabolisms such as 3-phosphoglycerate kinase (spot 9'), phosphoenolpyruvate carboxykinase (ATP) (spot 13'), malate dehydrogenase 2 (spot 2'), and PAPS synthetase 2 (spot 10'), besides uncharacterized protein LOC100194135 (Natterin-4, spot 11'). At the same time, it downregulated two proteins related to photosynthesis/carbon metabolism, rubisco large subunit (spot 3') and pyruvate phosphate dikinase 1 (spot 14'); three

proteins related to energy metabolism, ATP synthase subunit beta (spots 4’ and 5’) and arginine decarboxylase (spot 8’); and one protein related to response to stress, ferredoxin (spot 6’ and 7’) (Table 6, C x H comparison).

Table 5. Additional information on differentially regulated proteins identified by 2-D gels and mass spectrometry ESI-Q-TOF in maize leaves. Spot synthetic numbers refer to those shown in Figure 13.

Spot synthetic	Accession number (NCBI/SwissProt)	Protein (Species)	Localization	Biological process	Theor. MW(kDa)/pI [a]	Experim. MW(kDa)/pI [b]	MS/MS protein score	Sequence covered (%)	Matched peptides	Ion score	m/z [c]	z [d]
1'	ACG33555.1	FtsH6 - *Zea mays* FtsH protease [*Zea mays*]	Chloroplast	Photoinhibition, oxygen and reactive oxygen species metabolic process, thylakoid membrane organization, and PSII associated light-harvesting complex II catabolic process	72.72 / 5.78	70 / 5.2	136	3	(612)QLSDEAYEIALR(623)	61	704,3622	2
									(652)AILSEFAEIPVENR(665)	75	794,4275	2
2'	AQK92335.1	Malate dehydrogenase 2 [*Zea mays*]	Mitochondrion	Malate metabolic process	26.44 / 8.81	29 / 6.1	89	12	(48)LNPLVSSLSLYDIAGTPGVAADVSHINSPALVK(80)	89	1106,9318	3
3'	AAN63285.1	Ribulose-1,5-bisphosphate carboxylase/oxygenase large subunit, partial [*Pauridiantha afzelii*]	Chloroplast	Ribulose-bisphosphate carboxylase activity and carbon fixation	50.12 / 5.66	7 / 5.3	66	2	(121)CSQGPPHGIQVER(133)	66	489,2522	3
4'	ATPB_MAIZE	ATP synthase subunit beta [*Zea mays*]	Chloroplast	ATP synthesis coupled proton transport	54.06 / 5.31	14 / 6.2	77	4	(88)GMEVIDTGTPLSVPVGGATLGR(109)	77	1072,0546	2
5'	CAB65458.1	ATP synthase beta subunit, partial [*Scabiosa* sp. Albach]	Chloroplast and Mitochondrion	ATP synthesis coupled proton transport	28.86 / 5.87	20 / 5.0	221	10	(130)VGLTALTMAEYFR(142)	70	744,3799	2
									(159)MVQAGSEVSALLGR(172)	74	717,3849	2
									(159)FVQAGSEVSALLGR(172)	83	717,3849	2
6'	NP_001336742.1	Ferredoxin [*Zea mays*]	Chloroplast	Oxidation-reduction process	39.64 / 8.53	25 / 6.0	95	4	(135)LYSIASSAIGDFGDSK(150)	95	815,8967	2
7'	NP_001336742.1	Ferredoxin [*Zea mays*]	Chloroplast	Oxidation-reduction process	39.64 / 8.53	25 / 5.7	85	4	(135)LYSIASSAIGDFGDSK(150)	85	815,9017	2

Table 2 continue

Spot synthetic	Accession number (NCBI/SwissProt)	Protein (Species)	Localization	Biological process	Theor. MW(kDa)/pI [a]	Experim. MW(kDa)/pI [b]	MS/MS protein score	Sequence covered (%)	Matched peptides	Ion score	m/z [c]	z [d]
8'	ACG41098.1	Arginine decarboxylase [*Zea mays*]	Chloroplast	Arginine catabolic process and spermidine biosynthetic process	71.05 / 5.18	31 / 5.6	643	23	(35)WTEPGQEIDVHSVIVEALATQPNDSTSK(62)	58	1017,8437	3
									(79)IETLHNAFNSAMESTGYTSR(98)	63	749,0119	3
									(161)DADYIALALSAR(172)	74	639,8391	2
									(211)KFEPVIGIR(219)	71	529,8206	2
									(240)FGMLADQIYEVAETLGK(256)	75	942,9831	2
									(240)FGMLADQIYEVAETLGK(256)	85	950,98	2
									(302)WLATLDCGGGLGVDYDGTR(320)	107	1013,4796	2
									(321)SGDSDMSVAYGIQEYASAVVQAVR(344)	86	835,0656	3
									(321)SGDSDMSVAYGIQEYASAVVQAVR(344)	82	840,3956	3
									(321)SGDSDMSVAYGIQEYASAVVQAVR(344)	126	1260,1068	2
									(345)LKCDYNGVAHPVVCTESGR(363)	59	721,3416	3
									(345)LKCDYNGVAHPVVCTESGR(363)	59	721,669	3
9'	AAO32643.1	3-phosphoglycerate kinase, partial [*Zea mays*]	Cytosol	Glycolytic process	31.66 / 5.01	35 / 5.8	84	6	(64)LASVADLYVNDAFGTAHR(81)	84	640,6531	3
10'	NP_001147427.1	Bifunctional 3-phosphoadenosine 5-phosphosulfate synthetase 2 [*Zea mays*]	Mitochondrion	Sulfate assimilation	52.49 / 8.30	36 / 5.1	289	16	(290)NPILLLHPLGGYTK(303)	80	768,4559	2
									(319)VLEDGVLDPETTIVSIFPSPMHYAGPTEVQWHAK(352)	64	945,7232	4
									(355)INAGANFYIVGR(366)	89	647,85	2
									(441)TGENPPDGFMCPGGWK(456)	59	883,3754	2
11'	NP_001132659.1	Uncharacterized protein LOC100194135 (Natterin-4) [*Zea mays*]	-	-	42.29 / 6.53	39 / 6.6	341	18	(125)SPNWIWCDTDDTSTDNRDTLFEVVR(149)	126	1014,7953	3
									(150)VGDDADAVYGLR(161)	94	625,8045	2
									(196)IEEAVLLR(203)	63	471,7812	2
									(320)ILATQGTCQVPFSYTQEDILTTGEK(344)	57	934,1342	3
12'	AQL02522.1	Chaperonin 60 subunit beta 2 [*Zea mays*]	Chloroplast	Protein folding and protein refolding	63.36 / 5.35	47 / 4.9	155	3	(97)IVNDGVTVAR(106)	71	5.222.965	2
									(154)VVAAGANPVQITR(166)	84	6.483.745	2

Table 2 continue

Spot synthetic	Accession number (NCBI/SwissProt)	Protein (Species)	Localization	Biological process	Theor. MW(kDa)/pI [a]	Experim. MW(kDa)/pI [b]	MS/MS protein score	Sequence covered (%)	Matched peptides	Ion score	m/z [c]	z [d]
13'	PCKA_MAIZE	Phosphoenolpyruvate carboxykinase (ATP) [*Zea mays*]	Cytosol	Gluconeogenesis	73.78 / 6.57	81 / 6.2	65	2	(166)GSFITSTGALATLSGAK(182)	67	791,4275	2
14'	PPDK1_MAIZE	Pyruvate, phosphate dikinase 1 [*Zea mays*]	Chloroplast	Photosynthesis and pyruvate metabolic process	103.52 / 5.74	89 / 5.0	413	8	(211)FLDMFGNVVMDIPR(224)	76	827,4162	2
									(211)FLDMFGNVVMDIPR(224)	88	835,4175	2
									(423)IAVDMVNEGLVEPR(436)	112	779,4057	2
									(503)AETSPEDVGGMHAAVGILTER(523)	61	714,016	3
									(503)AETSPEDVGGMHAAVGILTER(523)	77	719,3473	3
									(610)VLANADTPDDALTAR(624)	76	771,8959	2
									(746)LGISYPELTEMQAR(759)	62	804,4164	2
15'	ABC59693.1	Lipoxygenase [*Zea mays*]	Chloroplast	Circadian rhythm, green leaf volatile biosynthetic process, and response to stress abiotic and biotic	102.48 / 6.11	94 / 4.5	305	5	(109)TLLLELVSSELDAK(122)	91	765,9387	2
									(380)LVEDTTDHVLR(390)	76	433,2248	3
									(380)LVEDTTDHVLR(390)	82	649,3427	2
									(435)LDPEVYGPAESAITK(449)	67	795,4116	2
									(699)SDEAVAADPELR(710)	65	636,8073	2
16'	AAL33595.1	Glycine cleavage complex P-protein, partial [*Zea mays*]	Mitochondrion	Glycine metabolic process	40.45 / 5.91	96 / 6.5	77	4	(63)LGTVTVQDLPFFDTVR(78)	77	904,4908	2
17'	NP_001132564.1	NAD(P)-binding Rossmann-fold superfamily protein [*Zea mays*]	Chloroplast	Defense to abiotic stress	31.91 / 9.11	16 / 6.7	201	13	(104)DPESIAPAIEGIDALIILTSAVPK(127)	77	8117896	3
									(202)KAEQYLADSGLPYTIIR(218)	65	646,6812	3
									(203)AEQYLADSGLPYTIIR(218)	59	905,4815	2
18'	NP_001148598.2	Chlorophyll a-b binding protein 8 [*Zea mays*]	Chloroplast	Photosynthesis and light harvesting	28.96 / 8.94	6 / 4.9	136	11	(100)YAMLGAVGAIAPEIFGK(116)	69	854,4669	2
									(117)MGIIPPETALPWFK(130)	59	800,4401	2
									(117)MGIIPPETALPWFK(130)	67	808,4367	2
19'	ATPA_MAIZE	ATP synthase subunit alpha [*Zea mays*]	Chloroplast	ATP synthesis coupled proton transport	55.73 / 5.87	19 / 5.2	80	2	(256)HTLIIYDDLSK(266)	80	659,3565	2
	ONM62969.1	DNA-directed RNA polymerase subunit beta [*Zea mays*]	Chloroplast	Transcription and DNA-templated	26.62 / 5.98		80	0	(2096)HTLIIYDDLSK(2106)	80	659,3565	2

Table 2 continue

Spot synthetic	Accession number (NCBI/SwissProt)	Protein (Species)	Localization	Biological process	Theor. MW(kDa)/pI [a]	Experim. MW(kDa)/pI [b]	MS/MS protein score	Sequence covered (%)	Matched peptides	Ion score	m/z [c]	z [d]
20'	NP_001148598.2	Chlorophyll a-b binding protein 8 [*Zea mays*]	Chloroplast	Photosynthesis and light harvesting	28.96 / 8.94	7 / 5.6	68	6	(100)YAMLGAVGAIAPEIFGK(116)	68	862,4522	2
21'	ACG36798.1	Fructose-bisphosphate aldolase [*Zea mays*]	Cytosol and chloroplast	Gluconeogenesis and glycolytic process	41.92 / 7.63	25 / 5.9	138	7	(73)LASIGLENTEANR(85)	69	6.943.619	2
									(122)IVDILVEQGIVPGIK(136)	69	7.969.834	2
22'	AQK86959.1	Phosphoglycerate kinase [*Zea mays*]	Cytosol	Gluconeogenesis, glycolytic process, and positive regulation of oxidative phosphorylation	49.98 / 6.29	50 / 5.2	75	2	(253)ELDYLVGAVSSPK(265)	75	689,3683	2
23'	AQK66518.1	Oxygen-evolving enhancer protein 1-1 [*Zea mays*]	Chloroplast	Photosynthetic electron transport chain	39.34 / 5.57	7 / 6.0	68	5	(258)QLVATGKPDSFGGPFLVPSYR(278)	68	746,0575	3
24'	ACG35092.1	2-cys peroxiredoxin BAS1 [*Zea mays*]	Chloroplast	Cell redox homeostasis, hydrogen peroxide catabolic, and response to oxidative stress	28.30 / 5.81	8 / 4.5	72	6	(197)EGVIQHSTINNLAIGR(212)	72	574,6458	3
									(197)EGVIQHSTINNLAIGR(212)	72	574,9774	3
25'	ONM22161.1	Sterile alpha motif (SAM) domain-containing protein [*Zea mays*]	Chloroplast	Protein folding	19.73 / 9.69	11 / 5.1	73	6	(119)TAGGLLLTQATK(130)	73	587,3458	2
26'	XP_004151190.1	PREDICTED: FRIGIDA-like protein 5 isoform X1 [*Cucumis sativus*]	Nucleous	-	13.29 / 6.37	13 / 5.7	68	0	(96)NELSELNR(103)	70	487,2659	2
27'	OEL16006.1	Fruit protein pKIWI502 [*Dichanthelium oligosanthes*]	Mitochondrion	Oxidation-reduction process	29.94 / 6.90	16 / 4.6	69	4	(204)IIPVLSQPDDSWK(216)	69	749,397	2
28'	PAN10940.1	Hypothetical protein PAHAL_B01754 [*Panicum hallii*]	Chloroplast	RNA modification and innate immune response	32.47 / 4.57	24 / 3.9	69	4	(216)IYVGNLPWQVDDSR(219)	69	831,4138	2
29'	CYSK_MAIZE	Cysteine synthase [*Zea mays*]	Mitochondrion and cytosol	Cysteine biosynthesis and response to salt stress	34.29 / 5.91	27 / 6.1	95	5	(176)IDGLVSGIGTGGTITGTGR(194)	95	866,4685	2

Table 2 continue

Spot synthetic	Accession number (NCBI/SwissProt)	Protein (Species)	Localization	Biological process	Theor. MW(kDa)/pI [a]	Experim. MW(kDa)/pI [b]	MS/MS protein score	Sequence covered (%)	Matched peptides	Ion score	m/z [c]	z [d]
30'	ACG36798.1	Fructose-bisphosphate aldolase [*Zea mays*]	Chloroplast	Gluconeogenesis and glycolytic process	41.92 / 7.63	29 / 5.5	346	18	(58)GILAMDESNATCGK(71)	91	741,8268	2
									(73)LASIGLENTEANR(85)	102	694,3564	2
									(122)IVDILVEQGIVPGIK(136)	68	796,9819	2
									(201)YAAISQDNGLVPIVEPEILLDGEHGIER(228)	86	1016,5206	3
	XP_008648857.1	Photosystem II stability/assembly factor HCF136 [*Zea mays*]	Chloroplast	Photosynthesis	43.04 / 8.71		378	18	(125)SIPSAEDEDFNYR(137)	69	771,8348	2
									(170)IPLSAQLPGNMVYIK(184)	72	830,4599	2
									(212)AAVQETVSATLNR(224)	80	680,3605	2
									(307)GTGITEDFEEVQVQSR(322)	84	897,9262	2
									(307)GTGITEDFEEVQVQSR(322)	69	897,9284	2
									(333)SQEEAWAAGGSGVLLK(348)	73	801,9085	2
31'	AQK86959.1	Phosphoglycerate kinase [*Zea mays*]	cytosol	Gluconeogenesis, glycolytic process, and positive regulation of oxidative phosphorylation	49.98 / 6.29	31 / 4.8	69	2	(253)ELDYLVGAVSSPK(265)	69	689,3637	2
32'	KPPR_SPIOL	Phosphoribulokinase [*Spinacia oleracea*]	Chloroplast	Reductive pentose-phosphate cycle	45.32 / 5.82	32 / 4.7	73	3	(76)LTSVFGGAAEPPK(88)	73	637,3395	2
33'	ACG35888.1	Elongation factor Tu [*Zea mays*]	Chloroplast	Mitochondrial translational elongation; translational elongation	50.95 / 6.06	36 / 5.5	221	7	(235)ALEALMVNPALK(246)	74	643,3604	2
									(306)IGDTVDIVGIR(316)	77	579,3261	2
									(306)IGDTVDIVGIR(316)	74	579,3276	2
									(320)NCTVTGVEMFQK(331)	69	715,3243	2
34'	IF4A_MAIZE	Eukaryotic initiation factor 4A [*Zea mays*]	Nucleous	mRNA processing, mRNA splicing, and mRNA transport	46.85 / 5.38	38 / 5,5	68	3	(182)MFVLDEADEMLSR(194)	68	794,3499	2
35'	ADD09775.1	Ribulose-1,5-bisphosphate carboxylase/oxygenase	Chloroplast	Ribulose-bisphosphate carboxylase	18.49 / 5.89	42 / 5,0	72	7	(129)TMQGPPHGIQVER(141)	74	489,2485	3

		large subunit, partial [*Ceratodon purpureus*]		activity and carbon fixation								
36'	AGJ75817.1	Ribulose-1,5-bisphosphate carboxylase/oxygenase large subunit, partial [*Pauridiantha afzelii*]	Chloroplast	Ribulose-bisphosphate carboxylase activity and carbon fixation	23.75 / 5.35	42 / 5,0	67	6	(127)TMQGPPHGIQVER(139)	69	489,2494	3
37'	AHM26656.1	Aldehyde dehydrogenase 2-1 [*Zea mays*]	Mitochondrion	Oxidation reduction and aldehyde metabolic process	59.77 / 6.69	43 / 6,5	83	2	(289)IAFTGSTDTGK(299)	83	549,2756	2
38'	TKTC_MAIZE	Transketolase [*Zea mays*]	Chloroplast	Reductive pentose-phosphate cycle	73.35 / 5.47	46 / 5.8	88	1	(257)VTTTIGFGSPNK(268)	88	611,33	2
39'	AQL02522.1	Chaperonin 60 subunit beta 2 [*Zea mays*]	Chloroplast	Protein folding and protein refolding	63.36 / 5.35	53 / 5.0	82	2	(155)VVAAGANPVQITR(166)	82	648,3722	2
40'	ATPA_MAIZE	ATP synthase subunit alpha [*Zea mays*]	Chloroplast	ATP synthesis coupled proton transport	55.73 / 5.87	51 / 6.1	715	24	(129)LIESPAPGIISR(140)	86	626,838	2
									(129)LIESPAPGIISR(140)	95	626,8614	2
									(142)SVYEPLQTGLIAIDSMIPIGR(162)	85	1137,112	2
									(142)SVYEPLQTGLIAIDSMIPIGR(162)	76	1145,1046	2
									(177)TAVATDTILNQK(188)	74	637,8471	2
									(256)HTLIIYDDLSK(266)	73	659,3382	2
									(423)QSQSNPLPVEEQVATIYTGTR(443)	87	1159,5815	2
									(423)QSQSNPLPVEEQVATIYTGTR(443)	87	1160,0697	2
									(423)QSQSNPLPVEEQVATIYTGTR(443)	64	1160,073	2
									(444)GYLDSLEIEQVK(455)	72	697,3608	2
									(467)DTKPQFQEIISSSK(480)	91	804,4121	2
									(481)TFTEQAETLLK(491)	67	640,8303	2
									(492)EAIQEQLER(500)	71	558,2805	2
41'	AQL02522.1	Chaperonin 60 subunit beta 2 [*Zea mays*]	Chloroplast	Protein foldinga and protein refolding	63.36 / 5.35	57 5.2	257	7	(107)EVELEDPVENIGAK(120)	71	771,3838	2
									(154)VVAAGANPVQITR(166)	81	648,3712	2
									(333)TQYLDDIAILTGATVIR(349)	105	932,014	2

	ATPA_MAIZE	ATP synthase subunit alpha	Chloroplast	ATP synthesis coupled proton transport	55.73 / 5.87	57 5.2	74	3	(42)IIGLGEIMSGELVEFAEGTR(61)	74	1.061,06	2
42'	AQK81560.1	Filamentation temperature-sensitive H 2B [*Zea mays*]	Chloroplast	Photoinhibition, reactive oxygen species metabolic process, thylakoid membrane organization, PSII associated light-harvesting complex II catabolic process, and photosystem II	49.28 / 6.16	68 / 5.2	82	2	(385)LAEDIDSAVK(394)	82	530,7757	2
43'	HSP70_MAIZE	Heat shock 70 kDa protein [*Zea mays*]	Chloroplast	Protein folding and response to stress abiotic and biotic	70.87 / 5.22	76 / 5.1	81	1	(306)FEELNMDLFR(315)	81	665,3138	2
44'	ONM07983.1	Heat shock 70 kDa protein 6 [*Zea mays*]	Chloroplast	Protein folding and response to stress abiotic and biotic	69.64 / 5.21	84 / 4.7	80	2	(174)IINEPTAASLAYGFEK(194)	80	862,4517	2
45'	NP_001150334.1	Uncharacterized protein LOC100283964 (Malonyl CoA-acyl carrier protein transacylase) [*Zea mays*]	Chloroplast	Fatty acid biosynthetic process	38.82 / 5.64	26 / 4.7	78	2	(281)LESALAATEIR(291)	78	587,3248	2
46'	CAC04365.1	Ribulose 1,5-bisphosphate carboxylase, partial [*Polyosma cunninghamii*]	Chloroplast	Ribulose-bisphosphate carboxylase activity and carbon fixation	51.39 / 6.32	44 / 6.7	154	5	(138)TFQGPPHGIQVER(150)	71	489,25	3
									(277)DNGILLHIHR(286)	82	396,5516	3
47'	NP_001132659.1	Uncharacterized protein LOC100194135 (Natterin-4) [*Zea mays*]	-	-	42.29 / 6.53	40 / 6.9	98	3	(150)VGDDADAVYGLR(161)	98	625,8005	2
48'	ACG31393.1	Triosephosphate isomerase [*Zea mays*]	Cytosol	Gluconeogenesis and glycolytic process	26.91 / 5.12	13 / 5.2	373	26	(124)VIACVGETLEER(135)	88	688,346	2
									(136)EAGSTMDVVAAQTK(149)	70	712,3364	2
									(176)VATPAQAQEVHASLR(190)	71	526,6102	3
									(195)INVSPEVSESTR(206)	71	659,3323	2
									(195)INVSPEVSESTR(206)	71	659,335	2
									(207)IIYGGSVTAANCK(219)	73	677,3417	2

49'	AQK43989.1	Putative plastid-lipid-associated protein 2 [*Zea mays*]	Chloroplast	Structural molecule activity	33.65 / 5.89	22 / 4.6	77	4	(248)GIFSSIENAASSVAK(262)	80	740,8836	2
50'	ACG36184.1	Malate dehydrogenase [*Zea mays*]	Mitochondrion	Carbohydrate metabolic process, malate metabolic process, and tricarboxylic acid cycle	35.66 / 7.63	29 / 6.5	72	3	(168)LFGVTTLDVVR(178)	72	610,3538	2
51'	AQK51681.1	Ribonucleoprotein [*Zea mays*]	Chloroplast	RNA modification, RNA processing, and innate immune response	31.27 / 4.69	11 / 4.0	70	4	(204)AYVGNLPWQVDDSR(217)	70	810,392	2
52'	NP_001336742.1	Ferredoxin [*Zea mays*]	Chloroplast	Oxidation-reduction process	39.64 / 8.53	25 / 5.4	99	4	(135)LYSIASSAIGDFGDSK(150)	99	815,9017	2
53'	ACG32614.1	S-adenosylmethionine synthetase 1 [*Zea mays*]	Cytosol	Methionine adenosyl biosynthetic process, response to salt stress, and ethylene biosynthetic process	42.98 / 5.50	37 / 5.8	67	3	(240)FVIGGPHGDAGLTGR(254)	67	485,2517	3
54'	XP_002463468.1	Rubisco large subunit-binding protein subunit alpha [*Sorghum bicolor*]	Chloroplast	Protein folding and chloroplast organization	60.97 / 5.2		80	2	(145)LGMLSITSGANPVSVK(160)	80	795,4318	2
55'	ATPB_MAIZE	ATP synthase subunit beta [*Zea mays*]	Chloroplast	ATP synthesis coupled proton transport	54.06 / 5.31	43 / 6.5	70	2	(76)AVAMSATEGLMR(87)	70	634,8059	2

[a] Theor. MW (kDa)/pI - Theoretical molecular weight (kDa)/isoelectrical point (pI)

[b] Experim. MW (kDa)/pI - Experimental molecular weight (kDa)/isoelectrical point (pI)

[c] m/z - mass to charge ratio of peptides

Table 6. Identification and regulation level of proteomic profile in maize leaves no-pretreated (C) and pretreated (H) with H2O2 under no-saline conditions, and no-pretreated (S) and pretreated (HS) with H2O2 under saline conditions for twelve days. Numbers highlighted in blue bars indicate higher protein abundance, and numbers highlighted in red bars denote lower protein abundance between comparisons in response to H2O2 priming or salinity (80 mM NaCl). The values indicate how many times the protein was upregulated or downregulated. Yellow cells indicate proteins exclusive of a specific treatment in each comparison, being repressed or de novo synthesized. For each comparison, only significant differences in relative abundance intensity ≥ 1.5-fold ($p < 0.05$) were considered. Also, C treatment was taken as a reference for comparisons C x H and C x S, while S for S x HS. For more details of proteins, see Table 5.

Spot synthetic	ID Spot C x H	ID Spot C x S	ID Spot S x HS	Accession nº	Protein	Regulation level C x H	Regulation level C x S	Regulation level S x HS
Photosynthesis/Carbon metabolism								
23’	-	23	-	AQK66518.1	Oxygen-evolving enhancer protein 1-1		1,68	
30’	-	171	-	XP_008648857.1	Photosystem II stability/assembly factor HCF136		1,58	
18’	486	493	-	NP_001148598.2	Chlorophyll a-b binding protein 8	C	C	
20’	489	501	-	NP_001148598.2	Chlorophyll a-b binding protein 8	C	C	
16’	451	595	-	AAL33595.1	Glycine cleavage complex P-protein, partial	1,59	C	
3’	33	24	-	AAN63285.1	Ribulose-1,5-bisphosphate carboxylase/oxygenase large subunit, partial	1,50	1,94	
36’	-	274	-	AGJ75817.1	Ribulose-1,5-bisphosphate carboxylase/oxygenase large subunit, partial		1,52	
46’	-	593	310	CAC04365.1	Ribulose 1,5-bisphosphate carboxylase, partial		8,05	1,55
35’	-	273		ADD09775.1	Ribulose-1,5-bisphosphate carboxylase/oxygenase large subunit, partial		1,68	
54’	-	-	318	XP_002463468.1	Rubisco large subunit-binding protein subunit alpha			1,54
21’	497	134	-	ACG36798.1	Fructose-bisphosphate aldolase	C	C	
30’	-	171	-	ACG36798.1	Fructose-bisphosphate aldolase		1,58	
38’	-	301	-	TKTC_MAIZE	Transketolase		1,68	
32’	-	202	-	KPPR_SPIOL	Phosphoribulokinase		1,64	
14’	427	-	-	PPDK1_MAIZE	Pyruvate, phosphate dikinase 1	1,56		
Energy metabolism								
19’	487	-	-	ATPA_MAIZE	ATP synthase subunit alpha	C		
40’	-	312	-	ATPA_MAIZE	ATP synthase subunit alpha		1,76	
41’	-	319	-	ATPA_MAIZE	ATP synthase subunit alpha		2,11	
5’	100	-	-	CAB65458.1	ATP synthase beta subunit, partial	1,86		
4’	80	-	-	ATPB_MAIZE	ATP synthase subunit beta	1,65		
55’	-	525	-	ATPB_MAIZE	ATP synthase subunit beta		1,50	
9’	233	-	237	AAO32643.1	3-phosphoglycerate kinase, partial	1,55		1,50
22’	500	518	-	AQK86959.1	Phosphoglycerate kinase	C	C	
31’	-	197	-	AQK86959.1	Phosphoglycerate kinase		1,67	
48’	-	-	77	ACG31393.1	Triosephosphate isomerase			1,62
37’	-	289	-	AHM26656.1	Aldehyde dehydrogenase 2-1		1,83	
13’	418	-	-	PCKA_MAIZE	Phosphoenolpyruvate carboxykinase (ATP)	1,83		
2’	6	596	432	AQK92335.1	Malate dehydrogenase 2	1,72	C	HS
50’	-	-	185	ACG36184.1	Malate dehydrogenase			1,76
10’	247	-	-	NP_001147427.1	Bifunctional 3-phosphoadenosine 5-phosphosulfate synthetase 2	1,51		
8’	207	522	-	ACG41098.1	Arginine decarboxylase	1,61	C	
Redox homeostasis								
6’	138	137	498	NP_001336742.1	Ferredoxin	3,41	1,56	S
7’	139	-	148	NP_001336742.1	Ferredoxin	2,24		2,20
52’	-	-	150	NP_001336742.1	Ferredoxin			1,65
27’	-	90	101	OEL16006.1	Fruit protein pKIWI502		1,56	1,72
24’	-	34	-	ACG35092.1	2-cys peroxiredoxin BAS1		2,92	
Response to stress								
53’	-	-	261	ACG32614.1	S-adenosylmethionine synthetase 1			1,50
12’	341	592	-	AQL02522.1	Chaperonin 60 subunit beta 2	1,55	C	
39’	-	311	-	AQL02522.1	Chaperonin 60 subunit beta 2		1,72	
41’	-	319	-	AQL02522.1	Chaperonin 60 subunit beta 2		2,11	
29’	-	159	176	CYSK_MAIZE	Cysteine synthase		1,68	1,56
15’	442	-	-	ABC59693.1	Lipoxygenase	1,57		
43’	-	360	-	HSP70_MAIZE	Heat shock 70 kDa protein		5,60	
44’	-	434	-	ONM07983.1	Heat shock 70 kDa protein 6		S	
17’	458	-	-	NP_001132564.1	NAD(P)-binding Rossmann-fold superfamily protein	H		
42’	-	337	-	AQK81560.1	Filamentation temperature-sensitive H 2B [Zea mays]		1,72	
1’	0	-	-	ACG33555.1	FtsH6 - Zea mays FtsH protease [Zea mays]	2,06		
RNA metabolism								
19’	487	-	-	ONM62969.1	DNA-directed RNA polymerase subunit beta	C		
28’	-	130	-	PAN10940.1	Hypothetical protein PAHAL_B01754		2,37	
51’	-	-	424	AQK51681.1	Ribonucleoprotein			HS
Protein synthesis								
34’	-	249	-	IF4A_MAIZE	Eukaryotic initiation factor 4A		1,95	
33’	-	236	-	ACG35888.1	Elongation factor Tu		1,96	
26’	-	71	-	XP_004151190.1	PREDICTED: FRIGIDA-like protein 5 isoform X1		1,57	
25’	-	53	-	ONM22161.1	Sterile alpha motif (SAM) domain-containing protein		1,57	
Other protein								
49’	-	-	131	AQK43989.1	Putative plastid-lipid-associated protein 2			1,54
11’	284	-	-	NP_001132659.1	Uncharacterized protein LOC100194135 (Natterin-4)	1,97		
47’	-	594	-	NP_001132659.1	Uncharacterized protein LOC100194135 (Natterin-4)		C	
45’	-	514	-	NP_001150334.1	Uncharacterized protein LOC100283964		C	

Salinity considerably affected protein modulation (Table 6). In C x S comparison, the salt stress repressed four proteins related to photosynthesis/carbon metabolism: chlorophyll a-b binding protein 8 (spots 18' and 20'), glycine cleavage complex P-protein (spot 16'), fructose-bisphosphate aldolase (spot 21'); three proteins related to energy metabolism: phosphoglycerate kinase (spot 22'), malate dehydrogenase 2 (spot 2'), arginine decarboxylase (spot 8'); a protein related to response to stress, chaperonin 60 subunit beta 2 (spot 12'); and two uncharacterized proteins: LOC100194135 (Natterin-4, spot 47'), and LOC100283964 (spot 45'). Also, the salinity downregulated much proteins-related to photosynthesis/carbon metabolism as the oxygen-evolving enhancer protein 1-1 (spot 23'), photosystem II stability/assembly factor HCF136 (spot 30'), rubisco large subunit (spots 3', 35', 36', and 46'), fructose-bisphosphate aldolase (spot 30'), transketolase (spot 38'), and phosphoribulokinase (spot 32'), as well as four protein related to energy metabolism: ATP synthase subunit alpha (spot 40'), ATP synthase subunit beta (spot 55'), phosphoglycerate kinase (spot 31'), aldehyde dehydrogenase 2-1(spot 37'); and three proteins related to redox homeostasis: ferredoxin (spot 6'), fruit protein pKIWI502 (spot 27'), and 2-cys peroxiredoxin BAS1 (spot 24'). Otherwise, the salinity upregulated ATP synthase subunit alpha (spot 41'), a protein related to energy metabolism, and, as expected, it also upregulated several stress-responsive proteins like chaperonin 60 subunit beta 2 (spots 39' and 41'), cysteine synthase (spot 29'), heat shock 70 kDa protein (spot 43'), and filamentation temperature-sensitive H 2B [Zea mays] (spot 42). The hypothetical protein PAHAL_B01754 (spot 28'), a protein related to RNA metabolism, as well as eukaryotic initiation factor 4A (spot 34'), elongation factor Tu (spot 33'), PREDICTED: FRIGIDA-like protein 5 isoform X1 (spot 26'), sterile alpha motif (SAM) domain-containing protein (spot 25'), all related to protein synthesis, were also upregulated by salt stress. Additionally, the heat shock 70 kDa protein 6 (spot 44'), a stress-responsive protein, was synthesized *de novo* by salinity.

In the S x HS comparison, there was an upregulation of two proteins related to photosynthesis/carbon metabolism: rubisco large subunit (spot 46') and rubisco large subunit-binding protein subunit alpha (spot 54'); two proteins related to redox homeostasis: ferredoxin (spot 52') and fruit protein pKIWI502 (spot 27'); as well as S-adenosylmethionine synthetase 1 (spot 53'), a responsive stress protein, and putative plastid-lipid-associated protein 2 (spot 49') (Table 6). In contrast, three proteins related to energy metabolism [3-phosphoglycerate kinase (spot 9'), triosephosphate isomerase (spot 48'), malate dehydrogenase (spot 50')], a protein related to redox homeostasis [ferredoxin (spot 7')], and a responsive stress protein [cysteine synthase (spot 29')] were downregulated. The H_2O_2 priming prompted a *de novo*

synthesis of malate dehydrogenase 2 (spot 2') and ribonucleoprotein (spot 51'), and repression of ferredoxin (spot 6') under salt stress.

The diagram shown in figure 14 highlights the benefits of H_2O_2 priming on the physiology and proteome of maize leaves under salinity. H_2O_2 priming not only reduced damage on growth, CO_2 assimilation (data not shown), and RWC, and favored less Na^+ accumulation in maize leaves, but also adjusted nine proteins not changed by salt stress and adjusted five proteins of the 38 proteins altered by salinity. The H_2O_2 priming upregulated two proteins [rubisco large subunit (spot 46') and fruit protein (spot 27')] previously downregulated by salinity; also, it downregulated the cysteine synthase (spot 29'), a stress-responsive protein, beforehand upregulated by salinity. The H_2O_2 priming suppressed ferredoxin (spot 6'), a redox homeostasis protein already downregulated by salt stress, and *de novo* synthesized the malate dehydrogenase 2, an energy metabolism protein previously suppressed by salt stress.

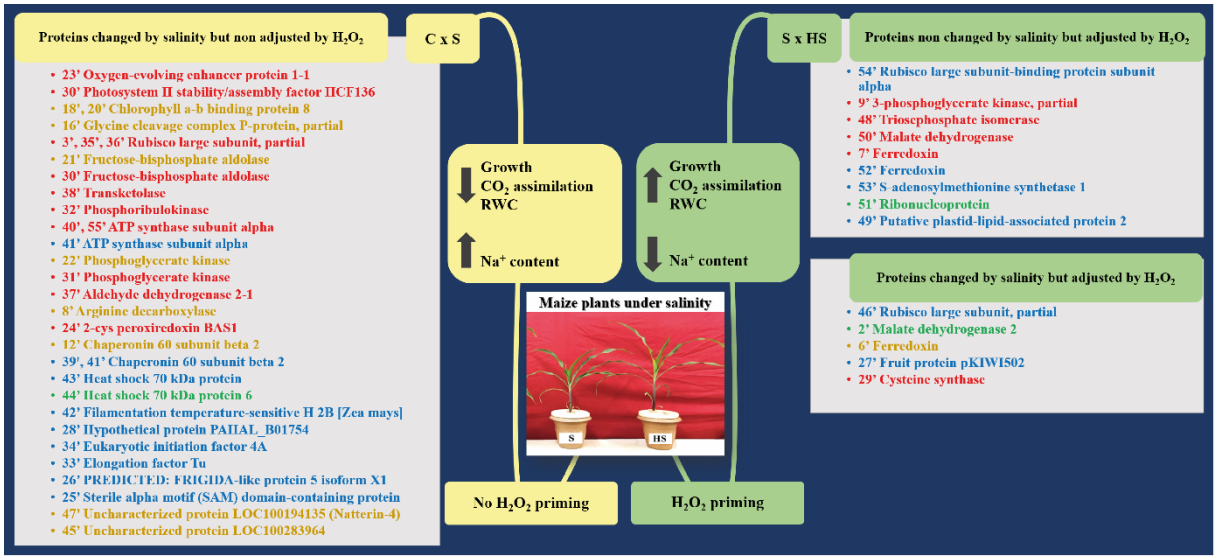

Figure 14. Diagram of impacts of H_2O_2 priming on the physiology, biochemistry, and proteomic profile of leaves from maize plants under salinity based on comparisons C x S and S x HS. The yellow text frames relate to the C x S comparison and highlight the salinity effects, while the green text frames relate to the S x HS comparison and highlight the H_2O_2 priming effects under salt conditions. The protein names in blue and red were significantly upregulated and downregulated, respectively. Also, the protein names in orange and green designate exclusive proteins that were suppressed and *de novo* synthesized, respectively. For more details, see Table 6.

7.4 Discussion

In this current study, salt stress caused drastic changes in maize plants, as shown by significant reductions in the leaf area, dry mass, RWC, and a remarkable increase in the Na^+/K^+ ratio (Figures 9, 11, and Table 4). However, there is evidence at H_2O_2 priming can mitigate such deleterious salt effects acting as a salinity acclimation inducer in maize and sunflower

(GONDIM *et al*. 2013; SILVA *et al*. 2019). Indeed, plants sprayed with H_2O_2 showed increases in RWC and reduced toxic Na^+ accumulation, followed by healthier phenotype and growth improvement under saline conditions compared to those plants without H_2O_2 priming (Figure 2). In another study, these same maize plants pretreated with H_2O_2 maintain normal levels of CO_2 assimilation even with low conductance in saline conditions (data not shown). Based on the beneficial effect of H_2O_2 priming in maize plants under salinity, the protein profiles and comparative analysis of the C, H, S, and HS treatments were performed to identify traits and regulatory mechanisms related to salt stress acclimation in maize plants. The C x H, C x S, and S x HS comparations showed 58 differentially synthesized proteins linked to diverse metabolic processes further discussed below (Figure 12 and Table 5).

7.4.1 *Responsive proteins to H_2O_2 priming*

H_2O_2 priming can produce a small oxidative burst that activates signaling networks in plants, and this allows the accumulation of latent defense proteins, which results in a primed state and induce protection to subsequent stresses (HOSSAIN *et al*., 2015). Indeed, H_2O_2 priming under no-saline conditions upregulated two proteins responsive to stress, lipoxygenase (spot 15') and FtsH6 - Zea mays FtsH protease (spot 1') in maize leaves, as well as synthesized de novo the NAD(P)-binding Rossmann-fold superfamily protein (spot 17') (Table 6, C x H comparison). These chloroplast proteins play an essential role in plant tolerance to multiple abiotic stressors and reflect a mechanism helping the plant cell to attenuate the detrimental effects of Na^+ on the photosynthetic machinery (Babenko et al. 2017). The increase of enzyme activities of lipoxygenase (spot 15') and FtsH6 - Zea mays FtsH protease (spot 1') has been correlated with rapid reactive oxygen species (ROS) scavenging and activation of defense-related marker genes (Zhao et al. 2016; Upadhyay et al. 2019). On the other hand, the NAD(P)-binding Rossmann-fold superfamily protein (spot 17'), that was synthesized *de novo*, can produce coenzyme $NAD(P)^+$ that is vital for proton transfer and energy reception in respiration that can reduce toxic substances accumulation (CHENG *et al*., 2016).

Proteins related to energy metabolism, such as phosphoenolpyruvate carboxykinase (spot 13') and malate dehydrogenase 2 (spot 2'), showed increased abundance by H_2O_2 priming in leaves from maize plants under no-saline conditions (Table 6, C x H comparison). These enzymes catalyze the conversion of oxaloacetate into phosphoenolpyruvate and CO_2, a critical step in the regulation of the metabolic flux toward gluconeogenesis, which provides an essential balance of reducing equivalents in the cytosol (SHAMEER *et al*., 2019). Interestingly, H_2O_2 priming also upregulated a glycine cleavage complex P-protein (spot 16') important to C3

plants through the photorespiration process. The glycine cleavage complex plays a critical role in the photorespiratory cycle by catalyzing two glycine molecules' conversion into serine (MAURINO; PETERHANSEL, 2010). This reaction releases CO_2, an essential and regulatory step of photorespiration and photosynthesis (TIMM *et al*. 2016; GIULIANI *et al*. 2019). Although the photorespiration in organisms with carbon-concentration mechanisms may be insignificant, C4 plants studies showed that photorespiration is essential for maintaining high photosynthesis (LEVEY *et al*., 2019). In which, mutants deficient of the photorespiratory enzymes, including maize plants, displayed a typical photorespiratory phenotype, exhibiting accelerated leaf senescence even under high CO_2. Thus, the photorespiratory pathway is essential in C4 plants as C3 plants. So, although the role of glycine cleavage complex P-protein (spot 16') needs to be better explored in plants C4, our results suggest that this protein's upregulation can be involved in priming action by H_2O_2 in maize plants.

Conversely, the H_2O_2 priming induced some similar proteomic changes the salinity without damage to growth such as to repress the proteins chlorophyll a-b binding protein 8 (spots 18' and 20'), fructose-bisphosphate aldolase (spot 21'), phosphoglycerate kinase (spot 22'), or downregulated others proteins negatively affected by salinity as rubisco large subunit (spot 3'), arginine decarboxylase (spot 8'), ferredoxin (spot 6'), chaperonin 60 subunit beta 2 (spot 12') (Table 6, C x H and C x S comparisons). Besides, the accumulation of crucial proteins, as stress-responsive protein, indicates that H_2O_2 priming may act as a stress elicitor in maize leaves, which is not surprising since H_2O_2 acts in signaling biotic and abiotic stimuli and mediating phytohormones action (ČERNÝ *et al*., 2018). Nevertheless, H_2O_2 priming positively affects metabolic pathways to preserve carbon fixation, energy metabolism, and oxidative stress defense without impacting plant growth despite negatively adjusting some proteins.

7.4.2 *Salt stress restraints diverse proteins related to carbon and energy metabolism and redox homeostasis*

Salinity severely affects photosynthesis/carbon metabolism that has critical importance for plant growth and development in many species (HOSSEINI *et al*. 2015; XIONG *et al*. 2017). Indeed, our results showed a decrease in plant growth and mass accumulation (Figures 1 and 2). The salt stress promoted a reduction of proteins related to the photosynthetic machinery such as oxygen-evolving enhancer protein (spot 23') and photosystem II stability/assembly factor HCF136 (spot 30') (Table 6, C x S comparison). Collectively, these proteins act as auxiliary components of photosystem II (PS II) and maintain their stability (LU, 2016). The dissociation of PSII complex reduces protein activities involved in the Calvin cycle, including isoforms of

rubisco large subunit (spots 3', 35', 36', and 46'), fructose-bisphosphate aldolase (spots 21' and 30'), transketolase (spot 38') and phosphoribulokinase (spot 32') which are insufficient to maintain CO_2 assimilation in leaves. Thus, the significant damage of salinity on photosynthesis, with a 24% reduction (data not shown), may due to the downregulation of PSII proteins that decrease carbon assimilation and impact maize growth and development, as also demonstrated by other studies with maize plants under salinity (ABREU *et al*., 2014; NOURI *et al*., 2015).

Salinity also provoked an alteration in proteins involved in energy metabolism, including reduction of alpha (spot 40') and beta (spot 55') ATP synthase subunits, and aldehyde dehydrogenase (spot 37') (Table 6, C x S comparison). The decrease of ATP synthase compounds impairs the generation of a proton gradient across the thylakoid membranes, once its activity is strongly repressed, the linear electron flow is highly restricted, and excess electron in the photosynthetic electron transport chain can lead to the production of ROS, and subsequently cause photodamage (KANAZAWA *et al*., 2017; TAKAGI *et al*., 2017). The reduction in aldehyde dehydrogenases negatively affects the removal of toxic aldehydes since these proteins function as aldehyde scavengers and thus play essential roles in stress responses on redox homeostasis (GUO *et al*., 2017; ZHAO *et al*., 2017). The salt stress repressed arginine decarboxylase (spot 8') and glycine cleavage complex P-protein (spot 16'). Arginine decarboxylase is involved in polyamine biosynthesis by putrescine production through direct decarboxylation of arginine. Polyamines, regulatory compounds in plant physiology, are involved in the stress-signaling scheme (WANG *et al*., 2019). Indeed, the accumulation of polyamines in maize and sorghum plants in salt conditions is genotype-dependent, in which the total polyamine content of the salt-tolerant genotype is higher than the salt-sensitive genotype (DU *et al*., 2018), mainly spermidine and spermine, suggesting that a decrease of polyamines precursors may defeat plant stress tolerance (FREITAS *et al*., 2018; OLIVEIRA *et al*., 2020). Further, the downregulation of the ferredoxin (spot 6'), a soluble protein that operates as electrons donor to different metabolic reactions, and the 2-cys peroxiredoxin (spot 24'), a protein that plays a crucial role in cellular ROS scavenging and participates in the transduction of redox signals, corroborates with the disruption of the redox state of maize plants in saline conditions (KAPOOR e*t al*., 2015; CALDERON *et al*., 2017). Also, the downregulation of fruit protein PKIWI502 (spot 27'), whose functions are related to FAD-dependent oxidoreduction, endorses the redox state's imbalance since this protein usually is upregulated in stress abiotic conditions (CHEN *et al*., 2014; KIM *et al*., 2014).

Conversely, salt stress induces different stress-responsive biomolecules as a part of their regulation in stressful environments. The cysteine synthase (spot 29'), a crucial enzyme for

mediating abiotic response by producing antioxidants and metal chelators, such as glutathione metallothionein and phytochelatin that protect the cellular environment from oxidative stress, was upregulated (LIU et al. 2016) (Table 6, C x S comparison). Additionally, chaperonins 60 subunit beta 2 (spots 39' and 41')] and heat shock protein (spots 43'), that were upregulated, and heat shock 70 kDa protein 6 (spot 44'), that was de novo synthesized, act in the stabilization of proteins and membranes, and can assist in protein refolding under stress conditions (JACOB *et al*., 2017; CHEN *et al*., 2018). Also, filamentation temperature-sensitive H 2B protein (spot 42'), a metalloprotease that functions in thylakoid membrane biogenesis and participates in the repair of PSII following damaged incurred during photoinhibition, was upregulated (KATO *et al*., 2012).

Some identified proteins in maize plants were attributed to protein synthesis, among them, initiation [eucaryotic initiation factor 4A (spot 34')] and elongation [elongation factor Tu (spot 33')] factors, sterile alpha motif (SAM) domain-containing protein (spot 25'), and PREDICTED: FRIGIDA-like protein 5 isoform X1 (spot 26') (Table 2). The upregulation of these proteins potentially gives the plants the ability to cope with salt stress by accelerating protein synthesis. Cellular response to environmental stress often leads to a change in cell state, explaining the enhanced biosynthesis or repair of salt-stressed proteins (AREFIAN *et al*. 2019). However, the protein biogenesis and degradation suggest that a complicated mechanism is involved in controlling protein metabolism under salinity. Overall, it was unable to mitigate the effects of salt stress in maize plants since these proteins' upregulation did not prevent Na^+ toxicity impairing the cell metabolism, photosynthetic and energetic processes. High Na^+ content in the cytosol can not only cause K^+ reduction, but it also affects various enzymatic processes that impose an energetic burden on the cell owing to the requirement of organic solute synthesis to compensate for the toxic ion exclusion for an osmotic adjustment (WU, 2018).

7.4.3 *H_2O_2 priming regulates crucial proteins and reduces the damage of salt stress in maize plants*

The proteins that participate in CO_2 assimilation, such as ribulose 1,5-bisphosphate carboxylase (spot 46') and rubisco large subunit-binding protein subunit alpha (spot 54'), were upregulated by H_2O_2 priming in plants exposed to salinity (Table 6, S x HS comparison). The upregulation of these proteins in maize plants was accompanied by the improvement of photosynthesis (data not shown) and, consequently, higher growth (Figures 9 and 10), minimizing the damage of salinity (SALESSE-SMITH *et al*., 2018). The plants pretreated with H_2O_2 also showed an adjustment in proteins of redox homeostasis once fruit protein pKIWI502

(spot 27') was upregulated, and adjustments were made on ferredoxin isoforms with the upregulation of the ferredoxin (spot 52'), the downregulation of the ferredoxin (spots 7'), and the repression of the ferredoxin (spots 6'). Moreover, H_2O_2 priming kept almost all proteins upregulated by salinity, downregulating only the cysteine synthase (spot 29') and upregulating another stress response protein, S-adenosylmethionine synthetase 1 (spot 53'), an essential enzyme to the synthesis of S-adenosylmethionine from methionine and ATP. It acts as a precursor for polyamine synthesis and as well as in the regulation of responses to abiotic stresses (SAHA *et al*., 2015). In agreement, overexpression of the S-adenosylmethionine synthetase gene has been directly related to enhanced salt tolerance by allowing high photosynthetic rates and biomass accumulation (MA *et al*., 2017). Furthermore, the ribonucleoprotein (spot 51') *de novo* synthesized can contribute a better response to environmental stress since it comprises a large family of RNA-binding proteins associated with mRNA metabolism, as well as a wide range of functions such as DNA repair, chromatin remodeling, telomere biogenesis, cell signaling, and development regulation (CIUZAN *et al*. 2015). Also, putative plastid-lipid-associated protein 2 (spot 49'), which was upregulated, can protect plants under stress conditions, preventing oxidation of thylakoid membranes (TAMBURINO *et al*., 2017).

The H_2O_2 priming in maize plants under salinity induced the downregulation of the 3-phosphoglycerate kinase (spot 9') and triosephosphate isomerase (spot 48'), proteins associated the glycolytic and metabolic processes, for adjusting energy metabolism (Table 6, S x HS comparison). Similar, plants that also abiotic stress-tolerant accumulated less protein related to energy metabolism than sensitive plants, which require the production of a large amount of ATP for stress tolerance (CHENG *et al*., 2016). Also, despite the downregulation of malate dehydrogenase (spot 50'), the malate dehydrogenase 2 (spot 2'), a mitochondrial isoenzyme, was synthesized de novo in the HS treatment, indicating a recovery from the repression caused by the salinity to this enzyme. Its activity is essential for mitochondrial redox state, which might regulate tricarboxylic acid cycle turnover. As observed in the C x S comparison (Table 6), the salt stress-induced repression of malate dehydrogenase 2 (spot 2') can promote photorespiratory perturbation resulting in the redox imbalance (LINDÉN *et al*., 2016). So, the H_2O_2 priming alleviated the effects deleterious of salinity by improving proteins involved in carbon assimilation, save energy, and maintain homeostasis redox in maize plants.

7.5 Conclusion

Although salinity increased stress-related proteins, it severely impacted several proteins related to energy and carbon metabolisms (Figure 14, left side). On the other hand, HS treatment recovered few proteins previously changed by salinity and up- and down-regulated some proteins that play a notable role in the face of salt stress (Figure 14, right side). H_2O_2 priming induced the proteome reprogramming, in which 14 proteins were relevant to improving adaptive tolerance mechanisms alleviating salt toxicity such as Na^+ reduction, growth preservation, and RWC increase. Among these, nine proteins were detected as new, and five were previously identified in the single salt treatment. However, all of them were adjusted by H_2O_2 pre-treatment, revealing an essential strategy to respond to salt stress efficiently. Highlighting malate dehydrogenase 2 (spot 2'), fruit protein pKIWI502 (spot 27'), putative plastid-lipid-associated protein 2 (spot 49'), and S-adenosylmethionine synthetase 1 (spot 53') that are related to the regulation of the tricarboxylic acid cycle, the redox homeostasis, the conservation of thylakoid membranes, and the biosynthesis of polyamines, the target molecules of different research on plant stress, respectively. This research provides new proteomic highlights to improve understanding and forward identifying biotechnological strategies to promote salt stress tolerance.

Acknowledgments

This work was supported by the Conselho Nacional de Desenvolvimento Científico e Tecnológico (CNPq), the Coodenação de Aperfeiçoamento de Pessoal de Nível Superior (CAPES), the Fundação Cearense de Apoio ao Desenvolvimento Científico e Tecnológico (FUNCAP).

8 CONSIDERAÇÕES FINAIS

A análise dos resultados fisiológicos, bioquímicos, estruturais, metabolômicos e proteômicos permitem revelar alguns mecanismos que as plantas de milho pré-tratadas com H_2O_2 usam para mitigar os efeitos prejudiciais do estresse salino. Redução do excesso de energia na maquinaria fotossintética e preservação da ultraestrutura dos cloroplastos foram essenciais para melhorar o desempenho fotossintético em plantas pré-tratadas sob salinidade. Adicionalmente, a modulação positiva de metabólitos, principalmente os envolvidos com o metabolismo de açúcares e aminoácidos, fornecem informações importantes relacionadas ao

restabelecimento da homeostase osmótica e redução do estresse oxidativo e, consequentemente, alivia os efeitos nocivos da salinidade. Por fim, reduções no acúmulo de íons Na^+ e a regulação de proteínas que participam de vias metabólicas associadas à fotossíntese e homeostase redox, que contribuem com o aumento do crescimento de plantas de pré-tratadas sob condições salinas.

O uso do pré-tratamento com H_2O_2 mostrou ser eficiente para aumentar a tolerância de plantas de milho à salinidade. Os resultados do presente estudo esclarecem informações sobre as respostas de defesa de plantas de milho pré-tratadas ao estresse salino, além disso, os dados encontrados poderão auxiliar na seleção de biomarcadores envolvidos na aclimatação dessas plantas à salinidade, os quais serão úteis para os programas de melhoramento genético dessa espécie.

REFERÊNCIAS

ABDELRAHEEM, A.; ESMAEILI, N.; O'CONNELLA, M.; ZHANGA, J. Progress and perspective on drought and salt stress tolerance in cotton. **Industrial Crops & Products**, [*s.l.*], v. 130, p.118-129, 2019.

ABREU, C.E.B.; ARAÚJO, G.S.; MOREIRA, A.N.O.M.; COSTA, J.H.; LEITE, H.B.; MORENO, F.B.M.B.; PRISCO, J.T.; GOMES-FILHO, E. Proteomic analysis of salt stress and recovery in leaves of *Vigna unguiculata* cultivars differing in salt tolerance. **Plant Cell Reports**, [*s.l.*], v. 33, p. 1289-1306, 2014.

AHMED M, HASANUZZAMAN M, RAZA MA, MALIK A, AHMAD S.Plant Nutrients for Crop Growth, Development and Stress Tolerance. In: Sustainable Agriculture in the Era of Climate Change. **Springer International Publishing**, Cham: Springer, p. 43-92, 2020.

AHUJA, I.; DE VOS, R.C.H.; BONES, A.M.; HALL, R.D. Plant molecular stress responses face climate change. **Trends in Plant Science**, [*s.l.*], v.15, n.12, p.664–674, 2010.

ALYEMENI, M.N. Plant Metabolites and Regulation Under Environmental Stress, **Academic Press**, [*s.l.*], p.281-309, 2018.

ANJUM, N.A. Plant acclimation to environmental stress: a critical appraisal. **Frontiers in Plant Science**, [*s.l.*], v. 6, p. 445, 2015.

ARAÚJO, G.S.; MIRANDA, R.S.; MESQUITA, R.O.; PAULA, S.O.; PRISCO, J.T.; GOMES- FILHO, E. Nitrogen assimilation pathways and ionic homeostasis are crucial for photosynthetic apparatus efficiency in salt-tolerant sunflower genotypes. **Plant Growth Regulation**, Dordrecht, v.86, p.375, 2018.

AREFIAN, M.; VESSAL, S.; MALEKZADEH-SHAFAROUDI, S.; SIDDIQUE, K.H.M.; BAGHERI, A. Comparative proteomics and gene expression analyses revealed responsive proteins and mechanisms for salt tolerance in chickpea genotype. **BMC Plant Biology**, [*s.l.*], v. 19, p. 300, 2019.

ASHFAQUE, F.; KHAN, M.I.R.; KHAN, N.A. Exogenously applied H_2O_2 promotes proline accumulation, water relations, photosynthetic efficiency and growth of wheat (*Triticuma estivum* L.) under salt stress. **Annual Research & Review in Biology**, [*s.l.*], v.4, p. 105–120, 2014.

ASHRAF, M.; ATHAR, H. R.; HARRIS, P. J. C.; KWON, T. R. Some prospective strategies for improving crop salt tolerance. **Advances in Agronomy**, [*s.l.*], v. 97, p. 45-110, 2008.

ASHRAF, M.A.; AKBAR, A.; ASKARI, S.H.; IQBAL, M.; RASHEED, R.; HUSSAIN, I. Recent Advances in Abiotic Stress Tolerance of Plants Through Chemical Priming: An Overview, in: Adv. Seed Priming, Springer Singapore, Singapore, p. 51–79, 2018.

AZEVEDO-NETO, A.D.; PRISCO, J.T.; ENÉAS-FILHO, J.; LACERDA, C.F.; SILVA, J.V.; COSTA, P.H.A.; GOMES-FILHO, E. Effects of salt stress on plant growth, stomatal response

and solute accumulation of different maize genotypes. **Brazilian Journal of Plant Physiology**, Munich, v.16, p.31-38, 2004.

BABENKO L.M.; SHCHERBATIUK M.M.; SKATERNA T.D.; KOSAKIVSKA I.V. Lipoxygenases and their metabolites information of plant stress tolerance. Ukrainian. Biochemical Journal, v. 89, p. 5-21, 2017.

BAGHERI, M.; GHOLAMI, M.; BANINASAB, B. Hydrogen peroxide-induced salt tolerance in relation to antioxidant systems in pistachio seedlings. **Scientia Horticulturae**, Amsterdam, v. 243, p. 207-213, 2019.

BATISTA, V.C.V.; PEREIRA, I.M.C.; PAULA-MARINHO, S.O.; CANUTO, K.M.; PEREIRA, R.C.A.; RODRIGUES, T.H.S.; DALOSO, D.M.; GOMES-FILHO, E.; CARVALHO, H.H. Salicylic acid modulates primary and volatile metabolites to alleviate salt stress-induced photosynthesis impairment on medicinal plant *Egletes viscosa*. **Environmental and Experimental Botany**, Amsterdam, v. 167, p. 103870, 2019.

BERTINI, L.; PALAZZI, L.; PROIETTI, S.; POLLASTRI, S.; ARRIGONI, G.; POLVERINO DE LAURETO, P.; CARUSO, C. Proteomic analysis of meja-induced defense responses in rice against wounding. **International Journal of Molecular Sciences**, [*s.l.*], v. 20, p. 2525, 2019.

BILGER, W.; SCHREIBER, U.; BOCK, M. Determination of the quantum efficiency of photosystem II and non-photochemical quenching of chlorophyll fluorescence in the field. **Oecologia**, [*s.l.*], v.102, p.425-432, 1995.

BISTGANI, Z.E.; HASHEMI, M.; DACOSTA, M. ; CRAKER, L.; MAGGI, F.; MORSHEDLOO, M.R. Effect of salinity stress on the physiological characteristics, phenolic compounds and antioxidant activity of *Thymus vulgaris* L. and *Thymus daenensis* Celak. **Industrial Crops & Products**, [*s.l.*], v. 135, p. 311–320, 2019.

BOLOURI-MOGHADDA, M.R.; ROY, K.L.; XIANG, L.; ROLLAND, F.; ENDE, W.V. Sugar signalling and antioxidant network connections in plant cells. **FEBS Journal**, v.277, p.2022–2037, 2010.

BORGES R.; MIGUEL, E.C.; DIAS, J.M.R.; DA CUNHA, M.; BRESSAN-SMITH, R.E.; DE OLIVEIRA, J.G.; DE SOUZA FILHO, G.A. Ultrastructural, physiological and biochemical analyses of chlorate toxicity on rice seedlings, **Plant Science**, Shannon, v. 166, p. 1057–1062, 2004.

BORRELLI, G.M.; FRAGASSO, M.; NIGRO, F.; PLATANI, C.; PAPA, R.; BELEGGIA, R.; TRONO, D. Analysis of metabolic and mineral changes in response to salt stress in durum wheat (*Triticum turgidum* ssp. *durum*) genotypes, which differ in salinity tolerance. **Plant Physiology and Biochemistry**, Paris, v.133, p.57–70, 2018.

BRADFORD, M.M. A rapid and sensitive method for the quantification of microgram quantities of protein utilizing the principle of dye binding. **Analytical Biochemistry**, Cambridge, v.72, p.248-254, 1976.

BRUCE, T.J.A.; MATTHES, M.C.; NAPIER, J.A.; PICKETT, J.A. Stressful "memories" of plants: evidence and possible mechanisms. **Plant Science**, Shannon, v. 173, p. 603-608, 2007.
BUDAK, H.; AKPINAR, B.A.; UNVER, T.; TURKTAS, M. Proteome changes in wild and modern wheat leaves upon drought stress by two-dimensional electrophoresis and nanoLC-ESI–MS/MS. **Plant Molecular and Biology**, [*s.l.*], v. 83, p.89–103, 2013.

CALDERÓN, A.; LÁZARO-PAYO, A.; IGLESIAS-BAENA, I.; CAMEJO, D.; LÁZARO, J.J.; SEVILLA, F.; JIMÉNEZ, A. Glutathionylation of pea chloroplast 2- Cys Prx and mitochondrial Prx IIF affects their structure and peroxidase activity and sulfiredoxin deglutathionylates only the 2-Cys Prx. **Frontiers in Plant Science**, [*s.l.*], v. 8, p. 118, 2017.

CALLISTER, A.N.; ARNDT, S.K.; ADAMS, M.A. Comparison of four methods for measuring osmotic potential of tree leaves. **Physiologia Plantarum**, [s.l.], v. 127, p.383-392, 2006.

CATALDO, D.A.; HAROON, M.; SCHRADER, L.E.; YOUNGS, V.L. Rapid col- orimetric determination of nitrate in plant tissue by nitration of salicylic acid. **Communications in Soil Science and Plant Analysis**, [*s.l.*], v.6, p.71–80, 1975.

CATSKY, J. Determination of water deficits in disc cut out from leaf blades. **Biologia Plantarum**, [*s.l.*], v. 2, p. 929- 938, 1960.

ČERNÝ, M.; HABÁNOVÁ, H.; BERKA, M.; LUKLOVÁ, M.; BRZOBOHATÝ, B. Hydrogen peroxide: its role in plant biology and crosstalk with signalling networks. **Internacional Journal of Molecular Sciences**, Basel, v. 19, p. 2812, 2018.

CHEESEMAN, J.M. Hydrogen peroxide concentrations in leaves under natural conditions. **Journal of Experimental Botany**, [*s.l.*], v.57, n.10, p.2435-2444, 2006.

CHEN, Y.U.; CHEN, X.I.; WANG, H.; BAO, Y.; ZHANG, W. Examination of the leaf proteome during flooding stress and the induction of programmed cell death in maize. **Proteome Science**, [*s.l.*], v.12, p.33, 2014.

CHEN, Z.; ZHU, D.; WU, J.; CHENG, Z.; YAN, X.; DENG, X.; YAN, Y. Identification of differentially accumulated proteins involved in regulating independent and combined osmosis and cadmium stress response in Brachypodium seedling roots. **Scientific Reports**, [*s.l.*], v. 8, p.7790, 2018.

CHENG, L.; WANG, Y.; HE, Q.; LI, H.; ZHANG, X.; ZHANG, F. Comparative proteomics illustrates the complexity of drought resistance mechanisms in two wheat (*Triticum aestivum* L.) cultivars under dehydration and rehydration. **BMC Plant Biology**, [*s.l.*], v.16, p.188, 2016.

CHOUDHURY, F.K; RIVERO, R.M; BLUMWALD, E.; MITTLER, R. Reactive oxygen species, abiotic stress and stress combination. **The Plant Journal**, [*s.l.*], v. 90, p. 856-867, 2017.

CIUZAN, O.; HANCOCK, J.; PAMFIL, D.; WILSON, I.; LADOMERY, M. The evolutionarily conserved multifunctional glycine-rich RNA-binding proteins play key roles in development and stress adaptation. **Physiology Plant**, [*s.l.*], v.153, p.1–11, 2015.

DAS, P.; NUTAN, K.K.; SINGLA-PAREEK, S.L.; PAREEK, A. Oxidative environment and redox homeostasis in plants: dissecting out significant contribution of major cellular organelles. **Frontiers in Environmental Science**, Paris, v. 2, p. 70, 2015.

DEBNATH, M.; ASHWATH, N.; HILL, C.B.; CALLAHAN, D.L.; DIAS, D.A.; JAYASINGHE, N.S.; MIDMORE, D.J.; ROESSNER, U. Comparative metabolic and ionomic profiling of two cultivars of *Stevia rebaudiana* Bert. (Bertoni) grown under salinity stress. **Plant Physiology and Biochemistry**, Paris, v.129, p. 56–70, 2018.

DOUBNEROVÁ, V.; RYŠLAVÁ, H. What can enzymes of C_4 photosynthesis do for C_3 plants under stress? **Plant science**, Shannon, v. 180, n.4, p.575-83, 2011.

DU, J.; GUO, S.; SUN, J.; SHU, S. Proteomic and physiological analyses reveal the role of exogenous spermidine on cucumber roots in response to Ca(NO3)2 stress. **Plant Molecular Biology**, [*s.l.*], v. 97, p.1–21, 2018.

ECHEVARRÍA, C.; PACQUIT, V.; BAKRIM, N.; OSUNA, L.; DELGADO, B.; ARRIO-DUPONT, M.; VIDAL, J. The effect of pH on the covalent and metabolic control of C4 phosphoenolpyruvate carboxylase from Sorghum leaf. **Archives of Biochemistry and Biophysics**, [*s.l.*], v.315, p.425-430, 1994.

FERNANDO, C.D.; SOYSA, P. Optimized enzymatic colorimetric assay for determination of hydrogen peroxide (H_2O_2) scavenging activity of plant extracts. **Methods X**, [*s.l.*], p. 283-291, 2015.

FILIPPOU, P.; TANOU, G.; MOLASSIOTIS, A.; FOTOPOULOS, V. Plant acclimation to environmental stress using priming agents. In: TUTEJA, N.; GILL, S.S. (Ed.). **Plant acclimation to environmental stress**. New York: Springer Science Business Media, p. 1-27, 2013.

FOOD AND AGRICULTURE ORGANIZATION (FAO). Electronic forum on biotechnology in food and agriculture: conference 15: Statistical Databases. [WWW Document]. URL. (Accessed November 2019). http://www.fao.org/ /biotech/C15doc.htm, 2019.

FOOD AND AGRICULTURE ORGANIZATION (FAO).The role of agricultural biotechnologies for production of bioenergy in developing countries. In: FAO Biotechnol. Forum. (Accessed May 2018). http://www.fao.org/biotech/C15doc.htm, 2008.

FREITAS, V.S.; MIRANDA, R.S.; COSTA, J.H.; OLIVEIRA, D.F.; PAULA, S.O.; MIGUEL, E.C.; FREIRE, R.S.; PRISCO, J.T.; GOMES-FILHO, E. Ethylene triggers salt tolerance in maize genotypes by modulating polyamine catabolism enzymes associated with H_2O_2 production. **Environmental and Experimental Botany**, Amsterdam, v. 145, p. 75–86, 2018.

FRUKH, A.; AHMAD, A.; SIDDIQI, T.O. Chapter 31: Proteomics Insights Into Salt Stress Signaling in Plants. In: KHAN, M.I.K.; REDDY, P.S.; FERRANTE, A.; KHAN, N.A. Plant signaling molecules. **Woodhead Publishing**, p.479-498, 2019.

GANGOLA, M.P.; RAMADOS, B.R. Chapter 2 - Sugars play a critical role in abiotic stress tolerance in plants. In: WANI, S.H. Biochemical, physiological and molecular avenues for combating abiotic stress in plants. **Academic Press**, [*s.l.*], p.12-38, 2018.

GAO, Y.; GUO, Y.K.; LIN, S.H.; FANG, Y.Y.; BAI, J.G. Hydrogen peroxide pretreatment alters the activity of antioxidant enzymes and protects chloroplast ultrastructure in heat-stressed cucumber leaves. **Scientia Horticulturae**, Amsterdam, v.126, p.20-26, 2010.

GAUFICHON, L.; REISDORF-CREN, M.; ROTHSTEIN, S.J.; CHARDON, F.; SUZUKI, A. Biological functions of asparagine synthetase in plants. **Plant Science**, Shannon, v.179, p.141–153, 2010.

GIULIANI, R.; KARKI, S.; COVSHOFF, S.; LIN, H.C.; COE, R.A.; KOTEYEVA, N.K.; QUICK, W.P.; VON CAEMMERER, S.; FURBANK, R.T.; HIBBERD, J.M.; EDWARDS, G.E.; COUSINS, A.B. Knockdown of glycine decarboxylase complex alters photorespiratory carbon isotope fractionation in *Oryza sativa* leaves. **Journal of Experimental Botany**, [*s.l.*], v.70, n.10, p.2773–2786, 2019.

GONDIM, F.A., MIRANDA, R.S., GOMES-FILHO, E.; PRISCO, J.T. Enhanced salt tolerance in maize plants induced by H_2O_2 leaf spraying is associated with improved gas Exchange rather than with non-enzymatic antioxidante system. **Theoretical and Experimental Plant Physiology**, [*s.l.*], v. 25, p. 251–260, 2013.

GONDIM, F.A.; GOMES-FILHO, E.; COSTA, J.H.; ALENCAR, N.L.M.; PRISCO, J.T. Catalase plays a key role in salt stress acclimation induced by hydrogen peroxide pretreatment in maize. **Plant Physiology and Biochemistry**, Paris, v.56, p.62-71, 2012.

GONZÁLEZ-BOSCH, C. Priming plant resistance by activation of redox-sensitive genes. **Free Radical Biology and Medicine**, v.122, p.171-180, 2018.

GUO, X.; WANG, Y.; LU, H. CAI, X.; WANG, X.; ZHOU, Z.; WANG, C.; WANG, Y, ZHANG, Z.; WANG, K. LIU, F.Genome-wide characterization and expression analysis of the aldehyde dehydrogenase (ALDH) gene superfamily under abiotic stresses in cotton. **Gene**, [*s.l.*], v. 628, p. 230-245, 2017.

HAKEEM, K.R.; CHANDNA, R.; ULREHMAN, R.; TAHIR, I.; SABIR, M.; IQBAL, M. Unravelling salt stress in plants through proteomics. Salt Stress in Plants. New York: **Springer**, p. 47-61, 2013.

HASANUZZAMAN, M.; NAHAR, K.; GILL, S.S.; ALHARBY, H.F.; RAZAFINDRABE, B.H.N.; FUJITA, M. Hydrogen peroxide pretreatment mitigates cadmium-induced oxidative stress in *Brassica napus*: an intrinsic study on antioxidant defense and glyoxalase systems. **Frontiers in Plant Science**, [*s.l.*], v. 8, p.115, 2017.

HASSINI, I.; RIOS, J.J.; GARCIA-IBAÑEZ, P.; BAENAS, N.; CARVAJAL, M.; MORENO, D.A. Comparative effect of elicitors on the physiology and secondary metabolites in broccoli plants. **Journal of Plant Physiology**, Munich, v. 239, p. 1-9, 2019.

HOAGLAND, D.R.; ARNON, D.I. **The water-cultured method for growing plants without soil**. California: California Agricultural Experiment Station, Circular nº 37, 32 p., 1950.

HOSSAIN, M. A.; BHATTACHARJEE, S.; ARMIN, S. M.; QIAN, P.; XIN, W.; LIH, Y.; BURRITT, D. J.; FUJITA, M.; TRAN, L. Hydrogen peroxide priming modulates abiotic oxidative stress tolerance: insights from ROS detoxification and scavenging. **Frontiers in Plant Science**, [*s.l.*], v.6, p. 420, 2015.

HOSSAIN, M.S.; PERSICKE, M.; ELSAYED, A.I.; KALINOWSKI, J.; DIETZ, K.J. Metabolite profiling at the cellular and subcellular level reveals metabolites associated with salinity tolerance in sugar beet. **Journal of Experimental Botany**, [*s.l.*], v.68, p.5961-5976, 2017.

HOSSEINI, S.A.; GHARECHAHI, J.; HEIDARI, M.; KOOBAZ, P.; ABDOLLAHI, S.; MIRZAEI, M.; NAKHODA, B.; SALEKDEH, G.H. Comparative proteomic and physiological characterisation of two closely related rice genotypes with contrasting responses to salt stress. **Functional Plant Biology**, [*s.l.*], v.42, p.527–542, 2015.

HOU, Q.Z.; WANG, Y.P.; LIANG, J.Y.; JIA, L.Y.; FENG, H.Q.; WEN, J.; EHMET, N.; BAI, J.Y. H_2O_2-induced acclimation of photosystem II to excess light is mediated by alternative respiratory pathway and salicylic acid. **Photosynthetica**, [*s.l.*], v. 56, p. 1154-1160, 2018.

HUANG, C.; WEI, G.; JIE, Y.; WANG, L.; RAN, H. Z. C.; HUANG, Z.; JIA H.; ANJUM, S. A. Effects of concentrations of sodium chloride on photosynthesis, antioxidative enzymes, growth and fiber yield of hybrid ramie. **Plant Physiology and Biochemistry**, Paris, v.76, p. 86-93, 2014.

HYSKOVÁA, V.D.H.; NSKAA, L.M.; DOBRÁB, J.; VANKOVAB, R.; RYSLAVÁA, H. Phosphoenolpyruvate carboxylase, NADP-malic enzyme, and pyruvate, phosphate dikinase are involved in the acclimation of *Nicotiana tabacum* L. to drought stress. **Journal of Plant Physiology**, Munich, v.171, p.19-25, 2014.

IGAMBERDIEV, A.U.; KLECZKOWSKI, L.A. The glycerate and phosphorylated pathways of serine synthesis in plants: the branches of plant glycolysis linking carbon and nitrogen metabolism. **Frontiers in Plant Science**, [*s.l.*], v.9, p.318, 2018.

ISAH, T. Stress and defense responses in plant secondary metabolites production. **Biological Research**, [*s.l.*], v.52, p.39, 2019.

ISAYENKOV, S.V.; MAATHUIS, F.J.M. Plant salinity stress: many unanswered questions remain. **Frontiers in Plant Science**, [*s.l.*], v.10, p.80, 2019.

JACOB, P.; HIRT, H.; BENDAHMANE, A. The heat-shock protein/chaperone network and multiple stress resistance. **Plant Biotechnology Journal**, [*s.l.*], v.15, p. 405–414, 2017.

JIAO, Y.; BAI, Z.; XU, J. M. ; ZHAO, Y.; KHAN, Y., HU, L. SHI, Metabolomics and its physiological regulation process reveal the salt-tolerant mechanism in *Glycine soja* seedling roots, **Plant Physiology and Biochemistry**, Paris, v. 126, p. 187–196, 2018.

KALAJI, H.M.; JAJOO, A.; OUKARROUM, A.; BRESTIC, M.; ZIVCAK, M.; SAMBORSKA, I.A.; CETNER1, M.D.; GOLTSEV, I.L.V.; LADLE, R.J. Chlorophyll a fluorescence as a tool to monitor physiological status of plants under abiotic stress conditions. **Acta Physiology Plant**, [*s.l.*], v.38, p.102, 2016.

KANAZAWA, A.; OSTENDORF, E.; KOHZUMA, K.; HOH, D.; STRAND, D.D.; SATO-CRUZ, M.; SAVAGE, L.; CRUZ, J.A.; FISHER, N.; FROEHLICH, J.E.; KRAMER, D.M. Chloroplast ATP synthase modulation of the thylakoid proton motive force: implications for photosystem I and photosystem II photoprotection. **Frontiers in Plant Science**, [*s.l.*], v.8, p.719, 2017.

KAPOOR, D.; SHARMA, R.; HANDA, N.; KAUR, H.; RATTAN, A.; YADAV, P.; GAUTAM, V.; KAUR, R.; BHARDWAJ, R. Redox homeostasis in plants under abiotic stress: role of electron carriers, energy metabolism mediators and proteinaceous thiols. **Frontiers in Environmental Science**, [*s.l.*], Paris, v. 3, p. 13, 2015.

KATO, Y.; SUN, X.; ZHANG, L.; SAKAMOTO, W. Cooperative D1 degradation in the photosystem II repair mediated by chloroplastic proteases in *Arabidopsis*. **Plant Physiology**, [*s.l.*], v.159, p.1428–1439, 2012

KHAN, H.A.; SIDDIQUE, K.H.M; MUNIR, R.; COLMER, T.D. Salt sensitivity in chickpea: Growth, photosynthesis, seed yield components and tissue ion regulation in contrasting genotypes. **Journal of Plant Physiology**, Munich, v. 182, p. 1–12, 2015.

KHAN, M.I.R.; KHAN, N.A.; MASOOD, A.; PER, T.S.; ASGHER, M. Hydrogen peroxide alleviates nickel-inhibited photosynthetic responses through increase in use-efficiency of nitrogen and sulfur, and glutathione production in mustard. **Frontier in Plant Science**, [*s.l.*], v.7, p.44, 2016.

KHAN, M.N.; SIDDIQUI, M.H.; MOHAMMAD, F.; NAEEM, M. Interactive role of nitric oxide and calcium chloride in enhancing tolerance to salt stress. **Nitric Oxide**, [*s.l.*], v. 27, n. 4, p. 210-218, 2012.

KIM, S.G.; BAE, H.H.; JUNG, H.J.; LEE, J.S.; KIM, J.T.; GO, T.H.; SON, B.Y.; BAEK, S.B.; KWON, Y.U.; WOO, M.O.; SHIN, S. Physiological and protein profiling response to drought stress in KS141, a Korean maize inbred line. **Journal of Crop Science and Biotechnology**, [*s.l.*], v. 17, p. 273–280, 2014.

KLEIN, A.; HÜSSELMANN, L.; KEYSTER, M.; LUDIDI, N. Exogenous nitric oxide limits salt-induced oxidative damage in maize by altering superoxide dismutase activity. **South African Journal of Botany**, [*s.l.*], v.115, p. 44-49, 2018.

KOYRO, H.; HUCHZERMEYER, B. Chapter 14 - Coordinated regulation of photosynthesis in plants increases yield and resistance to different types of environmental stress. In: AHMAD, P.; AHANGER, M.A.; SINGH, V.P.; TRIPATHI, D.K.; ALAM, P.; LEVEY, M.; TIMM, S.; METTLER-ALTMANN, T.; BORGHI G.L.; KOCZOR, M.; ARRIVAULT, S.; WEBER, A.P.M.; BAUWE, H.; GOWIK, U.; WESTHOFF, P. Efficient 2-phosphoglycolate degradation is required to maintain carbon assimilation and allocation in the C4 plant *Flaveria bidentis*. **Journal of Experimental Botany**, [*s.l.*], v 70, p.575–587, 2019.

LINDÉN, P.; KEECH, O.; STENLUND, H.; GARDESTRÖM, P. MORITZ, T. Reduced mitochondrial malate dehydrogenase activity has a strong effect on photorespiratory metabolism as revealed by 13C labelling. **Journal of Experimental Botany**, [*s.l.*], v.67, n.10 p. 3123–3135, 2016

LISEC, J.; SCHAUER, N.; KOPKA, J.; WILLMITZER, L.; FERNIE, A.R. Gas chromatography mass spectrometry–based metabolite profiling in plants. **Nature Protocols**, [*s.l.*], v.1, p.387–396, 2006.

LIU, X.; YU, W.; WANG, G.; CAO, F.; CAI, J.; WANG, H. Comparative proteomic and physiological analysis reveals the variation mechanisms of leaf coloration and carbon fixation in a xantha mutant of *Ginkgo biloba* L. **International Journal of Molecular Science**, [*s.l.*], v.17, n.11, p.1794, 2016.

LIU, Z.; CHENG, R.; XIAO, W.; GUO, Q.; WANG, N. Effect of off-season flooding on growth, photosynthesis, carbohydrate partitioning, and nutrient uptake in *Distylium chinense*. **PLoS One**, [*s.l.*], v.9, n.9, e107636, 2014.

LJUNG, K.; NEMHAUSER, J.L.; PERATA, P. New mechanistic links between sugar and hormone signalling networks. **Current Opinion in Plant Biology**, [*s.l.*], v.25, p.130–137, 2015.

LLANES, A.; ANDRADE, A.; ALEMANO, S.; LUNA, V. Metabolomic approach to understand plant adaptations to water and salt stress. In: AHMAD, P.; AHANGER, LONG, R.; GAO, Y.; SUN, H.; ZHANG, T.; LI, X.; LI, M.; SUN, Y.; KANG, J.; WANG, Z.; DING, W.; YANG, Q. Quantitative proteomic analysis using iTRAQ to identify salt-responsive proteins during the germination stage of two Medicago species. **Scientific Reports**, [*s.l.*], v. 8, p. 9553, 2018.

LOPES, L.S.; CARVALHO, H.H.; MIRANDA, R.S.; GALLÃO, M.I.; GOMES-FILHO, E. The influence of dissolved oxygen around rice roots on salt tolerance during pre-tillering and tillering phases. **Environmental and Experimental Botany**, Amsterdam, p. 104169, 2020.

LOPES, L.S.; PRISCO, J.T.; GOMES-FILHO, E. Inducing salt tolerance in castor bean through seed priming. **Australian Journal of Crop Science**, [*s.l.*], v. 12, p. 943–953, 2018.

LU, Y. Identification and roles of photosystem ii assembly, stability, and repair factors in arabidopsis. **Frontiers in Plant Science**, [*s.l.*], v.7, p.168, 2016.

M.A.; SINGH, V.P.; TRIPATHI, D.K.; ALAM, P.; ALYEMEN, M.N. Plant Metabolites and Regulation Under Environmental Stress, **Academic Press**, [*s.l.*], p.133-144, 2018.

MA, C.; WANG, Y.; GU, D.; NAN, J.; CHEN, S.; LI, H. Overexpression of s-adenosyl-l-methionine synthetase 2 from sugar beet m14 increased arabidopsis tolerance to salt and oxidative stress. **International Journal of Molecular Science**, [*s.l.*], v.18, p.847, 2017.

MALAVOLTA, E.; VITTI, G. C.; OLIVEIRA, S.A. Avaliação do estado nutricional das plantas: Princípios e Aplicações. Associação Brasileira para Pesquisa da Potassa e do Fosfato, Piracicaba, 1989.

MAURINO, V.G.; PETERHANSEL, C. Photorespiration: current status and approaches for metabolic engineering. **Current Opinion in Plant Biology**, [*s.l.*], v.13, p.249–256, 2010.

MESQUITA, R. O.; SOARES, E. A.; BARROS, E. G.; LOUREIRO, M. E. Method optimization for proteomic analysis of soybean leaf: improvements in identification of new and low-abundance proteins. **Genetics and Molecular Biology**, [*s.l.*], v. 35, p. 353-361, 2012

MHLONGO, M.I.; STEENKAMP, P.A.; PIATER, L.A.; MADALA, N.E.; DUBERY, I.A. Profiling of altered metabolomic states in *nicotiana tabacum* cells induced by priming agents, **Frontiers in Plant Science**, [*s.l.*], v. 7, p. 1527, 2016.

MIRANDA, R.S.; ALVAREZ-PIZARRO, J.C.; ARAÚJO, C.M.S.; PRISCO, J.T.; GOMES-FILHO, E. Influence of inorganic nitrogen sources on K^+/Na^+ homeostasis and salt tolerance in sorghum plants. **Acta Physiologiae Plantarum**, [*s.l.*], v. 35, p. 841-852, 2013.

MIRANDA, R.S.; MESQUITA, R.O.; FREITAS, N.S.; PRISCO, J.T.; GOMES-FILHO, E. Nitrate: ammonium nutrition alleviates detrimental effects of salinity by enhancing photosystem II efficiency in sorghum plants. **Revista Brasileira de Engenharia Agrícola e Ambiental**, Campina Grande, v. 18, p. 8–12, 2014.

MOURTZINIS, S.; CANTRELL, K.B.; ARRIAGA, F.J.; BALKCOM, K.S.; FREDERICK, J.R.; KARLEN, D.L. Carbohydrate and nutrient composition of corn stover from three southeastern USA locations. **Biomass and Bioenergy**, [*s.l.*], v. 85, p-153-158, 2016.

MÜLLER, P.; LI, X.P.; NIYOGI, K.K. Non-Photochemical Quenching. A Response to Excess Light Energy. **Plant Physiology**, [s.l.], v. 125, p. 1558–1566, 2001.

MURPHY, M.P.; O'NEILL, L.A.J. Krebs Cycle reimagined: the emerging roles of succinate and itaconate as signal transducers. **Cell**, [*s.l.*], v.174, n.4, p.780-784, 2018.

NEUHOFF, V.; AROLD, N.; TAUBE, D.; EHRHARD, T.W. Improved staining of proteins in polyacrylamide gels including isoelectric focusing gels with clear background at nanogram sensitivity using Coomassie Brilliant Blue G-250 and R-250. **Electrophoresis**, [*s.l.*], v.9, p.255–262, 1988.

NOURI, M.Z.; MOUMENI, A.; KOMATSU, S. Abiotic stresses: insight into gene regulation and protein expression in photosynthetic pathways of plants. **International Journal of Molecular Science**, [*s.l.*], v.16, p.20392-20416, 2015

O'LEARY, B.; PARK, J.; PLAXTON, W.C. The remarkable diversity of plant PEPC (phospho-enolpyruvate carboxylase): recent insights into the physiological functions and post-translational controls of non-photosynthetic PEPCs. **Biochemistry Journal**, [*s.l.*], v.436, p.15–34, 2011.

OLIVEIRA, D.F.; LOPES, L.S.; GOMES-FILHO, E. Metabolic changes associated with differential salt tolerance in sorghum genotypes. **Planta**, Heidelberg, v. 252, p. 34, 2020a

OLIVEIRA, F.D.B.; MIRANDA, R.S.; ARAÚJO, G.S.; COELHO, D.G.; LOBO, M.D.P.; PAULA-MARINHO, S.O.; LOPES, L.S.; MONTEIRO-MOREIRA, A.C.O.; CARVALHO,

H.H.; GOMES-FILHO, E. New insights into molecular targets of salt tolerance in sorghum leaves elicited by ammonium nutrition. **Plant Physiology and Biochemistry**, Paris, v. 154, p. 723–734, 2020b.

POÓR, P.; CZÉKUS, Z.; ÖRDÖG, A. Chapter 12 - Role and regulation of glucose as a signal molecule to salt stress. In: KHAN, M.I.K.; REDDY, P.S.; FERRANTE, A.; KHAN, N.A. Plant signaling molecules. **Woodhead Publishing**, p.193-205, 2019.

RICHTER, J.A.; ERBAN, A.; KOPKA, J.; ZÖRB, C. Metabolic contribution to salt stress in two maize hybrids with contrasting resistance. **Plant Science**, Shannon, v. 233, p.107–115, 2015.

ROESSNER-TUNALI, U.; LUEDEMANN, A.; BRUST, D.; FIEHN, O.; LINKE, T.; WILLMITZER, L.; FERNIE, A.R. Metabolic profiling allows comprehensive phenotyping of genetically or environmentally modified plant systems. **The Plant Cell Online**, [*s.l.*], v.13, p.11–29, 2001.

SABAGH, A. EL; HOSSAIN, A.; AAMIR IQBAL, M.; BARUTÇULAR, C.; ISLAM, M.S.; ÇIĞ, F.; ERMAN, M.; SYTAR, O.; BRESTIC, M.; WASAYA, A.; JABEEN, T.; ASIF BUKHARI, M.; M. MUBEEN, H.-R. ATHAR, F. AZEEM, H. AKDENIZ, Ö. KONUŞKAN, F. KIZILGECI, M. IKRAM, S. SOROUR, W. NASIM, M. ELSABAGH, M. RIZWAN, R. SWAROOP MEENA, S. FAHAD, A. UEDA, L. LIU, H. SANEOKA, Maize Adaptability to Heat Stress under Changing Climate, in: **Plant Stress Physiology** [Working Title].

SAGE, R.F. The evolution of C_4 photosynthesis. **New Phytologist**, [*s.l.*], v.161, p. 341-370, 2004.

SAHA, J.; BRAUER, E.K.; SENGUPTA, A.; POPESCU, S.C.; GUPTA, K.; GUPTA, B. Polyamines as redox homeostasis regulators during salt stress in plants. **Frontiers in Environmental Science**, Paris, v. 3, p. 21, 2015.

SALESSE-SMITH, C.E.; SHARWOOD, R.E.; BUSCH, F.A.; KROMDIJK, J.; BARDAL, J.; STERN, D.B. Overexpression of rubisco subunits with RAF1 increases rubisco content in maize. **Nature Plants**, [*s.l.*], v. 802, n.4, p. 802–810, 2018.

SANCHEZ, D.H.; LIPPOLD, F.; REDESTIG, H.; HANNAH, M.A.; ERBAN, A.; KRÄMER, U.; KOPKA, J.; UDVARDI, M.K. Integrative functional genomics of salt acclimatization in the model legume *Lotus japonicas*. **The Plant Journal**, [*s.l.*], v. 53, p. 973–987, 2007.

SATHIYARAJ, G.; SRINIVASAN, S.; KIM, Y.J.; LEE, O.R.; PARVIN, S.; BALUSAMY, S.R.D. Acclimation of hydrogen peroxide enhances salt tolerance by activating defense-related proteins in panax ginseng c.a.meyer. **Molecular Biology Reports**, [*s.l.*], v. 41, p. 3761-3771, 2014.

SAVVIDES, A.; ALI, S.; TESTER, M.; FOTOPOULOS, V. Chemical priming of plants against multiple abiotic stresses: mission possible? **Trends in Plant Science**, [*s.l.*], v. 21, p. 329-340, 2016.

SEKHON, R.S.; BREITZMAN, M.W.; SILVA, R.R.; SANTORO, N.; ROONEY, W.L.; DELEON, N.; KAEPPLER, S.M. Stover composition in maize and sorghum reveals

remarkable genetic variation and plasticity for carbohydrate accumulation. **Frontiers in Plant Science**, [*s.l.*], v.7, p.822, 2016.

SENGUPTA, S.; MUKHERJEE, S.; BASAK, P.; MAJUMDER, A.L. Significance of galactinol and raffinose family oligosaccharide synthesis in plants. **Frontiers in Plant Science**, [*s.l.*], v. 6, p. 656, 2015.

SHAMEER, S.; RATCLIFFE, R.G.; SWEETLOVE, L.J. Leaf energy balance requires mitochondrial respiration and export of chloroplast NADPH in the light. **Plant Physiology**, [*s.l.*], v.180, p.1947–1961, 2019.

SHARMA, A.; SHAHZAD, B.; REHMAN, A.; BHARDWAJ, R.; LANDI, M.; ZHENG, B. Response of phenylpropanoid pathway and the role of polyphenols in plants under abiotic stress. **Molecules**, [*s.l.*], v. 24, p. 2452, 2019.

SHELKE, D.B., PANDEY, M., NIKALJE, G.C., ZAWARE, B.N., SUPRASANNA, P., NIKAM, T.D. Salt responsive physiological, photosynthetic and biochemical attributes at early seedling stage for screening soybean genotypes. **Plant Physiology and Biochemistry**, Paris, v. 118, p. 519-528, 2017.

SHEN, J.; WANG, Y.; SHU, S.; JAHAN, M.S.; ZHONG, M.; WU, J.; SUN, J.; GUO, S. Exogenous putrescine regulates leaf starch overaccumulation in cucumber under salt stress. **Scientia Horticulturae**, Amsterdam, v. 253, p. 99-110, 2019.

SHEVCHENKO, A.; TOMAS, H.; HAVLIS, J.; OLSEN, J.V.; MANN, M. In-gel digestion for mass spectrometric characterization of proteins and proteomes. **Nature Protocols**, [*s.l.*], v.1, p.2856–2860, 2006.

SHI, J.; YI, K.; YU, L.; LI, X.; ZHONGJING, Z.; YUE, C.; ZHANGHUA, H.; ZHENG, T.; RENHU, L.; YUNLONG, C.; CHEN, J. Phosphoenolpyruvate carboxylase in arabidopsis leaves plays a crucial role in carbon and nitrogen metabolism. **Plant Physiology**, [*s.l.*], v.167,

SHU, S.; YUAN, L.; GUO, S.; SUN, J.; YUAN, Y. Effects of exogenous spermine on chlorophyll fluorescence, antioxidant system and ultrastructure of chloroplasts in cucumis sativus L. under salt stress. **Plant Physiology and Biochemistry**, Paris, v. 63, p. 209-216, 2013.

SILVA, P.C.C.; AZEVEDO-NETO, A.D; GHEYI, H.R. Mobilization of seed reserves pretreated with H_2O_2 during germination and establishment of sunflower seedlings under salinity. **Journal of Plant Nutrition**, [*s.l.*], v. 42, p. 2388-2394, 2019.

SINGH, A.; KUMAR, A.; YADAV, S.; SINGH, I.K. Reactive oxygen species-mediated signaling during abiotic stress, **Plant Gene**, [*s.l.*], v. 18, p. 100173, 2019.

SINGH, M.; SINGH, A.; PRASAD, S.M.; SINGH, R.K. Regulation of plants metabolism in response to salt stress: an omics approach. **Acta Physiologiae Plantarum**, [*s.l.*], v.39, p.48, 2017.

SLAMA, I.; ABDELLY, C.; BOUCHEREAU, A.; FLOWER, T.; SAVOURÉ, A. Diversity, distribution and roles of osmoprotective compounds accumulated in halophytes under abiotic stress. **Annals of Botany**, Oxford, v.115, p.433–447, 2015.

SOZHARAJAN, R.; NATARAJAN, S. NaCl stress causes changes in photosynthetic pigments and accumulation of compatible solutes in *Zea mays* L. **Journal of Applied and Advanced Research**, [*s.l.*], v.1, n.1, p.3-9, 2016.

SUN, X.; WANG, Y.; XU, L.; LI, C.; ZHANG, W.; LUO, X.; JIANG, H.; LIU, L. Unraveling the root proteome changes and its relationship to molecular mechanism underlying salt stress response in radish (*Raphanus sativus* L.). **Frontiers in Plant Science**, [*s.l.*], v. 8, p.1192, 2017.

TAKAGI, D.; AMAKO, K.; HASHIGUCHI, M.; FUKAKI, H.; ISHIZAKI, K.; GOH, T.; FUKAO, Y.; SANO, R.; KURATA, T.; DEMURA, T.; SAWA, S.; MIYAKE, C. Chloroplastic ATP synthase builds up proton motive force for preventing reactive oxygen species production in photosystem I. **The Plant Journal**, [*s.l.*], v. 91, p.306–324, 2017.

TAMBURINO, R.; VITALE, M.; RUGGIERO, A.; SASSI, M.; SANNINO, L.; ARENA, S.; COSTA, A.; BATELLI, G.; ZAMBRANO, N.; SCALONI, A.; GRILLO, S.; SCOTTI, N. Chloroplast proteome response to drought stress and recovery in tomato (*Solanum lycopersicum* L.). **BMC Plant Biology**, [*s.l.*], v.17, p.40, 2017.

THAKUR, M.; SHARMA, P.; ANAND, A. Seed priming-induced early vigor in crops: an alternate strategy for abiotic stress tolerance, in: Priming Pretreat. Seeds Seedlings, Springer Singapore, Singapore, p. 163–180, 2019.

TIMM, S.; FLORIAN, A.; FERNIE, A.R.; BAUWE, H. The regulatory interplay between photorespiration and photosynthesis. **Journal of Experimental Botany**, [*s.l.*], v.67, p.2923–2929, 2016.

UPADHYAY, R.K.; HANDA, A.K.; MATTOO, A.K. Transcript abundance patterns of 9- and 13-lipoxygenase subfamily gene members in response to abiotic stresses (heat, cold, drought or salt) in tomato (*Solanum lycopersicum* L.) highlights member-specific dynamics relevant to each stress. **Genes**, [*s.l.*], v.10, p.683, 2019.

VERMA, V.; RAVINDRAN, P.; KUMAR, P.P. Plant hormone-mediated regulation of stress responses. **BMC Plant Biology**, [*s.l.*], v.16, p.86, 2016.

WANG, N.; ZHONG, X.; CONG, Y.; WANG, T.; YANG, S.; LI, Y.; GAI, J. Genome-wide analysis of phosphoenolpyruvate carboxylase gene family and their response to abiotic stresses in soybean. **Scientific Reports***,* [*s.l.*], v.6, p. 38448, 2016.

WANG, Y.; ZENG, X.; XU, Q.; MEI, X.; YUAN, H.; JIABU, D.; SANG, Z.; NYIMA, T. Metabolite profiling in two contrasting Tibetan hulless barley cultivars revealed the core salt-responsive metabolome and key salt-tolerance biomarkers. **AoB PLANTS**, [*s.l.*], v.11, doi:10.1093/aobpla/plz021, 2019.

WASEEM, M.; AHMAD, F. The phosphoenolpyruvate carboxylase gene family identification and expression analysis under abiotic and phytohormone stresses in *Solanum lycopersicum* L. **Gene**, [*s.l.*], v.690, p.11–20, 2019.

WELLBURN, A. R. The spectral determination of chlorophylls a and b, as well as total carotenoids, using various solvents with spectrophotometers of different resolution. **Journal Plant Physiology**, [*s.l.*], v. 144, p. 307-313, 1994.

WU, H. Plant salt tolerance and Na^+ sensing and transport**. The Crop Journal**, [*s.l.*], v. 6, p. 215-225, 2018.

XIA, J.; SINELNIKOV, I.V.; HAN, B.; WISHART, D.S. MetaboAnalyst 3.0 - making metabolomics more meaningful. **Nucleic Acids Research**, [*s.l.*], v.43, p.251–257, 2015.

XIONG, J.; SUN, Y.; YANG, Q.; TIAN, H.; ZHANG, H.; LIU, Y.; CHEN, M. Proteomic analysis of early salt stress responsive proteins in alfalfa roots and shoots. **Proteome Science**, [*s.l.*], v.15, p.19, 2017.

YAMANE, K.; MITSUYA, S.; TANIGUCHI, M.; MIYAKE, H. Salt-induced chloroplast protrusion is the process of exclusion of ribulose-1,5-bisphosphate carboxylase/ oxygenase from chloroplasts into cytoplasm in leaves of rice. **Plant, Cell and Environment**, [*s.l.*], v. 35, p. 1663-1671, 2012.

ZECHMANN, B. Ultrastructure of plastids serves as reliable abiotic and biotic stress marker. **PLoS ONE**, [*s.l.*], v.14, p.4, 2019.

ZHANG, X.L.; JIA, X.F.; YU, B.; GAO, Y.; BAI, J.G. Exogenous hydrogen peroxide influences antioxidant enzyme activity and lipid peroxidation in cucumber leaves at low light. **Scientia Horticulturae**, Amsterdam, v. 129, p 656–662, 2011.

ZHAO, F.; ZHANG2, D.; ZHAO, Y.; WEIWANG; YANG, H.; TAI, F.; LI, C.; HU, X. The difference of physiological and proteomic changes in maize leaves adaptation to drought, heat, and combined both stresses. **Frontiers in Plants Science**, [*s.l.*], v.7, p.1471, 2016.

ZHAO, J.; MISSIHOUN, T.D.; BARTELS, D. The role of Arabidopsis aldehyde dehydrogenase genes in response to high temperature and stress combinations. **Journal of Experimental Botany**, [*s.l.*], v.68, n.15, p.4295-4308, 2017.